ELECTROMAGNETIC COUPLING OF GROUNDED WIRES ON AN ANISOTROPIC, POLARIZABLE, LAYERED EARTH

by

Louis John O'Connor

A Thesis Submitted to the Faculty of the

DEPARTMENT OF GEOSCIENCES

In Partial Fulfillment of the Requirements
For the Degree of

MASTERS OF SCIENCE

In the Graduate College

THE UNIVERSITY OF ARIZONA

1 9 9 0

STATEMENT BY AUTHOR

This thesis has been submitted in partial fulfillment of requirements for an advanced degree at The University of Arizona and is deposited in the University Library to be made available to borrowers under rules of the Library.

Brief quotations from this thesis are allowable without special permission, provided that accurate acknowledgment of source is made. Requests for permission for extended quotation from or reproduction of this manuscript in whole or in part may be granted by the head of the major department or the Dean of the Graduate College when in his or her judgment the proposed use of the material is in the interests of scholarship. In all other instances, however, permission must be obtained from the author.

SIGNED: Louis J. O'Connor

APPROVAL BY THESIS DIRECTOR

This thesis has been approved on the date shown below:

J. R. Wait

J. R. WAIT
Regents Professor, Emeritus

29 Dec. 1989
Date

ACKNOWLEDGEMENTS

I would like to thank the members of my Committee, Dr. James R. Wait, Dr. John S. Sumner, and Dr. Robert Butler for their strong encouragement to complete this thesis and for the great patience and good cheer they exhibited while waiting for the final product. I would also like to thank the GeoElectromagnetics Program and Cominco American Resources Incorporated for their financial assistance during portions of my graduate studies. Other people who assisted me and deserve thanks include Steve Sorenson, who introduced me to the Reflection Seismology Convex Computer and Maureen Mackey, who guided me through the paperwork required by the Graduate College. Finally, I would like to thank my wife Trink for her love and support. Her companionship during this effort was invaluable.

TABLE OF CONTENTS

LIST OF ILLUSTRATIONS

LIST OF ILLUSTRATIONS--Continued

LIST OF ILLUSTRATIONS--Continued

LIST OF ILLUSTRATIONS--Continued

LIST OF ILLUSTRATIONS--Continued

ABSTRACT

An explicit derivation is given for the electromagnetic coupling of grounded wires on the surface of a two-layer earth with each layer having independent, complex horizontal and vertical conductivities.

An existing program that calculates the EM coupling of grounded wires for the isotropic complex resistivity case is extended to calculate models with anisotropic resistivities. Numerical results are computed for multi-frequency dipole-dipole IP measurements on one and two-layer models. Distinctly different coupling curves occur when the ratio of the horizontal to vertical conductivity is greater than or less than one.

CHAPTER 1

INTRODUCTION

Induced polarization (IP) is an electrical method of geophysical exploration that has been used in the search for minerals, oil and ground water. The widespread use of the method is indicated by the many books and scientific articles that have been published relating to the method. Texts covering the basic theory and practice of IP are notably those by Wait (1959a), Sumner (1976), and Bertin and Loeb (1976). The method was basically developed in the late 1940's and early 1950's, after it was recognized that strong IP responses were associated with rocks that contained the oxides and sulphides of some economically important metals. Over the last thirty years, with improvements in the measurement techniques and instrumentation, the detection of subtle variations in IP response has become possible.

The basis of the technique is the measurement of a quantity related to the frequency dependence of the electrical resistivity of the ground. Measurement procedures are similar to those used in the four electrode direct current (dc) resistivity measurement. A current is driven through two grounded electrodes, and the resulting voltage between the other two grounded electrodes is measured. The IP

method is different from a dc resistivity measurement in that instead of a dc current, a time dependent waveform is used. Several methods have been developed to measure the frequency dependence, and to arrange the transmitter and receiver electrode geometry. Choice of measurement method and field array depends on the economics and objectives of the field survey.

From early on in the field use of the method, workers recognized that the induced polarization response of the ground could often be distorted or obscured by electromagnetic (EM) effects between the transmitting and receiving circuits of the field array (Wait, 1959c). Voltage measured at the receiver is in part the result of the electromagnetic coupling between the transmitter and receiver circuits. This coupling is a complicated function of transmitter waveform, resistivity structure of the ground, and geometry of the transmitting and receiving wires. Prior to recognition as an important factor in IP measurements, electromagnetic coupling had been studied by electrical engineers and mathematicians interested in its effects on power transmission and communication lines. These studies were generally limited to layered earth models with real resistivities. An excellent summary and bibliography of this work is given by Sunde (1949).

In an IP survey, measured voltage is the result of three forms of coupling between the transmitting and receiving wires: capacitive, resistive and inductive. Capacitive coupling is related to electrostatic effects between the transmitting and receiving wires and between the receiving wires and the ground. It is generally small for surface arrays and can be controlled by proper field techniques, such as keeping wires separated from each other and maintaining low contact impedances at the electrodes (Wait, 1959c; Madden and Cantwell, 1967). In situations where current and voltage lines cannot be separated, such as in borehole work, shielding of the potential lines can reduce capacitive coupling.

The commonly more important forms of coupling are mutual resistance and mutual inductance between the wires. Mutual resistance or resistive coupling results from the current driven into the ground at the grounding points of the transmitting wire. The mutual induction or inductive coupling component is related to coupling of the current in the transmitter circuit to the receiver circuit.

Early analytical work on EM coupling has been adapted and extended by geophysicists interested in its analysis and calculation in a geophysical context. The difficult form of the solution of mutual impedance (ratio of voltage in the receiver circuit to current in the transmit-

ting circuit), even in simple geologic models, has placed practical restrictions on numerical treatment of the problem. The standard approach has been to use field procedures that minimize the unwanted effects of electromagnetic coupling; or to use master curves for simple geologic models and commonly used arrays so that an estimate could be made of the influence of EM coupling on the data. More recently, with the increasing availability of computers, coupling for more complicated models has been studied. Now the trend is towards interpretation of the information contained in the EM coupling component of an IP survey, as has been done previously with loop-loop and grounded dipole-loop EM sounding data.

In the last decade, research in IP has concentrated on the measurement of variations in rock resistivity in the frequency range from dc to greater than one kiloHertz. Many researchers believe that spectral resistivity measurements can provide information that aids the identification of rock type and mineralization (Fraser et al., 1964; Zonge and Wynn, 1975; Pelton et al., 1978; Halverson et al., 1981). However, comparison of field results with laboratory measurements or theoretical models requires accurate subtraction of the distorting effects of the EM coupling response from the field data.

The common approach is to use empirical models and numerical techniques in an attempt to separate the IP and EM responses of the ground. Some examples of this approach are Hallof (1974), Hallof and Pelton (1980), Tyne (1981), Trofimenkoff et al., (1982), Anderson and Smith (1984, 1986), Coggon (1984), Song (1984), Brown (1985), and Wang et al. (1985). These numerical techniques have a limited ability to separate IP and EM effects (Major and Silic, 1981). The problem is complicated because resistivity structure and frequency dependence are inherently involved in both the IP and EM responses. Direct inversion of field data has been avoided due to problems in choosing appropriate earth models and complexity of numerical calculations.

To study behavior of the electromagnetic coupling present in a wide band spectral resistivity survey, I review the mathematical formulation of mutual impedance for a two-layer earth with anisotropic resistivities. Using anisotropic resistivities provides a general formulation of the layered earth response that might prove useful in the study of EM coupling in ore environments. Anisotropic resistivities are also important for the study of positive and negative coupling effects associated with layered earth responses. Parts of this problem have been studied previously by Wynn (1974, 1979) and Wynn and Zonge (1975, 1977), but the derivations in those papers do not agree with those

of Wait (1966a, 1966b) and the numerical results are questionable.

CHAPTER 2

FREQUENCY DEPENDENCE AND ANISOTROPY OF RESISTIVITY

In geophysical exploration, the primary objective is to locate zones whose physical properties indicate a subsurface geologic target. A quantitative interpretation of geophysical survey data requires finding an earth model that best fits the observations. In order of increasing complexity, the geophysical model may be one, two- or three-dimensional in describing variations in the geologic structure.

A common approach in interpretation of geophysical data is to assume a one dimensional earth model consisting of a several infinite, horizontal layers with different physical properties. Although layering is a common phenomena in most rock types, an infinite, horizontally stratified earth is at best a local approximation to the geologic environment. Because it is mathematically convenient and formal analytic solutions can be found, an initial interpretation often is in terms of a layered earth model.

Electromagnetic methods use the measurement of components of an electromagnetic field to determine the

subsurface resistivity structure. The most common interpretation assumes a one-dimensional model with layers of constant thickness and resistivities that are linear, homogeneous, isotropic, and independent of frequency.

In reality, measurements both laboratory and field measurements show that rock resistivities are both frequency dependent and anisotropic. By careful choice of resistivity anisotropy, a more general layered earth model allowing both anisotropy and frequency dependence of resistivity in each layer can be applied. To provide background for the mathematical analysis of EM coupling between grounded wires for this model, a general discussion of frequency dependence and anisotropy is given in this chapter.

Frequency Dependence of Resistivity

Observations of the resistivity of rocks have been made for at least the last sixty years, but the systematic study of rock resistivity began with the interest in explaining IP phenomena. As a result of early studies of rock samples in the laboratory, it became clear that rock resistivity can be conveniently described as a complex function of frequency (Wait, 1959b). For time harmonic fields written for a time factor of

$$e^{iwt}, \tag{2.1}$$

the current density, J, is related to the electric field, E, by

$$J_j = \sigma(w)_j E_j \; ; \quad j = x, y \text{ or } z \tag{2.2}$$

where the complex conductivity is

$$\sigma_j(w) = \sigma_j + iw \epsilon_j \tag{2.3}$$

and the following definitions hold:

$i = (-1)^{1/2}$,

$w = 2\pi f$,

f = frequency,

σ_j = conductivity (a real quantity),

and

ϵ_j = permittivity (a real quantity).

Complex conductivity and complex resistivity are related by

$$\rho_j(w) = 1/\sigma_j(w) \; . \tag{2.4}$$

Current in phase with the electric field is referred to as the conduction current and is proportional to rock conductivity. The current flowing out-of-phase with the inducing field is proportional to the angular frequency and

permittivity and is referred to as the quadrature current. Conduction current is related to the ordered motion of free charges; in rocks this takes place largely through the motion of ions in pore fluids. Quadrature current is related to time changes in the distribution of bound charges.

In general, both conductivity and permittivity can be complex functions of frequency in the sense that not all conduction currents (motion of free charge) or displacement currents are exactly in phase or in quadrature with the electric field. However, neither the complex nature of the permittivity nor the conductivity is resolvable, since only the total in phase and quadrature components of the field can be readily measured. Hence, only the effective conductivity and permittivity can be measured and it is sufficient to consider both of these as real quantities (Fuller and Ward, 1970).

Polarization mechanisms in rocks of importance to IP responses are often described as electrode or membrane type behavior (Madden and Cantwell, 1967). The electrode polarization mechanism occurs at the interface between ionic conduction in pore fluids and semiconductor behavior in solid mineral phases of certain metal oxides and sulphides. Membrane polarization occurs in the presence of certain clay minerals.

Two approaches have been taken in the study and modeling of the IP response of rocks. Both are based on a consideration of the physical processes involved in the electrical conduction in rocks. The empirical approach attempts to represent these processes by circuit elements; resistivity of the rock is then derived from the impedance of the equivalent circuit (Madden and Cantwell, 1967; Zonge, 1972; Pelton et al., 1978). The other approach is to build a physical model of the conduction process at the particle level and solve for the rock impedance (Wait, 1959b; Wong, 1979; Wong and Strangway, 1981). A current review of the physical model approach is given by Wait (1989).

Both methods have relevance in describing and understanding the electrical behavior of rocks. The empirical approach provides a handy means of classifying rock behavior in terms of the contribution of a few parameters in the equivalent circuit formulation. The problem is that the equivalent circuit elements are not easily related to actual physical quantities describing the rock. They are difficult to use to predict rock behavior, but they are useful for cataloging measured responses. The physical model approach, even when it is a gross simplification of the rock system, provides a direct way to predict the influence of physical properties such as particle size, shape,

and pore fluid electrochemistry on the electrical response of rocks.

A currently popular model for the complex resistivity of the ground is the Cole-Cole model (Pelton et al., 1978). The complex resistivity is derived from

$$\rho(w) = R(1 - m(1 - \frac{1}{1 + (iw\, t_o)^c})) \qquad (2.5)$$

The model has four parameters R, m, t_o and c. The R value is the dc resistivity term. The m value is the chargeability, t_o is time constant and c is referred to as the frequency dependence.

The above equation was applied empirically by Pelton et al. (1978) to laboratory and in-situ measurements of multifrequency dipole-dipole data. By fitting data to the model equation, parameters for typical mineralized environments were cataloged. In both laboratory and field measurements, it was found that m and t_o were associated with grain size and volume percentage of sulphide minerals. An increase in concentration of sulphide minerals increased both the time constant and the chargeability. An increase in grain size resulted in an increase in time constant, but a decrease in chargeability.

Later analysis by Halverson et al. (1981) and Wait (1982, 1989) demonstrate that the Cole-Cole equation is

derivable from Wait's original model for IP phenomena (Wait, 1959b). The Cole-Cole equation can be related to the effective resistivity of a medium loaded with spherical conducting particles having an impedance boundary. The empirical data of Pelton agree with predictions of the Wait model.

Resistivity Anisotropy

Electrical resistivity anisotropy refers to the directional dependence of resistivity. It results from the directional mixing of media of different resistivities. In anisotropic rocks, currents are distorted in the direction of the lowest resistivity. This results in a different current density and electric field than observed in isotropic ground. Two scales of resistivity anisotropy are defined by Keller and Frischnecht (1966). Microanisotropy can be related to the preferential orientation of particles or to fine scale layering in a rock. Macroanisotropy is related to interbedding of rock types of different resistivities. Microanisotropy is a property of a rock type and is observable in laboratory measurements of a hand sample. Macroanisotropy is the result of larger scale features such as interbedded formations in a sedimentary section, structural features, faulting or large veins.

Data on the anisotropy of rocks is limited, with few published laboratory studies. Available information suggests that microanisotropy is a common feature in many rock

types. Hill (1972) made a study of the three-dimensional resistivity anisotropy of Precambrian metasediments and metavolcanics. His study showed that even somewhat dry, unmineralized, crystalline rocks could be highly anisotropic. Anisotropy was found to be a complex function of frequency.

A common assumption is that resistivity anisotropy can be reduced to two components: one perpendicular and one parallel to the preferred orientation of the layering in the rocks. For this case, the coefficient of anisotropy is expressed as

$$\lambda = (\sigma_l/\sigma_t) \qquad (2.6)$$

where

σ_l = longitudinal conductivity (parallel to bedding)

σ_t = the transverse conductivity (perpendicular to bedding).

Commonly this ratio is only measured at dc, but for the general case the ratio is a complex function of frequency. Typical dc values of this ratio for unmineralized rocks range from one to three, with exceptional values approaching seven (Keller and Frischnecht, 1966). Few values of this parameter have been reported for mineralized rocks; however it can be expected that anisotropy is much

larger in those environments since sulphide minerals are often three to five orders of magnitude more conductive than the host rocks. Sumner (1976, p. 99) reported a sample of schist from the Homestake mine with $\lambda = 14.5$ for the dc resistivity and 4.7 for the percent frequency effect between .3 and 3.0 Hz. The percent frequency effect is

$$PFE = \frac{\rho_{.3} - \rho_3}{\rho_3} 100. \qquad (2.7)$$

with $\rho_{.3}$ the apparent resistivity at .3 Hertz and ρ_3 the apparent resistivity at 3 Hertz.

For the model analyzed here, I assume a layered earth with complex, microanisotropic conductivities. Within each layer, horizontal and vertical conductivities are independent. Cartesian components of the conductivity are

$$\sigma_x = \sigma_y = \sigma_h(w) \qquad (2.8)$$

and

$$\sigma_z = \sigma_v(w) \qquad (2.9)$$

where $\sigma_h(w)$ is the horizontal complex conductivity and $\sigma_v(w)$ is the vertical complex conductivity.

Note that the ratio

$$k(w) = (\sigma_h(w)/\sigma_v(w))^{1/2} \qquad (2.10)$$

is not always the same as the coefficient of anisotropy defined for layered rocks. Theoretically, the coefficient of anisotropy for layered rocks is always greater than or equal to one. The ratio k defined here can be either greater or less than one. A k(w) greater than one is expected for flat-lying rocks containing laminated sulphides or interbedded graphitic layers. A k(w) less than one is expected for steeply dipping structures such as fractures, stockwork veining, or steeply dipping bedding.

Other more complicated orientations for anisotropy are possible. LeManse and Vasseur (1981) derived expressions for the electromagnetic field components on half-spaces where either the x and z or the y and z directions have the same conductivities. They use their expressions to predict the influence of vertical water-bearing fissures on the electromagnetic coupling of loops on the surface of a half-space. They did not consider electromagnetic coupling between grounded wires.

CHAPTER 3

ANALYSIS OF ELECTROMAGNETIC COUPLING

Mathematical analysis of the mutual impedance of grounded wires for various earth models has been studied by many workers in the past eighty years. The problem is important in both electrical engineering and geophysical prospecting. A comprehensive reference to the work done in the first half of this century is Sunde (1949). He presents the basic approach to formulating and solving the boundary value problem associated with the mutual impedance of grounded wires on a homogeneous half-space and a two-layer earth. He also discusses analytical approximations for special cases that allow computation of numerical results. His bibliography provides numerous references to earlier work on the subject.

Since the early 1950's some studies of mutual impedance and electromagnetic coupling have appeared in the geophysical literature. These studies were stimulated by a growing interest in electromagnetic exploration techniques and the recognition of distorting effects that EM coupling has on induced polarization surveys (Wait, 1959c). Numerical results for the mutual impedance of grounded wires have been presented by: Millet (1967) for a homogeneous and

isotropic half-space; Hohmann (1973) for a two-layer earth with isotropic resistivities; and Dey and Morrison (1973) for multilayered earths with either real or complex resistivities. Ramachandran Nair and Sanyal (1980) studied EM coupling for a variety of electrode configurations on an isotropic half-space.

A computer program for computation of the mutual impedance of wires on a layered earth model with isotropic resistivities has been written by Kauahikaua and Anderson (1979). Their program allows complex resistivities in the model to compute the combined effects of IP and EM coupling. Using this program, Washburne (1982) calculated a set of coupling curves for dipole-dipole arrays on two layer earths with complex isotropic resistivities. For problems of two- and three-dimensional geometries, results are few because these geometries require costly numerical methods. Some results have been presented by Hohmann (1975) and Hohmann and Ward (1981).

The first work on anisotropic earth models dates from the original work on DC resistivity interpretation. For EM fields, Wait (1966a, 1966b, 1982) presented solutions for the EM fields on the surface of an anisotropic layered earth and for the resulting EM coupling in grounded wire arrangements. For EM coupling in IP surveys on layered anisotropic earths, Wynn (1974, 1979) and Wynn and Zonge

(1975, 1977) published results. But as pointed out by Wait (1982, p. 165), several discrepancies in the theoretical derivations make these results questionable. The results of Xiong et al. (1986) are for the most complicated IP and EM coupling model published to date. They computed the IP and EM coupling response for a three-dimensional block in the second layer of a two-layer anisotropic earth.

In this chapter, I present a detailed derivation of electromagnetic coupling for a two-layer earth using the stratified, anisotropic resistivity model in Chapter 2. Results can be shown to be equivalent to Wait's solution for the fields of a dipole over a multilayered earth (1966b). This model is more general than the isotropic resistivity model, but unlike the two- and three-dimensional models, it has a relatively straightforward analytical solution due to symmetry about the vertical axis. The model can be described with only a few parameters and can be computed in only a fraction of the time required for two- and three-dimensional EM problems. It could be useful for interpreting EM effects in multi-frequency IP surveys.

General Approach

The derivation starts by solving for the electromagnetic field generated by a horizontal dipole placed in the air over a two-layer earth. The general form of the solutions are found by applying Maxwell's equations in the

regions of the problem; that is, the air and the layers of the earth. Then by applying boundary conditions on the field components at the interfaces between air and the first layer and between the first and second layer, coefficients in the general solutions are determined.

Allowing the dipole to approach the air-earth interface then integrating over the length of the transmitter wire results in the general expression for the field of a finite length grounded wire source on the surface of the earth. Mutual impedance is found by integrating the expression for the electric field at the surface of the earth over the length of the receiver wire and normalizing by the transmitter current.

Maxwell's Equations

In the frequency domain, the electric and magnetic fields can be written as

$$E = \begin{vmatrix} E_x \\ E_y \\ E_z \end{vmatrix} \qquad (3.1)$$

and

$$H = \begin{vmatrix} H_x \\ H_y \\ H_z \end{vmatrix} . \qquad (3.2)$$

Then, Maxwell's equations for source free regions with

linear, homogeneous, complex, anisotropic resistivities can be written as

$$\nabla \times E = iw\mu H \ , \tag{3.3}$$

$$\nabla \times H = [\sigma]E \ , \tag{3.4}$$

$$\nabla \cdot B = \mu(\nabla \cdot H) = 0 \ , \tag{3.6}$$

and

$$\nabla \cdot D = \varepsilon(\nabla \cdot E) = 0 \ , \tag{3.7}$$

where

$$i = (-1)^{1/2} \tag{3.8}$$

and

$$w = 2\pi f \tag{3.9}$$

with

f = frequency

μ = magnetic permeability

and

ε = the permittivity.

The complex conductivity is:

$$[\sigma] = \begin{vmatrix} \sigma_h & 0 & 0 \\ 0 & \sigma_h & 0 \\ 0 & 0 & \sigma_v \end{vmatrix} \tag{3.10}$$

where

$$\sigma_j = (1/\rho_j) = \sigma_j + iw\varepsilon_j \tag{3.11}$$

with

$$j = x, y, \text{ and } z.$$

The three-dimensional analog of Ohm's Law is then

$$E_j = \rho_j J_j \ . \tag{3.12}$$

Maxwell's equations represent the relationship between the electric and magnetic fields in a region. Thus determination of these fields is often simplified by solving the problem using auxiliary function from which the fields can later be derived. The auxiliary function is introduced by letting $H = \nabla \times A$. Substitution of $H = \nabla \times A$ into Maxwell's equations then gives

$$\nabla \times E = -iw\,\mu(\nabla \times A) \tag{3.13}$$

and

$$\nabla \cdot B = 0 \ , \tag{3.14}$$

where by definition

$$\nabla \cdot \nabla \times A = 0 \ . \tag{3.15}$$

Letting Φ be an arbitrary scalar function, and using the vector identity $\nabla \times (-\nabla \Phi) = 0$ results in

$$\nabla \times (E + iw\,\mu A) = \nabla \times (-\nabla \Phi) \tag{3.16}$$

or

$$E + iw\ \mu A = -\nabla\Phi\ . \qquad (3.17)$$

When $w = 0$, Φ can be identified as the potential of the electrostatic field, because

$$E = -\nabla\Phi. \qquad (3.18)$$

Formulation for Anisotropy

Following Wait's approach (1966a, 1966b, 1982), I derive the partial differential equations governing the EM fields in the anisotropic earth problem by using the auxillary function A. Substituting for E and H in the equation involving the curl of H results in

$$\nabla \times \nabla \times A = [\sigma](-iw\ \mu A - \nabla\Phi)\ . \qquad (3.19)$$

Then using the vector identity

$$\nabla \times \nabla A = \nabla(\nabla \cdot A) - \nabla^2 A \qquad (3.20)$$

where

$$\nabla^2 A = a_x \nabla^2 A_x + a_y \nabla^2 A_y + a_z \nabla^2 A_z \qquad (3.21)$$

results in

$$\nabla^2 A - [\sigma]iw\ \mu A = \nabla(\nabla \cdot A + [\sigma]\Phi)\ . \qquad (3.22)$$

The scalar cartesian components of A are then

$$\nabla^2 A_x - \sigma_h \, iw \, \mu A_x = \frac{\partial}{\partial x} (\nabla \circ A + \sigma_h \Phi) \, , \qquad (3.23)$$

$$\nabla^2 A_y - \sigma_h \, iw \, \mu A_y = \frac{\partial}{\partial y} (\nabla \circ A + \sigma_h \Phi) \, , \qquad (3.24)$$

and

$$\nabla^2 A_z - \sigma_v \, iw \, \mu A_z = \frac{\partial}{\partial z} (\nabla \circ A + \sigma_v \Phi) \, . \qquad (3.25)$$

To get a unique solution to the components of the electromagnetic field, a condition must be set on the choice of A and Φ. The commonly chosen condition for isotropic conductivity is the Lorentz condition

$$\nabla \circ A + \sigma \Phi = 0 \, , \qquad (3.26)$$

but for anisotropic conductivity, the choice is

$$\nabla \circ A + \sigma_h \Phi = 0 \qquad (3.27)$$

since this provides the greatest simplification of the equations.

Substituting the relation between A and into the equations for the components of A and letting

$$k^2 = (\sigma_h/\sigma_v) \tag{3.28}$$

and

$$\gamma_h^2 = iw\mu\sigma_h \tag{3.29}$$

results in

$$\nabla^2 A_x - \gamma_h^2 A_x = 0 , \tag{3.30}$$

$$\nabla^2 A_y - \gamma_h^2 A_y = 0 , \tag{3.31}$$

and

$$\nabla^2 A_z - (1-(1/k^2))\frac{\partial}{\partial z}(\nabla \cdot A) - (1/k^2)\gamma_h^2 A_z = 0 . \tag{3.32}$$

These are the general equations to be solved for regions of the problem. The equations for A_x and A_y are of the same form as those treated by Sunde for the isotropic resistivity problem, but the equation for A_z is more complicated and reflects the coupling of the horizontal and vertical conductivities in A_z. Only in an isotropic region such as the air does the equation for A_z simplify.

Note that although k is defined in a form similar to the coefficient of anisotropy, they are not the same. As formulated here, σ_h and σ_v are arbitrary complex numbers; thus, k is also an arbitrary complex number and can have a magnitude less than one. The coefficient of anisotropy as defined in Chapter 2 is the ratio of the longitudinal to the

transverse conductivity and is always greater than or equal to one.

After solving for A, the magnetic field can be found from

$$H = \nabla \times A \ , \tag{3.33}$$

which in Cartesian coordinates reduces to

$$H_x = \frac{\partial A_z}{\partial y} - \frac{\partial A_y}{\partial z} \ , \tag{3.34}$$

$$H_y = \frac{\partial A_x}{\partial z} - \frac{\partial A_z}{\partial x} \ , \tag{3.35}$$

and

$$H_z = \frac{\partial A_y}{\partial x} - \frac{\partial A_x}{\partial y} \ . \tag{3.36}$$

The electric field components can be found by substituting into

$$[\sigma] \ E = \nabla(\nabla \cdot A) - \nabla^2 A \ . \tag{3.37}$$

Then

$$E_x = (1/\sigma_h)[\frac{\partial}{\partial x} (\nabla \cdot A) - \gamma_h^2 A_x] \tag{3.38}$$

$$E_y = (1/\sigma_h)[\frac{\partial}{\partial y} (\nabla \cdot A) - \gamma_h^2 A_y] \tag{3.39}$$

and

$$E_z = (1/\sigma_h) \left[\frac{\partial}{\partial z}(\nabla \cdot A) - \gamma_h^2 A_z\right] \qquad (3.40)$$

Of particular interest in the derivation of the mutual impedance of grounded wires are the equations for E_x and E_y, which are responsible for the voltage measured on the surface of the earth.

Boundary Conditions

Boundary conditions on the electromagnetic field are used to match solutions in the particular regions of the problem to find the complete expressions for the fields. The standard boundary conditions are the continuity of the tangential electric and magnetic fields. For the problem of horizontally stratified earth, this means the continuity of the x and y components of E and H. For problems with cylindrical symmetry about the z axis, as in the stratified earth model, only the A_x and A_y components of the auxiliary function need to be considered in the solution of the problem (Sommerfeld, 1949). The A_y component is not needed and can be set to zero.

Boundary conditions at the interfaces between regions of different physical properties can be written in a simple form with respect to the components of A. With A_y set to zero and integration with respect to x and y per-

mitted since conditions hold everywhere in the interface, the horizontal magnetic field components imply

$$A_{z,n} = A_{z,n+1} \tag{3.41}$$

and

$$\frac{\partial}{\partial z} A_{x,n} = \frac{\partial}{\partial z} A_{x,n+1} \tag{3.42}$$

at the interface (where the second subscript designates the layer). Similarly, from the electric field at the interface between layers n and n+1

$$A_{x,n} = A_{x,n+1} \tag{3.43}$$

and

$$\frac{1}{\gamma^2_{h,n}}\left(\frac{\partial}{\partial x} A_{x,n} + \frac{\partial}{\partial z} A_{z,n}\right) = \frac{1}{\gamma^2_{h,n+1}} \left(\frac{\partial}{\partial x} A_{x,n+1} + \frac{\partial}{\partial z} A_{z,n+1}\right) \tag{3.44}$$

Two-Layer Anisotropic Earth

The problem is illustrated in Figure 3.1. A horizontal, x oriented, electric dipole is located in the air at a height h above a two-layer earth. Each layer has independent horizontal and vertical conductivities. The origin of the cartesian coordinate system is at the air-earth

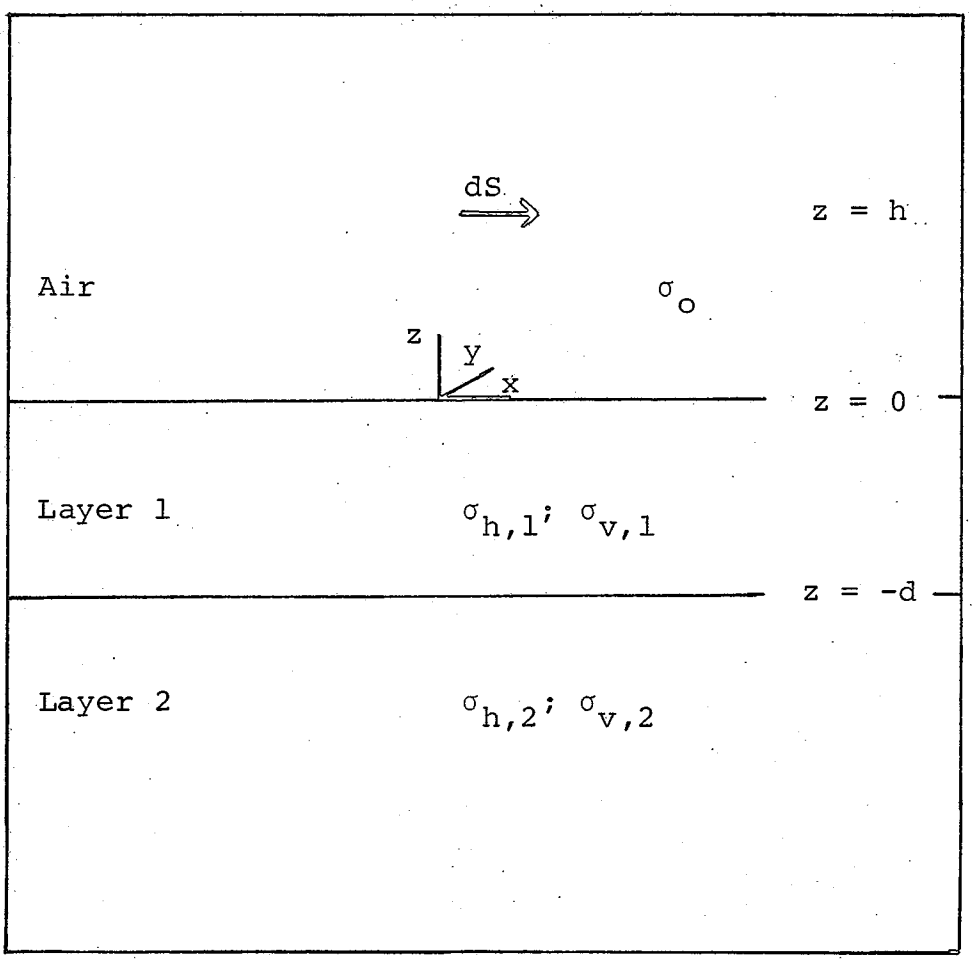

Figure 3.1. Dipole source over a two-layer, anisotropic earth. -- An infinitesimal x oriented dipole is located in the air at an elevation h over a two layer earth. The air extends along the z axis from zero to positive infinity and layer 2 extends from -d to negative infinity. The electric field is to be determined at the earth's surface where z is equal to zero. The horizontal complex conductivities are $\sigma_{h,1}(w)$ and $\sigma_{h,2}(w)$. The vertical complex conductivities are $\sigma_{v,1}(w)$ and $\sigma_{v,2}(w)$.

interface and the positive z axis is oriented upward. The magnetic permeability is assumed equal to the permeability of free space in each of the layers. The problem divides into three regions: the air (designated by subscript 0); layer 1, with z ranging from 0 to -d; and layer 2, with z ranging from -d to negative infinity.

In the air, conductivity is isotropic and is written as

$$\sigma_o = iw\,\varepsilon_o \,. \tag{3.45}$$

In each layer it is represented by a tensor

$$\begin{vmatrix} \sigma_{h,n} & 0 & 0 \\ 0 & \sigma_{h,n} & 0 \\ 0 & 0 & \sigma_{v,n} \end{vmatrix} . \tag{3.46}$$

Equations for the Air

In the air, the solution is the sum of a primary field and a secondary field. The primary field is caused solely by the source dipole, and the secondary field results from the presence of the earth. For a dipole oriented in the x direction, the primary field contributes only to the x component of A. Solutions of the partial differential equations in the air can then be written as

$$A_{x,o} = A^{p}_{x,o} + A^{s}_{x,o} \tag{3.47}$$

and

$$A_{z,o} = A^{s}_{z,o} \tag{3.48}$$

where the superscript p denotes the primary field component and superscript s denotes a secondary field.

Primary Field

Considering first the primary field of the dipole, I want a solution to

$$\nabla^2 A_{x,o} - \gamma_o^2 A_{x,o} = 0 \tag{3.49}$$

that has a singularity at the source at x = 0, y = 0 and z = h. Following Sommerfeld (1949) or Stratton (1941), such a solution is

$$A^{p}_{x,o} = \frac{c}{r} e^{-\gamma_o r} \tag{3.50}$$

where

$$r = (x^2 + y^2 + (z - h)^2)^{1/2} \tag{3.51}$$

This solution can readily be verified in spherical coordinates where ∇^2 reduces to

$$\nabla^2 = \frac{1}{r^2}\left(\frac{\partial}{\partial r}\left(r^2 \frac{\partial}{\partial r}\right)\right) \tag{3.52}$$

The constant C is evaluated using

$$\nabla \cdot A + \sigma_o \Phi = 0 \tag{3.53}$$

setting $w = 0$,

$$\Phi = \frac{I\, dS}{4\pi\sigma_o}\,, \tag{3.54}$$

the potential of a static electric dipole, and

$$C = \frac{I\, dS}{4\pi}\,. \tag{3.55}$$

Finally, the result is expressed in cylindrical coordinates by using the Fourier Bessel theorem and contour integration in the complex plane (Stratton 1941, p. 575). The result for a dipole at a height $z = h$ is the "Sommerfeld integral":

$$A^p_{x,o} = \frac{I\, dS}{4\pi} \int_o^\infty \frac{\lambda}{u_o} e^{-u_o|z - h|} J_o(\lambda r) d\lambda \tag{3.56}$$

$$u_o = (\lambda^2 + \gamma_o^2)^{1/2} \tag{3.57}$$

Secondary Field

For $A^s_{x,o}$ and $A^s_{z,o}$, the expression

$$\nabla^2 A - \gamma_o^2 A = 0 \tag{3.58}$$

is written in cylindrical coordinates as

$$\left(\frac{1}{r}\frac{\partial}{\partial r}\left(r\frac{\partial}{\partial r}\right) + \frac{1}{r^2}\frac{\partial^2}{\partial \phi^2} + \frac{\partial^2}{\partial z^2}\right) A - \gamma_o^2 A = 0 \tag{3.59}$$

A general form of the solution can be found by the technique of separation of variables. The general solution is a linear combination of the following forms

$$\begin{vmatrix} J_n(\lambda r) \\ Y_n(\lambda r) \end{vmatrix} \begin{vmatrix} \cos n\phi \\ \sin n\phi \end{vmatrix} \begin{vmatrix} e^{-u_o z} \\ e^{u_o z} \end{vmatrix} . \tag{3.60}$$

For the $A^s_{x,o}$ component, it is required that: (1) the fields vanish as r approaches positive infinity, (2) the fields be finite on the z axis, and (3) there is no angular dependence. Hence the general form of the solution is

$$A^{s}_{x,o} = \int_{o}^{\infty} C(\lambda)\, e^{-u_o z}\, J_o(\lambda r)\, d\lambda \,. \qquad (3.61)$$

For the $A^{s}_{z,o}$ component, the conditions are similar except that now the fields and hence the auxiliary function should be even with respect to the x-z plane. Therefore

$$A^{s}_{z,o} = \cos\phi \int_{o}^{\infty} D(\lambda)\, e^{-u_o z}\, J_o(\lambda r)\, d\lambda \,. \qquad (3.62)$$

Then using the identity

$$-\frac{\partial}{\partial x}\int_{o}^{\infty} \frac{J_o(\lambda r)}{\lambda}\, d\lambda = \cos\phi \int_{o}^{\infty} J_o(\lambda r)\, d\lambda \qquad (3.63)$$

the solution becomes

$$A^{s}_{z,o} = -\frac{\partial}{\partial x}\int_{o}^{\infty} \frac{D(\lambda)}{\lambda}\, e^{-u_o z}\, J_o(\lambda r)\, d\lambda \qquad (3.64)$$

Finally, the expressions for the auxiliary components in the air are given as:

$$A_{x,o} = \frac{I\, dS}{4\pi}\int_{o}^{\infty} \frac{\lambda}{u_o}\, [e^{-u_o|z - h|}$$

$$+ R_{\perp}(\lambda)\, e^{-u_o(z+h)}]\, J_o(\lambda r)\, d\lambda \qquad (3.65)$$

and

$$A_{z,o} = \frac{I\, dS}{4\pi} \frac{\partial}{\partial x} \int_o^\infty S(\lambda)\, e^{-u_o(z+h)} J_o(\lambda r)\, d\lambda \qquad (3.66)$$

where the new coefficients $R_{\perp}(\lambda)$ and $S(\lambda)$ absorb the manipulations with respect to the constants and functions of λ.

Equations for the First Layer

In the first layer the range of the z values is from 0 to -d. $A_{x,1}$ is a solution to an equation of the same form as $A^s_{x,o}$, but now the bounded range of z means that the general solution takes the form

$$A_{x,1} = \frac{I\, dS}{4\pi} \int_o^\infty [a_1 e^{u_1 z} + a_1' e^{-u_1 z}]\, J_o(\lambda r) d\lambda. \qquad (3.67)$$

For $A_{z,1}$, I want a solution to

$$\nabla^2 A_{z,1} - (1-(1/k_1^2)\, \frac{\partial}{\partial z} (\nabla \cdot A) - (1/k_1^2)\, \gamma_{h,1}^2 A_{z,1} = 0 . \qquad (3.68)$$

To do this, I follow the method of Wait (1966a). I assume a solution of the form

$$A_{z,1} = \frac{I\, dS}{4\pi} \frac{\partial}{\partial x} \int_0^\infty G(\lambda, z)\, J_o(\lambda r)\, d\lambda \qquad (3.69)$$

where the function $G(\lambda,z)$ is to be determined. Substitution of this form into the partial differential equation then gives

$$\frac{\partial}{\partial x} \int_0^\infty \left[\left(\frac{\partial^2 G}{\partial z^2} - \lambda^2 G \right) - \left(1 - (1/k_1^2) \frac{\partial}{\partial z} \left(A_{x,1} + \frac{\partial}{\partial z} G \right) \right. \right.$$

$$\left. \left. - (1/k_1^2) \gamma_{h,1}^2 G \right] J_o(\lambda r)\, d\lambda = 0 \right. \qquad (3.70)$$

where I have used:

$$\left(\frac{\partial^2}{\partial x^2} + \frac{\partial^2}{\partial y^2} \right) J_o(\lambda r) = -\lambda^2 J_o(\lambda r) \,. \qquad (3.71)$$

After simplifying, the non-trivial case for $G(\lambda,z)$ satisfies

$$\frac{\partial^2 G}{\partial z^2} - (k_1^2 \lambda^2 + \gamma_{h,1}^2) G =$$

$$(k_1^2 - 1) \left[u_1 a_1 e^{u_1 z} - u_1 a_1' e^{-u_1 z} \right] \,. \qquad (3.72)$$

For the homogeneous solution

$$G = B_1(\lambda)e^{v_1 z} + B_1'(\lambda)e^{-v_1 z} \tag{3.73}$$

with

$$v_1 = (\lambda^2 k^2 + \gamma_{h,1}^2)^{1/2} \tag{3.74}$$

where it is required that

$$\mathrm{Re}(v_1) > 0 \ . \tag{3.75}$$

Now using the method of undetermined coefficients, the particular solution is found by assuming

$$G_p(\lambda, z) = e^{u_1 z} G(\lambda) \ . \tag{3.76}$$

Substituting this into the partial differential equation for G and simplifying leads to the particular solution

$$G_p = \frac{-u_1}{\lambda^2} [a_1 e^{u_1 z} - a_1' e^{-u_1 z}] \tag{3.77}$$

and the general solution for A_z in the first layer is

$$A_{z,1} = \frac{I\,dS}{4\pi}\frac{\partial}{\partial z}\int_0^\infty [B_1(\lambda)\, e^{v_1 z} + B_1'(\lambda)e^{-v_1 z} - \frac{u_1}{\lambda^2}(a_1 e^{u_1 z} - a_1' e^{-u_1 z})]J_o(\lambda r)d\lambda \ . \qquad (3.78)$$

Equations for the Second Layer

The forms for the second layer can be derived directly from those of the first layer. Since the region is unbounded on the negative z axis, the terms involving negative exponentials are set to 0. Then

$$A_{x,2} = \frac{I\,dS}{4\pi}\int_0^\infty a_2 e^{u_2 z} J_o(\lambda r)\, d\lambda \qquad (3.79)$$

and

$$A_{z,2} = \frac{I\,dS}{4\pi}\int_0^\infty (B_2 e^{v_2 z} - \frac{u_2}{\lambda^2} a_2 e^{u_2 z})J_o(\lambda r)\, d\lambda \ . \qquad (3.80)$$

Solving for the Coefficients

Now the unknown coefficients are found by applying the boundary conditions on A_x and A_z at the interfaces at $z = 0$ and $z = -d$. A system of eight equations in eight unknowns results. The eight equations can be simplified and grouped into two sets of four equations each. To derive the fields at the surface only the $R_\perp(\lambda)$ and $S(\lambda)$ coefficients need to be determined. In matrix form, the two sets can be written as

$$\begin{vmatrix} -e^{-u_2 d} & e^{u_1 d} & e^{-u_1 d} & 0 \\ -u_2 e^{-u_2 d} & -u_1 e^{u_1 d} & u_1 e^{-u_1 d} & 0 \\ 0 & -u_o & -u_o & \lambda e^{-u_o h} \\ 0 & u_1 & -u_1 & -\lambda e^{-u_o h} \end{vmatrix} \begin{vmatrix} a_2 \\ a_1' \\ a_1 \\ R_\perp \end{vmatrix} = \begin{vmatrix} 0 \\ 0 \\ -\lambda e^{-u_o h} \\ -\lambda e^{u_o h} \end{vmatrix} \tag{3.82}$$

and

$$\begin{vmatrix} -e^{-v_2 d} & e^{v_1 d} & e^{-v_1 d} & 0 \\ -\alpha_2 e^{-v_2 d} & -\alpha_1 e^{v_1 d} & \alpha_1 e^{-v_1 d} & 0 \\ 0 & -e^{u_o h} & -e^{-u_o h} & 1 \\ 0 & -\frac{\alpha_1}{\alpha_2} e^{-u_o h} & -\frac{\alpha_1}{\alpha_2} e^{-u_o h} & 1 \end{vmatrix} \begin{vmatrix} B \\ B_1' \\ B_1 \\ S \end{vmatrix} = \begin{vmatrix} 0 \\ 0 \\ (R_\perp - 1)/\lambda \\ (R_\perp - 1)/\lambda \end{vmatrix} \tag{3.83}$$

where

$$\alpha_o = \frac{u_o}{\gamma_o^2} \quad \text{and} \quad \alpha_n = \frac{v_n}{\gamma_{h,n}^2} \, . \tag{3.84}$$

For the first set (Equation 3.82), a four-step forward elimination yields a solution for $R_\perp(\lambda)$. After some cancellation, it can be written as

$$R_{\perp} = \frac{u_o - u_1\left(\dfrac{u_2 + u_1 \tanh u_1 d}{u_1 + u_2 \tanh u_1 d}\right)}{u_o + u_1\left(\dfrac{u_2 + u_1 \tanh u_1 d}{u_1 + u_2 \tanh u_1 d}\right)} \quad . \tag{3.85}$$

Wait (1966b) expresses this result for an m layered earth as

$$R_{\perp} = \frac{N_o - Y_1}{N_o + Y_1} \tag{3.86}$$

where N_o and Y_1 are computed recursively from:

$$N_m = Y_m = \frac{u_m}{i\mu w} \tag{3.87}$$

$$N_n = \frac{u_n}{i\mu w} \quad ; \qquad n = m-1 \text{ to } 0 \tag{3.88}$$

and

$$Y_n = N_n \frac{Y_{n+1} + N_n \tanh u_n d_n}{N_n + Y_{n+1} \tanh u_n d_n} \quad ; \; n = m-1 \text{ to } 1 \tag{3.89}$$

Similarly, for the second set of equations, a four-step forward elimination gives a solution for $S(\lambda)$. After a lot of algebra, the solution can be reduced to

$$S = \frac{1}{\lambda}\left(R_{\perp} + \frac{\alpha_o - \alpha_1 \dfrac{\alpha_2 + \alpha_1 \tanh v_1 d}{\alpha_1 + \alpha_2 \tanh v_1 d}}{\alpha_o + \alpha_1 \dfrac{\alpha_2 + \alpha_1 \tanh v_1 d}{\alpha_1 + \alpha_2 \tanh v_1 d}}\right) . \qquad (3.90)$$

Or again in the notation of Wait (1966b),

$$S = \frac{1}{\lambda}\left(R_{\perp} + R_{\parallel}\right) \qquad (3.91)$$

and

$$R_{\parallel} = \frac{K_o - Z_1}{K_o + Z_1} , \qquad (3.92)$$

where for an m layered earth, K_o and Z_1 are computed recursively by

$$K_m = Z_m = \frac{v_m}{\sigma_{h,m}} \qquad (3.93)$$

$$K_n = \frac{v_n}{\sigma_{h,n}} ; \qquad n = m - 1 \text{ to } 1 \qquad (3.94)$$

$$K_o = \frac{u_o}{\sigma_o} \qquad (3.95)$$

and

$$Z_n = K_n \frac{Z_{n+1} + K_n \tanh v_n d_n}{K_n + Z_{n+1} \tanh v_n d_n} \quad ; \quad n = m-1 \text{ to } 1 \text{ .} \quad (3.96)$$

Electric Field at the Surface

Completing the expressions for the electric field on the surface of the earth requires two more steps. First, the expressions for S and $R_\perp$ must be substituted back into the equations for A. Then the x and y components of the electric field are determined from A and Φ. Finally, the elevation of the source wire is allowed to approach zero, and the field is determined at the air-earth interface.

For the frequencies of interest in the IP method, it is common to further simplify the results by making the "quasi-static" assumption. This means neglecting propagation effects at small distances with respect to the wavelength of radiation, where the fields are nearly in phase with the transmitter current (Grant and West, 1965, p. 470). A condition for the quasi-static region is $|\gamma_o r|^2 << 1$ (Wait, 1982, p. 169). Effectively, the quasi-static assumption means setting $\sigma_o = i\varepsilon_o w = 0$, then $u_o = \lambda$. This assumption implies that the propagation velocity on the current and voltage wires is infinite and that the current is independent of the position along the transmitter wire. With this assumption and using the notation of Sunde (1949), I

can express the tangential components of the electric field at z = 0. For a horizontal dipole at the surface, those components are:

$$E_x = I\, dS\, (-P(r) + \frac{\partial^2}{\partial x^2} Q(r)) \tag{3.97}$$

and

$$E_y = I\, dS\, (\frac{\partial^2}{\partial x \partial y} Q(r)) \ . \tag{3.98}$$

Using Wait's notation

$$P(r) = \frac{iw\mu_o}{2\pi} \int_o^\infty (\frac{\lambda}{\lambda + iw\mu_o Y_1}) J_o(\lambda r) d\lambda \tag{3.99}$$

and

$$Q(r) = \frac{1}{2\pi} \int_o^\infty \frac{1}{\lambda} (Z_1 - \frac{iw\mu_o}{\lambda + iw\mu_o Y_1}) J_o(\lambda r)\, d\lambda. \tag{3.100}$$

Mutual Impedance

To complete the expression for the mutual impedance of grounded wires on the surface, it is necessary to integrate the electric field over the length of the transmitting and receiving wires (Sunde, 1949, p. 31). The geometry for two straight grounded wires in the z = 0 plane is illustrated in Figure 3.2. The origin is located at an elementary section of the source wire dS, with the positive x axis

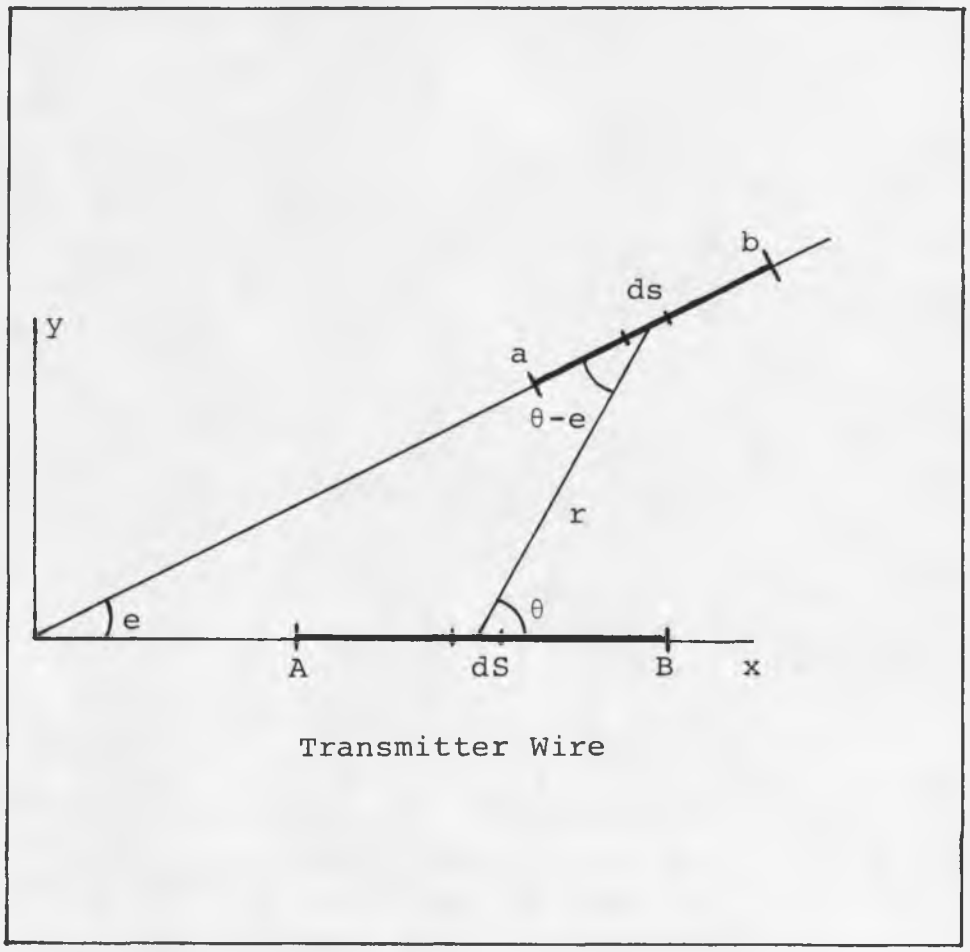

Figure 3.2. Geometry for the mutual impedance of straight grounded wires on the surface of the earth.

oriented along the positive direction of the path S of the source wire.

The voltage induced in a section ds of the receiver wire is given by

$$d\,V = E_s(r)ds \tag{3.101}$$

where

$$E_s\,(r) = \cos(e)E_x(r) + \sin(e)E_y\,(r) \tag{3.102}$$

Substituting for E_x and E_y,

$$dV = ds\ I\ dS(-P(r)\cos(e) + \frac{\partial^2}{\partial x^2}\,Q(r)\,\cos(e)$$

$$+ \frac{\partial^2}{\partial x\,\partial y}\,Q(r)\,\sin(e)) \tag{3.103}$$

Since the source is oriented along the x axis, dx = dS, and

$$dV = I\ ds\ dS\ (-P(r)\cos(e) +$$

$$\frac{\partial}{\partial S}(\frac{\partial}{\partial x}\,Q(r)\cos(e) + \frac{\partial}{\partial y}\,O(r)\sin(e)))\ . \tag{3.104}$$

Now following Sunde (1949, p. 31),

$$\frac{\partial}{\partial x} Q(r)\cos(e) + \frac{\partial}{\partial y} Q(r)\sin(e) =$$

$$\frac{d}{dr} Q(r)(\cos(\theta)\cos(e) + \sin(\theta)\sin(e))$$

$$= \frac{d}{dr} Q(r) \cos(\theta - e)$$

$$= - \frac{d}{ds} Q(r) \quad . \qquad (3.105)$$

A final expression for the mutual impedance is then

$$\frac{-V}{I} = \int_A^B dS \int_a^b ds(P(r)\cos(e) + \frac{d^2}{dS\, ds} Q(r)) \qquad (3.106)$$

where the double integration of Q(r) reduces to

$$Q(r_{Aa}) + Q(r_{Bb}) - Q(r_{Ab}) - Q(r_{Ba}) \quad . \qquad (3.107)$$

Comparison with the Derivation of Wynn

Wynn uses the horizontal and vertical Hertz vectors to derive his solution to the two-layer anisotropic earth. Unfortunately his development for the vertical Hertz vector ignores the coupling between the horizontal and the vertical components in the anisotropic layers. Wait (1981) noted

this and other theoretical errors in his communications with Wynn in 1981. In Wynn's 1979 publication, he assumes that he can use Sunde's (1949, p. 24) results for the isotropic case and expect the x and z Hertz vectors to satisfy

$$\nabla^2 \pi_j - \gamma_j^2 \pi_j = 0 \; ; \qquad j = x, y \tag{3.108}$$

where

$$\gamma_j^2 = iw\mu\sigma_j \; .$$

This assumption is incorrect. The actual equation for the vertical component in the anisotropic case should be similar to Equation 3.32 and should be

$$\nabla^2 \pi_z - (1-(1/k^2)) \frac{\partial}{\partial z}(\nabla \cdot \pi) - (1/k^2)\gamma_h^2 \pi_z = 0 \; . \tag{3.109}$$

Only the horizontal component satisfies Equation 3.108.

This mistake leads to other problems Wynn's solution, the most obvious is that his ratio for anisotropy is inverted. This is most easily seen in Wynn and Zonge (1977), where Equation 18 should be

$$v = (g^2 k^2 + 2i)^{1/2} \; . \tag{3.110}$$

CHAPTER 4

RESULTS FOR ANISOTROPIC MODELS

Numerical results for complex and anisotropic earth models have been computed for the collinear dipole-dipole array. Calculations were made using a revised version of a program for isotropic multi-layered earths (Kauahikaua and Anderson, 1979). Before discussing numerical results, I will point out some of the obvious properties of the P(r) and Q(r) functions and describe how they are rewritten for numerical evaluation.

General Behavior of the P(r) and Q(r) Functions

An inspection of the inductive component, P(r), indicates that it is a function of the transmitter frequency, and separation of the transmitter and receiver wires. For the horizontally stratified anisotropic model, it depends only on horizontal resistivities. In general, the function tends to zero as separation of the wires approaches infinity or frequency tends to zero.

The Q(r) function depends on r, frequency, and both horizontal and vertical resistivities. As separation of the transmitter and receiver gets very large, the Q function approaches zero. Also, if either the source or receiver are

ungrounded loops, this function equals zero and mutual impedance is independent of vertical resistivities.

For a half-space model (1 layer earth), the expression for P(r) (Equation 3.99) simplifies to

$$P(r) = \frac{iw\mu}{2\pi} \int_0^\infty \frac{\lambda}{\lambda + u_1} J_o(\lambda r)\, d\lambda \qquad (4.1)$$

Using

$$\frac{1}{\lambda + u_1} = \frac{\lambda - u_1}{\lambda^2 - u_1^2} = \frac{u_1 - \lambda}{\gamma_1^2} \qquad (4.2)$$

Equation 4.1 can be rewritten as

$$P(r) = \frac{iw\mu}{2\pi} \frac{1}{\gamma_1^2} \left(\int_o^\infty \lambda u_1 J_o(\lambda r) d\lambda - \int_o^\infty \lambda^2 J_o(\lambda r) d\lambda \right) \qquad (4.3)$$

and evaluated analytically. The first integral can be written as

$$\left[\frac{\partial^2}{\partial z^2} \int_o^\infty \frac{\lambda}{u_1} e^{-u_1 z} J_o(\lambda r) d\lambda \right]_{z=0} \qquad (4.4)$$

and the second integral as

$$- \left[\frac{\partial^2}{\partial z^2} \int_0^\infty \frac{\lambda}{u_1} e^{-u_1 z} J_o(\lambda r) d\lambda\right]_{\gamma=0,\ z=0} \qquad (4.5)$$

Recalling the equation for the primary field of a dipole, the first integral is

$$\frac{\partial^2}{\partial z^2} \left(\frac{e}{r^3} e^{-\gamma_1 r}\right)_{z=0}; \qquad r = (x^2 + y^2 + z^2)^{1/2} \ . \qquad (4.6)$$

This reduces to

$$\frac{(1 + \gamma_1 r) e^{-\gamma_1 r}}{r^3} \ . \qquad (4.7)$$

The second integral (Equation 4.5) therefore is

$$\frac{1}{r^3} \ . \qquad (4.8)$$

The expression for mutual inductance on the half space then is

$$\frac{1}{2\pi\sigma_{h,1}(w)} \int_A^B dS \int_a^b ds \ (\cos(e)\left(\frac{1}{r^3}\right.$$

$$- \left(\frac{1 + \gamma_1 r}{r^3} e^{-\gamma_1 r}\right)) \quad . \tag{4.9}$$

As noted before, the expression is the same as for an isotropic half space (Sunde, 1949, p. 123).

For Q(r) (Equation 3.100) on an anisotropic half space

$$Z_1 = \frac{v_1}{\sigma_{h,1}(w)} \tag{4.10}$$

and

$$Y_1 = \frac{u_1}{iw\,\mu_o} \quad . \tag{4.11}$$

Substituting into the general expression and simplifying results in

$$Q(r) = \frac{1}{2\pi\sigma_{h,1}(w)}\left(\int_o^\infty \frac{v_1 - u_1}{\lambda} J_o(\lambda r)d\lambda + \frac{1}{r}\right) \quad . \tag{4.12}$$

When the frequency goes to zero, the expression reduces to the potential on an anisotropic half space. Then the integral can be written as

$$(k-1)\int_o^\infty J_o(\lambda r)d\lambda = \left(\left(\frac{\sigma_{h,1}(w)}{\sigma_{v,1}(w)}\right)^{1/2} - 1\right)\frac{1}{r} \tag{4.13}$$

and

$$Q(r) = \frac{1}{2\pi r(\sigma_{h,1} \cdot \sigma_{v,1})^{1/2}} \qquad (4.14)$$

Numerical Evaluation

To get numerical results, I have modified an existing program for a multi-layered earth with isotropic resistivities. The program by Kauahikaua and Anderson (1979) numerically evaluates the P(r) and Q(r) functions using the linear digital filter method (Anderson 1974, 1979) and the double integration over the P(r) term by Gaussian quadrature. To generalize the program for an anisotropic model requires replacement of the expression for the isotropic Q(r) by the expression for the anisotropic Q(r).

In the FORTRAN program EMCUPL, the infinite integrals of Bessel functions in both the P(r) and Q(r) are written with the half space response for the first layer subtracted under the integral sign and the analytical results added back outside the integral. This improves convergence of the integrals for numerical evaluation. They are also expressed as a function of the dimensionless "induction number," B, where

$$B = \frac{r}{\delta_1} \qquad (4.15)$$

and

$$\delta_1 = \left(\frac{2}{w\mu_o\sigma_{h,1}(0)}\right)^{1/2} \qquad (4.16)$$

by making the substitutions

$$\lambda = \frac{q}{\delta_1} \qquad (4.17)$$

and

$$d\lambda = \frac{1}{\delta_1}\, dg \ . \qquad (4.18)$$

To derive the kernel function for P(r), the integral expression for the half-space is subtracted under the integral sign and the analytical result is added back outside the integral sign. Thus

$$P(r) = \frac{iw\,\mu_o}{2\pi} \int_o^\infty \left(\frac{\lambda}{\lambda + iw\mu_o Y_1} - \frac{\lambda}{\lambda + u_1}\right) J_o(\lambda r)\, d\lambda$$

$$+ \frac{1}{2\pi\sigma_{h,1}(w)} \left(\frac{1}{r^3} - \frac{(1 + \gamma_1 r)e^{-\gamma_1 r}}{r^3}\right) . \qquad (4.19)$$

The first term of 4.19 is written as a function of B by substituting for λ and r. Combining terms in the integral and recognizing that

$$\frac{iw\,\mu_o}{2\pi} = \frac{1}{2\pi\sigma_{h,1}(0)} \cdot \frac{2i}{\delta_1^2} \quad , \tag{4.20}$$

the first term is written as

$$\frac{1}{2\pi\sigma_{h,1}(w)} \frac{2i}{\delta_1^3} \frac{\sigma_{h,1}(w)}{\sigma_{h,1}(0)} \int_o^\infty \frac{g u_1'(1-F_1)}{(g+u_1')\,(g+u_1' F_i)} J_o(gB)\, dg \tag{4.21}$$

where, using the notation of Kauanikaua and Anderson (1979), for an m layered earth

$$iw\,\mu_o\, Y_1 = u_1'\, F_1 \quad , \tag{4.22}$$

$$F_m = 1 \quad . \tag{4.23}$$

and F_1 is computed recursively from the bottom layer to the surface using

$$F_n = \frac{u_{n+1}'\, F_{n+1} + u_n'\, E_n}{u_n' + u_{n+1}'\, F_{n+1}\, E_n} \quad ; \qquad n = m-1 \text{ to } 1 \tag{4.24}$$

and

$$E_n = \frac{1 - e^{(-2\ u_n'\ d_n/\delta_1)}}{1 + e^{(-2\ u_n'\ d_n/\delta_1)}} \qquad (4.25)$$

where

$$u_n = \frac{1}{\delta_1}\left(g^2 + 2i\frac{\sigma_{h,n}(w)}{\sigma_{h,1}(0)}\right) = \frac{1}{\delta_1}\ u_n' \ . \qquad (4.26)$$

The complete expression for P(r) is then

$$P(r) = \frac{1}{2\pi\sigma_{h,1}(w)}\left(\frac{2i}{\delta_1^3}\frac{\sigma_{h,1}(w)}{\sigma_{h,1}(0)}\int_0^\infty \frac{g u_1'(1 - F_1)}{(g+u_1')(g+u_1'F_1)} J_o(gB)\ dg\right.$$

$$\left. + \left(\frac{1}{r^3} - \frac{(1 + \gamma_1 r)e^{-\gamma_1 r}}{r^3}\right)\right) \ . \qquad (4.27)$$

This result is different from that used by Kauahikaua and Anderson (1979) by the multiplicative factor of

$$\frac{\sigma_{h,1}(w)}{\sigma_{h,1}(0)} \qquad (4.28)$$

in the first term of the expression. My results agree with those of Kauahikaua and Anderson (1979) only when the first

layer has a strictly real resistivity. They apparently overlooked that δ_1 is defined to be real even when the first layer has a complex resistivity.

To derive the expression for Q(r), I follow a similar procedure. By adding and subtracting the expression for an isotropic half-space and then rearranging terms, Q(r) becomes

$$Q(r) = \frac{1}{2\pi\sigma_{h,1}(w)} \int_0^\infty \frac{\sigma_{h,1}(w)}{\lambda} \left(Z_1 - \frac{iw\,\mu_o}{\lambda + iw\,\mu_o Y_1} - \right.$$

$$\left. \frac{\lambda}{\sigma_{h,1}(w)} \right) J_o(\lambda r)\,d\lambda + \frac{1}{2\pi r \sigma_{h,1}(w)} \,. \qquad (4.29)$$

Then making substitutions for r, λ and $d\lambda$ and factoring out a -1 results in

$$Q(r) = \frac{-1}{2\pi\sigma_{h,1}(w)} \left(\int_0^\infty \frac{\sigma_{h,1}(w)}{\delta_1 g} \left(\frac{iw\,\mu_o\,\delta_1^2}{g + iw\,\mu_o Y_1} + \frac{g}{\sigma_{h,1}(w)} \right. \right.$$

$$\left. \left. - \delta_1 Z_1 \right) J_o(gB)\,dg - \frac{1}{r} \right) \,. \qquad (4.30)$$

Substituting

$$iw\,\mu_o\delta_1^2 = 2i\,\frac{1}{\sigma_{h,1}(0)} \tag{4.31}$$

$$iw\,\mu_o\delta_1 Y_1 = u_1' F_1 \tag{4.32}$$

and

$$\delta_1\sigma_{h,1}(w)\,Z_1 = v_1'\,L_1 \tag{4.33}$$

and multiplying inside and outside of the integral in Equation 4.30 by i and -i,

$$Q(r) = \frac{-1}{2\pi\sigma_{h,1}(w)}\left(\frac{i}{\delta_1}\int_o^\infty \frac{1}{g}\left(iv_1'L_1 - i\,g - i\,\frac{u_1'^2 - g^2}{q + u_1'F_1}\right)J_o(gB)\,dg\right.$$

$$\left. - \frac{1}{r}\right)\,. \tag{4.34}$$

For an m layered earth, F_1 is computed using Equations 4.22 to 4.26 and L_1 is computed recursively from the bottom layer to the surface using

$$L_m = 1.0 \tag{4.35}$$

$$L_n = \frac{\sigma_{h,n}(w)v_{n+1}'L_{n+1} + \sigma_{h,n+1}(w)v_n'E_n'}{\sigma_{h,n+1}(w)\,v_n' + \sigma_{h,n}(w)\,v_{n+1}'L_{n+1}E_n'}\,;$$

$$n = m-1 \text{ to } 1 \tag{4.36}$$

$$E_n' = \frac{1 - e^{(-2\, v_n' d_n/\delta_1)}}{1 + e^{(-2\, v_n' d_n/\delta_1)}} \qquad (4.37)$$

where

$$v_n = \frac{1}{\delta_1}(g^2 k_n^2 + 2\, i\, \frac{\sigma_{h,n}(w)}{\sigma_{h,1}(0)})^{1/2} = \frac{1}{\delta_1} v_n' \,. \qquad (4.38)$$

An equivalent form for the kernel would be

$$\frac{1}{g}\,(i\, v_1' L_1 - ig + \frac{2\,\frac{\sigma_{h,1}(w)}{\sigma_{h,1}(0)}}{g + u_1' F_1}) \,. \qquad (4.39)$$

To express the kernel in a form comparable to the isotropic kernel given by Kauahikaua and Anderson (1979), I add and subtract iv_1' to the kernel in 4.34, and after some re-arranging get

$$\frac{1}{g}\,(iv_1'(L_1 - 1) - \frac{i(u_1' - g)}{g + u_1' F_1} + i\,\frac{(v_1' - g)(v_1' + g)}{v_1' + g}) \,. \qquad (4.40)$$

Combining the second and third terms and again making the substitutions

$$-i(u_1'^2 - g^2) = 2\,\frac{\sigma_{h,1}(w)}{\sigma_{h,1}(0)} \qquad (4.41)$$

and

$$v_1'^2 - g^2 = (k_1^2 - 1)\,g^2 + 2i\,\frac{\sigma_{h,1}(w)}{\sigma_{h,1}(0)} \qquad (4.42)$$

I obtain

$$\frac{1}{g}\left(iv_1'(L_1 - 1) - \frac{2\,\frac{\sigma_{h,1}(w)}{\sigma_{h,1}(0)}\,(v_1' - u_1'F_1) + ig^2(k_1^2 - 1)(g + u_1'F_1)}{(g + u_1'F_1)(v_1' + g)}\right). \qquad (4.43)$$

If the first layer is nonpolarizable and all layers are isotropic, then $k_n^2 = 1$, $v_n' = u_n'$ and the isotropic case reduces to

$$\frac{1}{g}\left(iu_1'(L_1 - 1) + \frac{2\,u_1'(1 - F_1)}{(g + u_1'F_1)\,(g + u_1')}\right), \qquad (4.44)$$

Equation 4.44 is used by Kauahikaua and Anderson (1979) in EMCUPL. In the report accompanying the program, it is printed incorrectly on page 7 as

$$f7(g) = \frac{i\, u_1'(L_1 - 1)}{g} + \frac{2\, u_1'(1 - F_1)}{(g + u_1'F_1)(g + u_1')} \quad . \quad (4.45)$$

From Equation 3.106, the final form for computation is

$$\frac{V}{I} = -\left(\int_A^B dS \int_a^b ds \cos(e)\, P(r) \right.$$

$$\left. - (Q(r_{Ra}) + Q(r_{Bb}) - Q(r_{Ab}) - Q(r_{Ba})) \right). \quad (4.46)$$

This equation follows the sign convention of Millet (1967). In practice, for frequencies approaching dc, this produces a positive real component and zero phase for the collinear dipole-dipole array. This sign convention has not been followed by everyone, so one must be careful when comparing results of different workers. For example, Dey and Morrison (1973) have negative real values and 180 degree phase shifts for their low frequency results.

Numerical Results

To get numerical results for a general set of models, I have replaced the kernel functions for P(r) and Q(r) in a 1981 version of EMCUPL with those derived in this chapter. Initial tests indicated that to avoid underflow, some models required double precision calculations of the

kernels when the program was run on a 32-bit computer. Further testing revealed another minor problem in the computation of Q(r). In subroutine finqdf, the statement

```
260  q4=finq(del,r3,tol)
```

was changed to

```
260  q4=finq(del,r4,tol)
```

to give correct results for arbitrarily oriented wires. This statement was corrected in a 1984 revision of the program (Kauahikaua, 1989).

Calculations for electromagnetic coupling have been restricted to the dipole-dipole array, probably the most commonly used geometry for the routine field measurement of IP. The dipole-dipole array consists of equal length, collinear transmitting and receiving wires separated by a multiple of the dipole length. Length of the dipole is typically referred to as the "a-spacing," and separation of the transmitting and receiving wires is referred to as the "N spacing" or "N separation." Typically for any given receiver location, N spacing is varied from 1 to 6, providing both lateral and vertical investigation of the ground. Figure 4.1 illustrates the array geometry and the conventional pseudo-section representation of the data. As separation of the transmitter and receiver dipoles

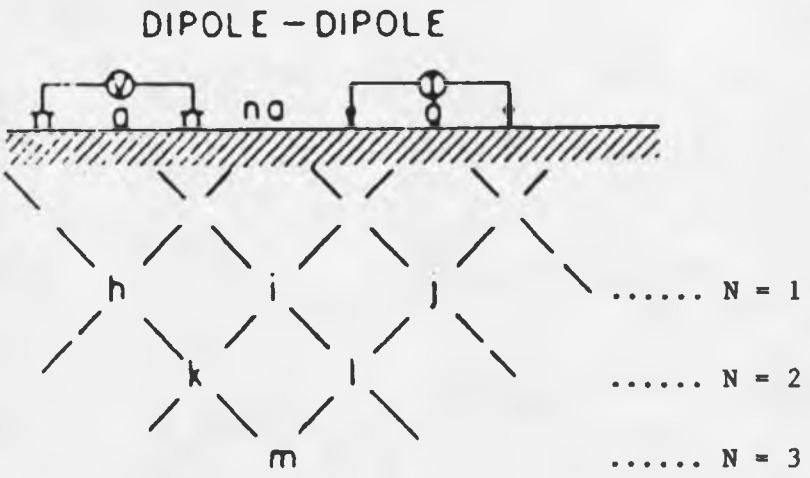

Figure 4.1. The field layout for a collinear dipole-dipole array and the pseudo-section representation of field data (after Sumner, 1976).

increases, measured voltage reflects deeper resistivity structure.

In the multi-frequency IP method, a common way of plotting field data is to normalize the real and imaginary components of the voltage by the real part of the lowest frequency then plot the data as a continuous curve in the complex plane. Figure 4.2 illustrates the complex plane plot and how other representations of the data such as the relative magnitude and phase of the received voltage can be determined from the plot. In this study, I have used the complex plane plot for all computed results.

Models with Real Resistivities

A set of models have been computed for a range of anisotropy values on a half-space with real resistivities. Figures 4.3a through 4.3i show the influence of varying the horizontal and vertical resistivity of the half-space. Results have been computed for a 100 meter dipole-dipole array at an N of 6 on a half-space with a constant mean conductivity of .01 mhos/meter. The ratio of horizontal to vertical conductivity, in this case a real quantity, has been varied between 25 and 1/25.

Figure 4.3a is the isotropic case where the ratio of horizontal to vertical is 1. Figures 4.3a-4.3d illustrate how increasing the horizontal conductivity affects the shape of the mutual impedance curve. Figures 4.3e-4.3i show the

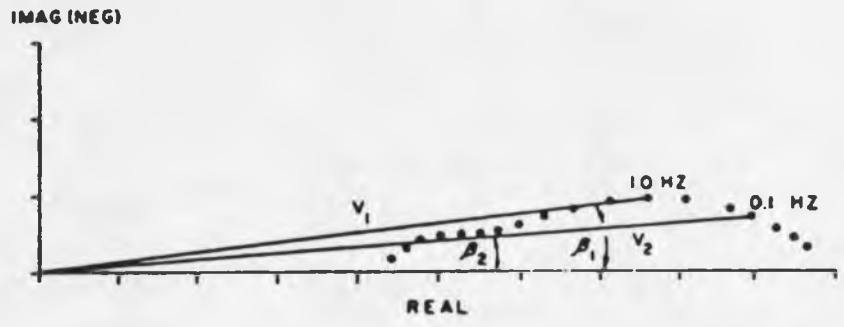

Figure 4.2. The complex plane plot of multi-frequency IP data. -- The normalized mutual impedance is plotted as data points defining a curve in the complex plane with frequency increasing to the left. The real part of the lowest frequency data has been used as the normalization factor (after Sumner, 1976).

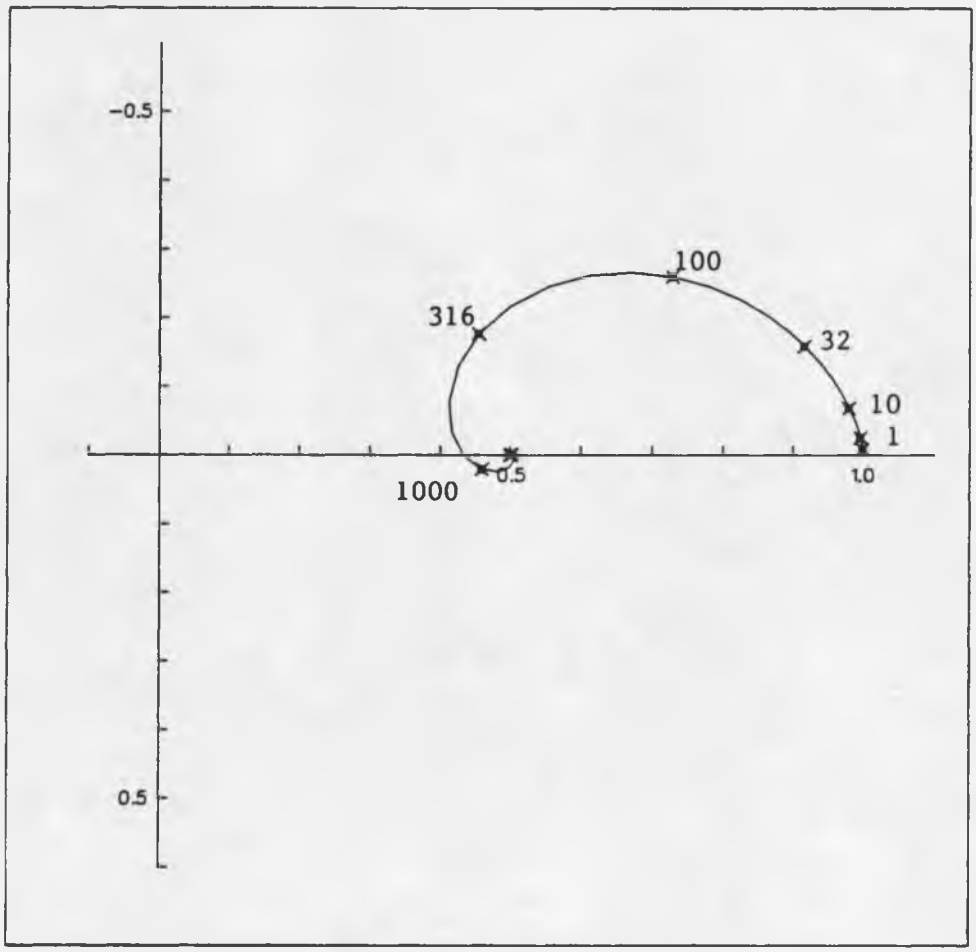

Figure 4.3a. Mutual impedance on a homogeneous, anisotropic half-space with real resistivities and a ratio of vertical to horizontal resistivity of 1.--Computed for a 100 meter dipole-dipole array at an N of 6 for frequencies between .001 and 10,000 Hertz. Half-space has a mean conductivity of .01 mhos/meter. Normalization factor is 947.4 x 10^{-6}.

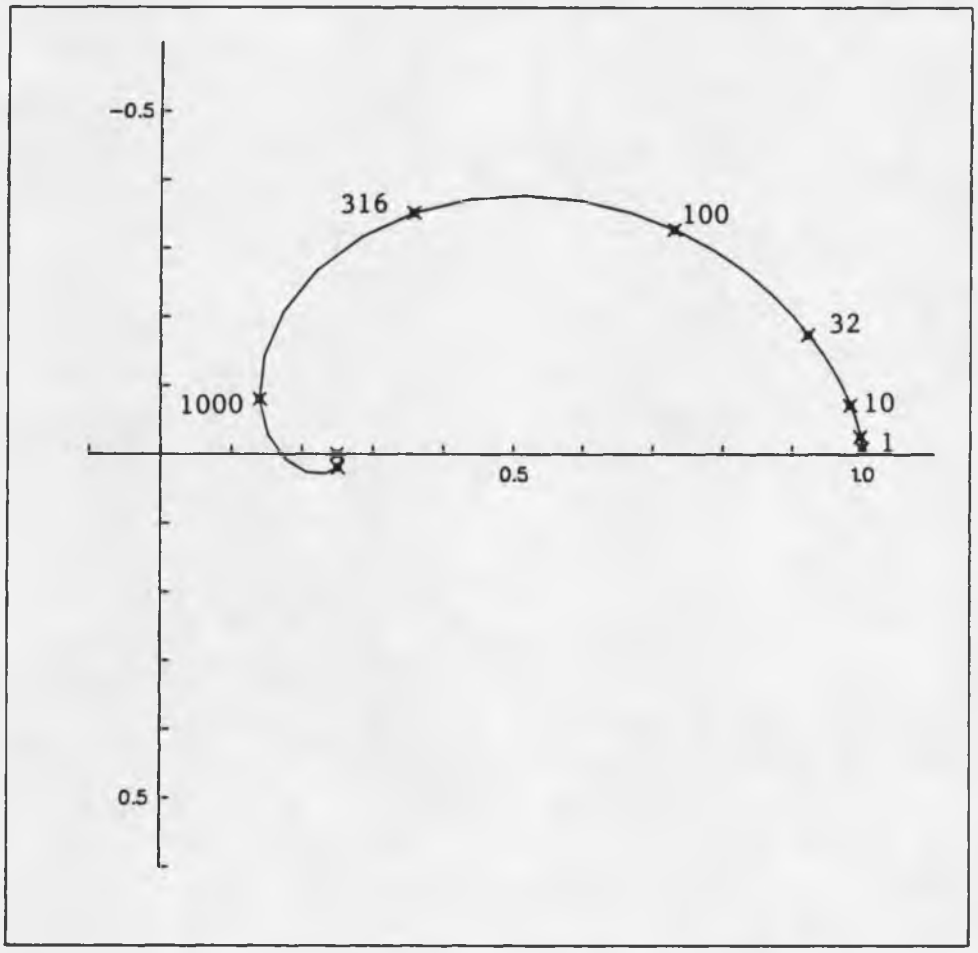

Figure 4.3b. Mutual impedance on a homogeneous, anisotropic half-space with real resistivities and a ratio of vertical to horizontal resistivity of 4.--Computed for a 100 meter dipole-dipole array at an N of 6 for frequencies between .001 and 10,000 Hertz. Half-space has a mean conductivity of .01 mhos/meter. Normalization factor is 947.4×10^{-6}.

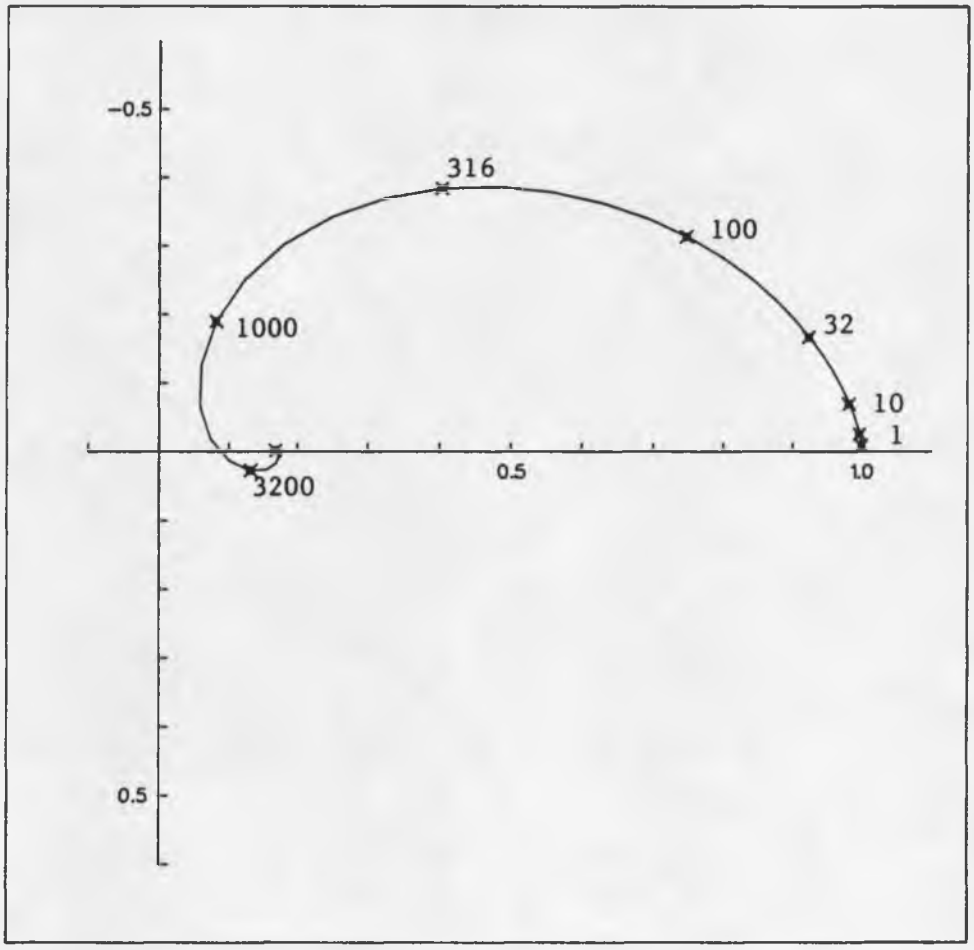

Figure 4.3c. Mutual impedance on a homogeneous, anisotropic half-space with real resistivities and a ratio of vertical to horizontal resistivity of 9.--Computed for a 100 meter dipole-dipole array at an N of 6 for frequencies between .001 and 10,000 Hertz. Half-space has a mean conductivity of .01 mhos/meter. Normalization factor is 947.4 x 10^{-6}.

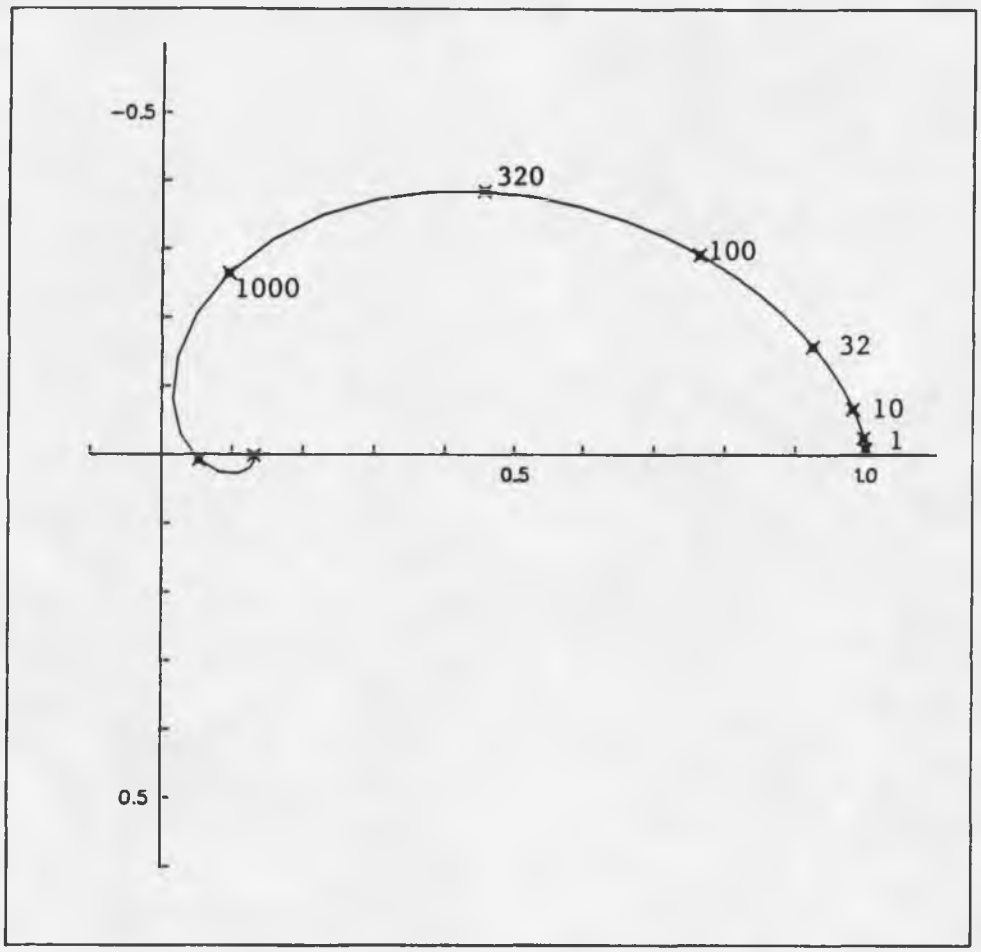

Figure 4.3d. Mutual impedance on a homogeneous, anisotropic half-space with real resistivities and a ratio of vertical to horizontal resistivity of 16. -- Computed for a 100 meter dipole-dipole array at an N of 6 for frequencies between .001 and 10,000 Hertz. Half-space has a mean conductivity of .01 mhos/meter. Normalization factor is 947.3×10^{-6}.

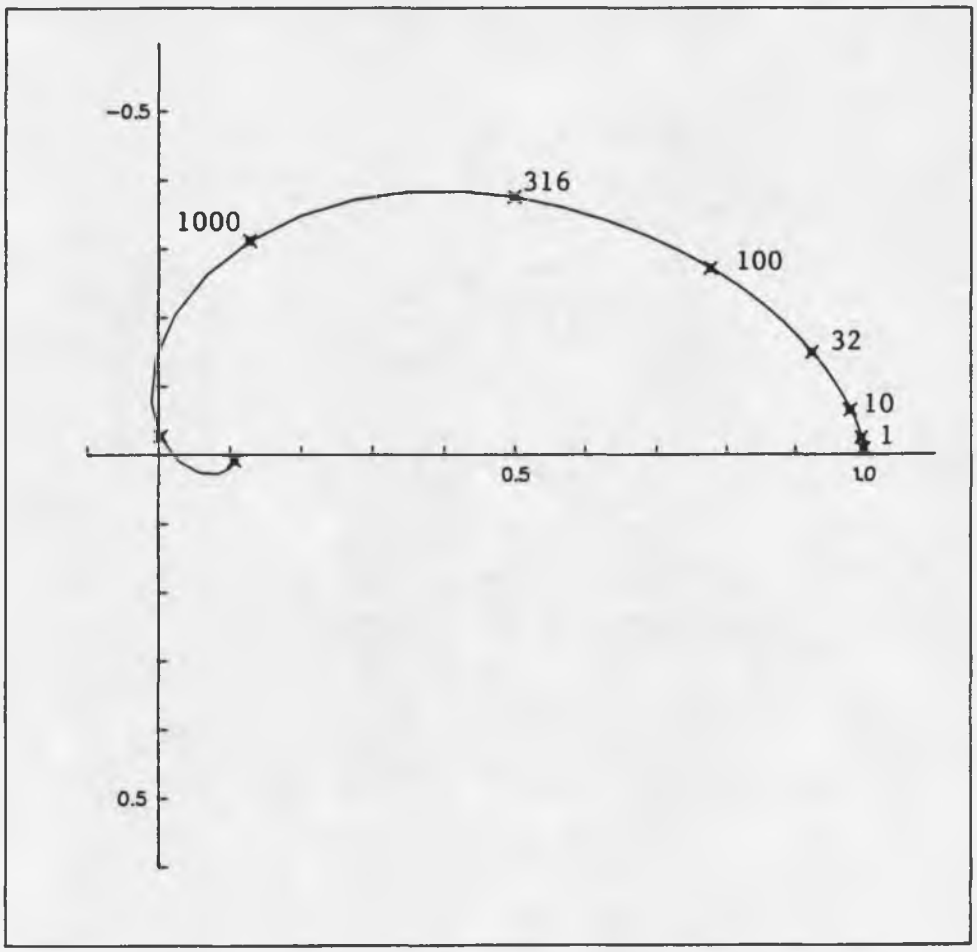

Figure 4.3e. Mutual impedance on a homogeneous, anisotropic half-space with real resistivities and a ratio of vertical to horizontal resistivity of 25. -- Computed for a 100 meter dipole-dipole array at an N of 6 for frequencies between .001 and 10,000 Hertz. Half-space has a mean conductivity of .01 mhos/meter. Normalization factor is 947.3×10^{-6}.

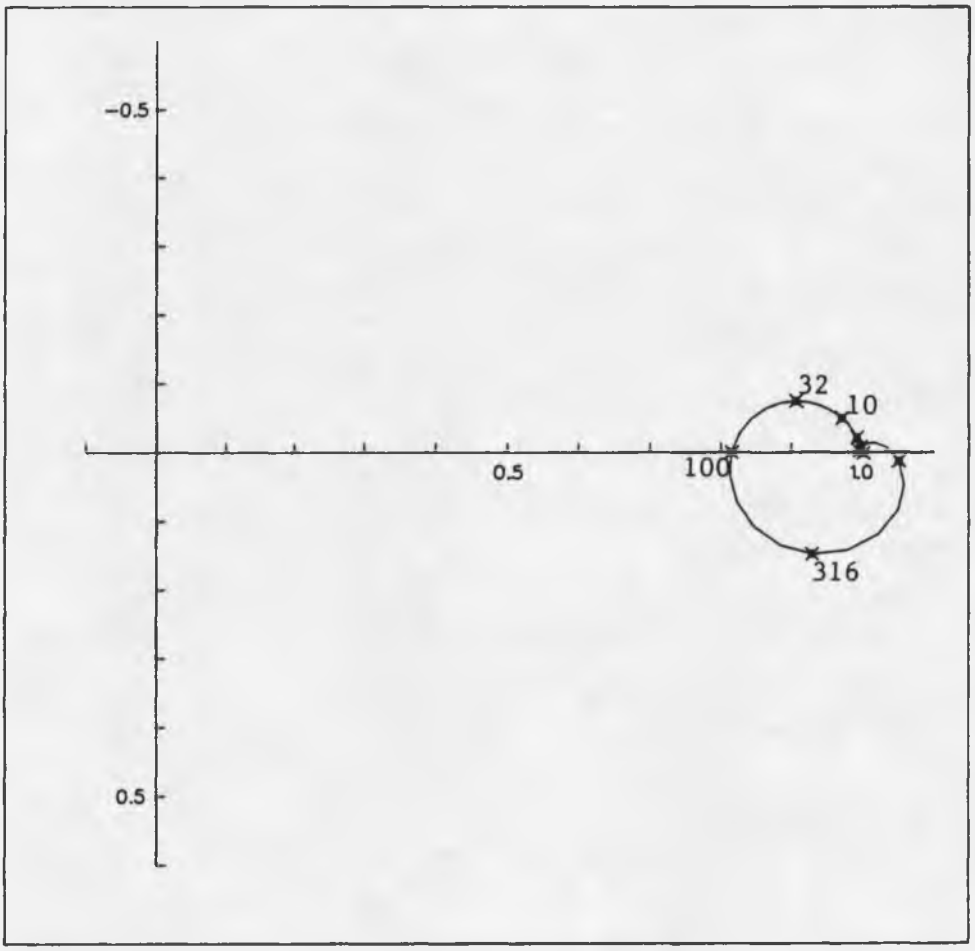

Figure 4.3f. Mutual impedance on a homogeneous, anisotropic half-space with real resistivities and a ratio of vertical to horizontal resistivity of .25. -- Computed for a 100 meter dipole-dipole array at an N of 6 for frequencies between .001 and 10,000 Hertz. Half-space has a mean conductivity of .01 mhos/meter. Normalization factor is 947.3×10^{-6}.

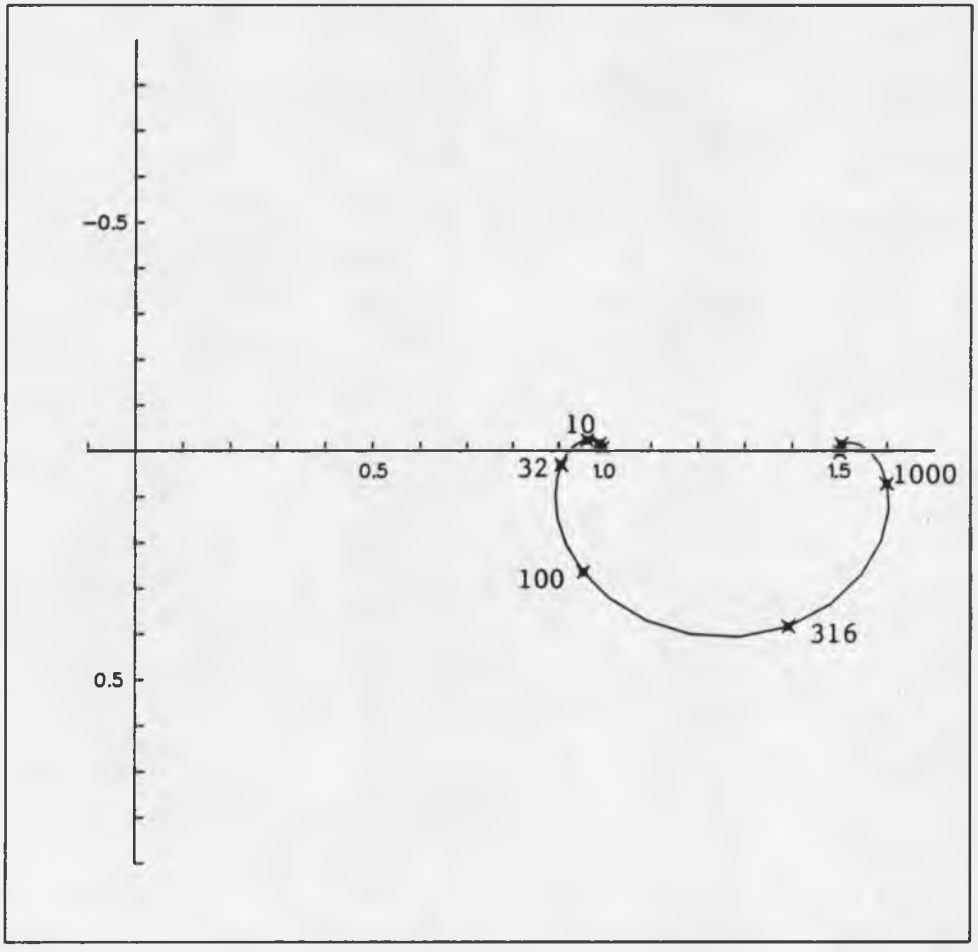

Figure 4.3g. Mutual impedance on a homogeneous, anisotropic half-space with real resistivities and a ratio of vertical to horizontal resistivity of .1111. -- Computed for a 100 meter dipole-dipole array at an N of 6 for frequencies between .001 and 10,000 Hertz. Half-space has a mean conductivity of .01 mhos/meter. Normalization factor is 947.4×10^{-6}.

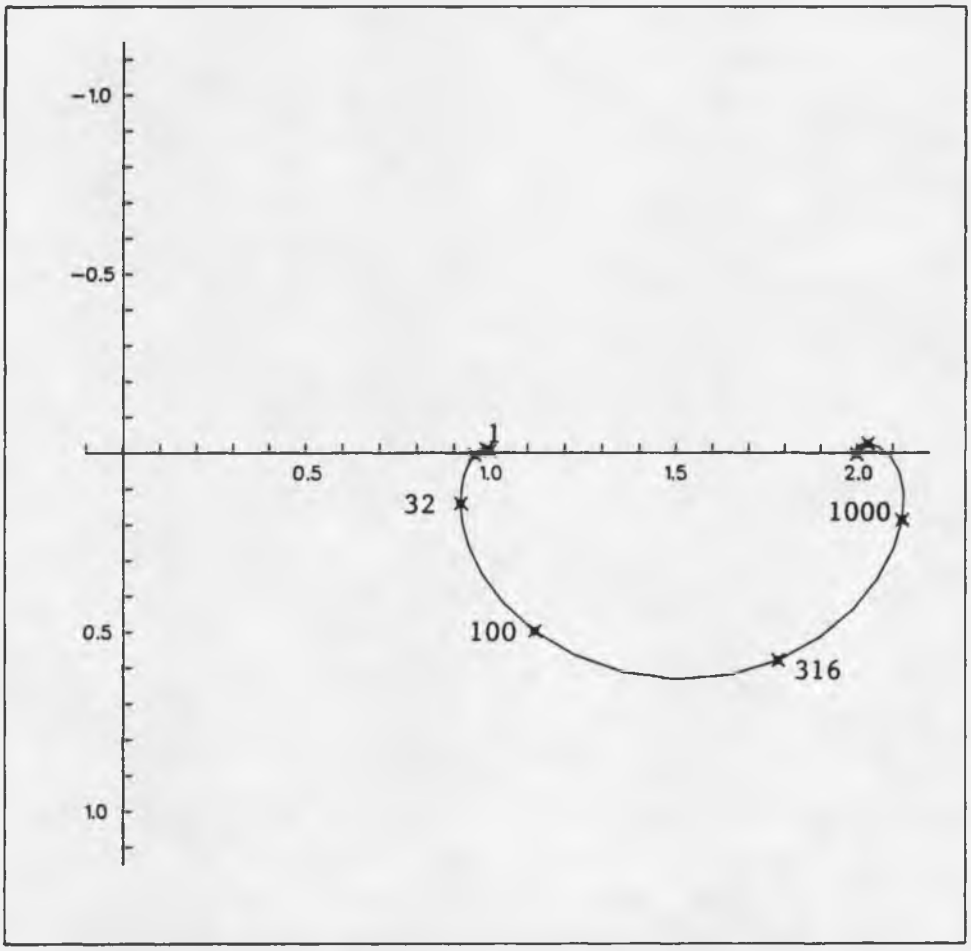

Figure 4.3h. Mutual impedance on a homogeneous, anisotropic half-space with real resistivities and a ratio of vertical to horizontal resistivity of .0625. -- Computed for a 100 meter dipole-dipole array at an N of 6 for frequencies between .001 and 10,000 Hertz. Half-space has a mean conductivity of .01 mhos/meter. Normalization factor is 947.4×10^{-6}.

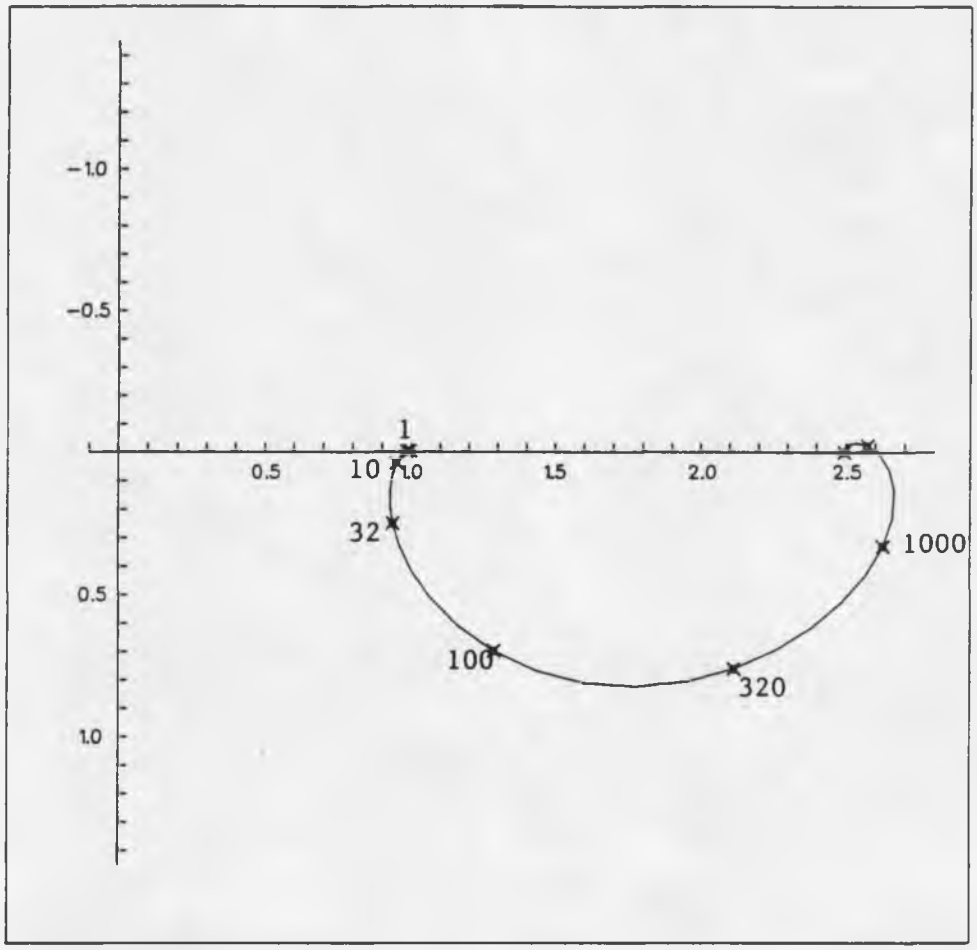

Figure 4.3i. Mutual impedance on a homogeneous, anisotropic half-space with real resistivities and a ratio of vertical to horizontal resistivity of .04. -- Computed for a 100 meter dipole-dipole array at an N of 6 for frequencies between .001 and 10,000 Hertz. Half-space has a mean conductivity of .01 mhos/meter. Normalization factor is 947.4×10^{-6}.

influence of increasing the vertical conductivity. Distinctly different results are found when the ratio is greater than or less than one. Increasing the horizontal conductivity has resulted in curves that plot in the first quadrant and have the same form as the isotropic half-space curve. At frequencies up to about 32 Hertz, values are very similar to the isotropic curve. But as the frequency is increased, quadrature component increases and the real part decreases compared to the isotropic case. The high frequency intercept with the real axis is shifted laterally toward the origin from the .5 intercept of the isotropic case. Visually, the curves appear to be stretched towards the origin.

When the ratio of horizontal to vertical is less than one, different curves result. The sign of the quadrature component changes at low frequency and curves plot almost entirely in the fourth quadrant. Another characteristic of the curves is that the real part goes through a minimum and increases beyond the value of one. Increasing anisotropy causes the value of the high frequency intersection with the real axis to increase.

In general, anisotropy appears to produce similar results to layering. Coupling curves associated with increased horizontal conductivity produce what has been commonly referred to as positive coupling (Hallof and

Pelton, 1980). Previously this effect has been observed as the result of a surface layer which is more conductive than the underlying strata. Physically, similarity of the two cases is that they both channel currents horizontally, and less current flows at depth than would for a homogeneous half-space.

The case of increased vertical conductivity produces what has been termed negative coupling (Hallof and Pelton, 1980) and has been previously attributed to a resistive surface layer over a more conductive subsurface. The physical similarity of the two cases is that they both channel currents deeper into the ground than the homogeneous half-space.

Interestingly, conventional sounding techniques on the same models as in Figure 4.3b-4.3i would only detect homogeneous, isotropic half-spaces. A dc resistivity sounding would only sense the constant mean conductivity of the half-space. A conventional EM sounding technique on these models would only detect horizontal conductivities and would indicate homogeneous isotropic half-spaces.

Comparisons with previous anisotropic results are for models computed by Wynn (1979). Figures 4.4 and 4.5 are for two-layer models with real resistivities. Both figures are for a 305 meter dipole-dipole array at an N of 3. Figure 4.4 is from Wynn's example 26, with a model consisting

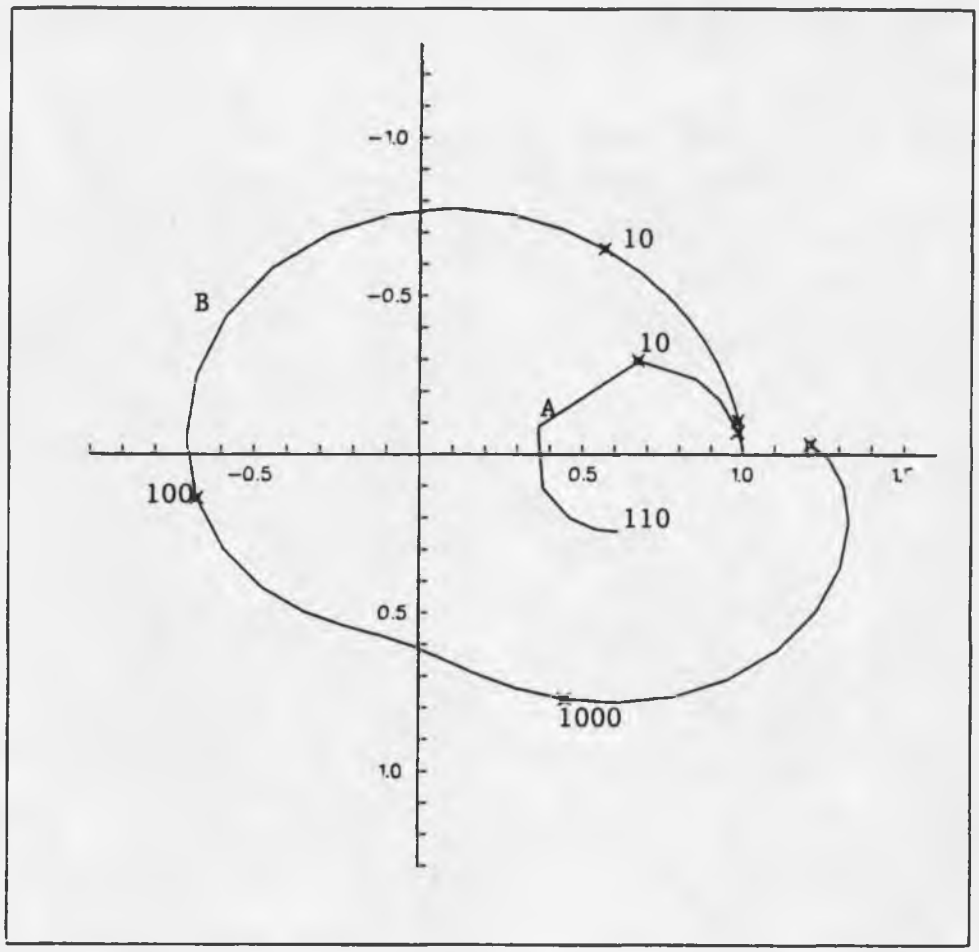

Figure 4.4. Comparison of results of this study with results of example 26 of Wynn (1979). -- EM coupling curve for a dipole-dipole array with a 305 meter dipole at an N spacing of 3 on a two-layer earth. The first layer is isotropic with a conductivity of .02 mhos/meter and a thickness of 61 meters. The second layer has a horizontal conductivity of .1 mhos/meter and a vertical conductivity of .02 mhos/meter. Curve A, Wynn (1979); Curve B, this study. Normalization factor is 395.6×10^{-6}.

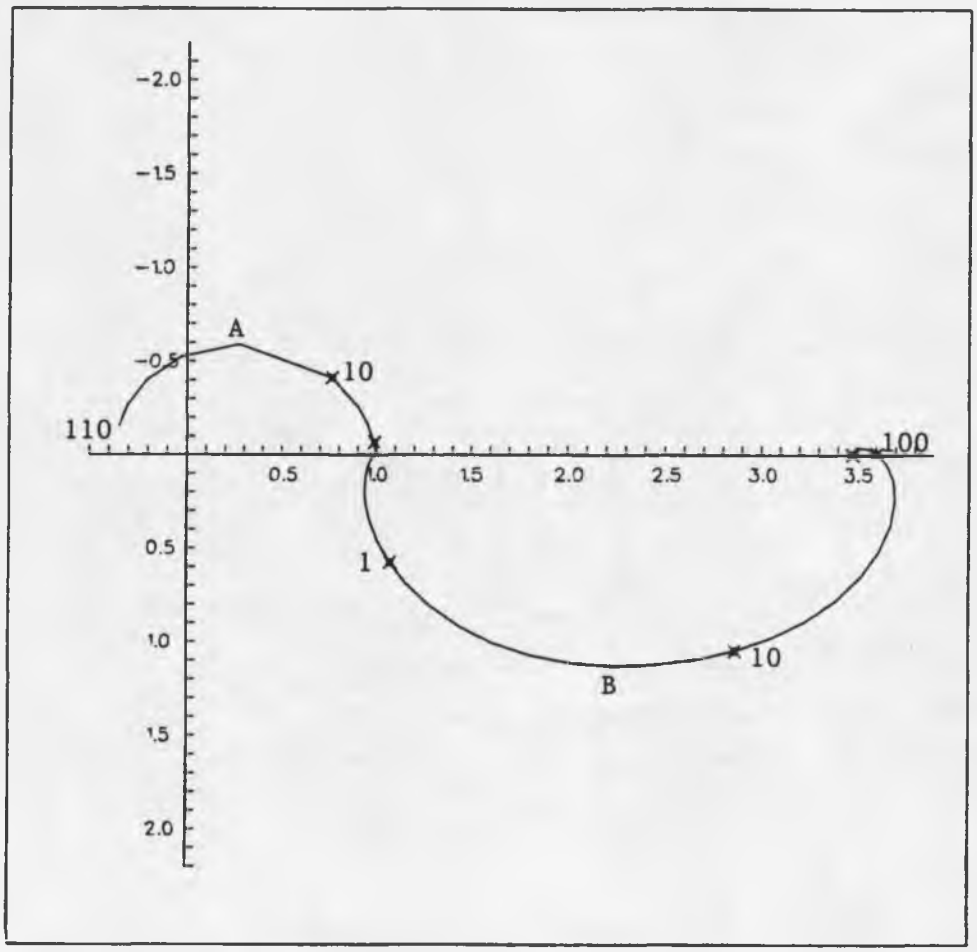

Figure 4.5. Comparison of the results of this study with results of example 28 of Wynn (1979). -- EM coupling curve for a dipole-dipole array with a 305 meter dipole at an N spacing of 3 on a two-layer earth. The first layer is isotropic with a conductivity of .02 mhos/meter and a thickness of 61 meters. The second layer has a horizontal conductivity of .02 mhos/meter and a vertical conductivity of 1 mhos/meter. Curve A, Wynn (1979); Curve B, this study. Normalization factor is 125.5×10^{-6}.

of a 61 meter thick 50 ohm-meter surface layer over a second layer that has a horizontal resistivity of 10 ohm-meters and a vertical resistivity of 50. In this model the second layer has a mean conductivity of 22.3 ohm-meters and an anisotropy ratio $k^2 = 5$. As a consequence, the curve is expected to have components of both a horizontally conductive half-space and also a two layer case with a high resistivity over a low resistivity. In my results, at low frequency, the array is seeing the properties of the second layer and responding to its increased horizontal conductivity. As frequency is increased, currents flow closer to the surface and mutual impedance responds to the high-over-low resistivity layering, causing a reversal in sign of the quadrature component and an increase in the real component. Wynn's results, plotted for reference on the figure, are quite different.

Figure 4.5 is a comparison with Wynn's (1979) example 28. The second layer has a horizontal resistivity of 50 ohm-m and a vertical resistivity of 1 ohm-meter. Thus the second layer has a mean conductivity of 7.1 ohm-meters and a $k^2 = 1/50$. The two-layer case has both increased vertical conductivity and a high-over-low resistivity layering. These effects combine to produce a coupling curve that plots entirely in the fourth quadrant.

Models with Complex Resistivities

The remaining models have been computed using complex resistivities. The form chosen for the complex resistivity is the Cole-Cole model (Pelton et al., 1978) discussed in Chapter 2. The expression for resistivity as a function of frequency is

$$\rho(w) = R\left(1 - m\left(1 - \frac{1}{1 + (iw\ t_o)^c}\right)\right) \qquad (4.47)$$

The model has four parameters: R, m, t_o and c. The R value is the dc resistivity term. The m value is the chargeability, t_o is time constant, and c is referred to as the frequency dependence. Through laboratory and in-situ measurements, parameters for the model can be related to typical mineralized environments (Pelton et al., 1978).

In Figures 4.6a-4.6i, I have plotted mutual coupling curves for an anisotropic half-space with horizontal and vertical resistivity functions represented by Cole-Cole resistivity functions. Cole-Cole parameters were chosen to be intermediate in the range of values for porphry-copper mineralization. The mean dc resistivity term was chosen to be 100 ohm-meters, m was set at .30, t_o at 1.0, and c at .50. Based on Figure 6 of Pelton et al. (1978), these values would be related to about 5 to 10 volume percent sulphides with grain sizes of about 5 to 10 mm. Since the

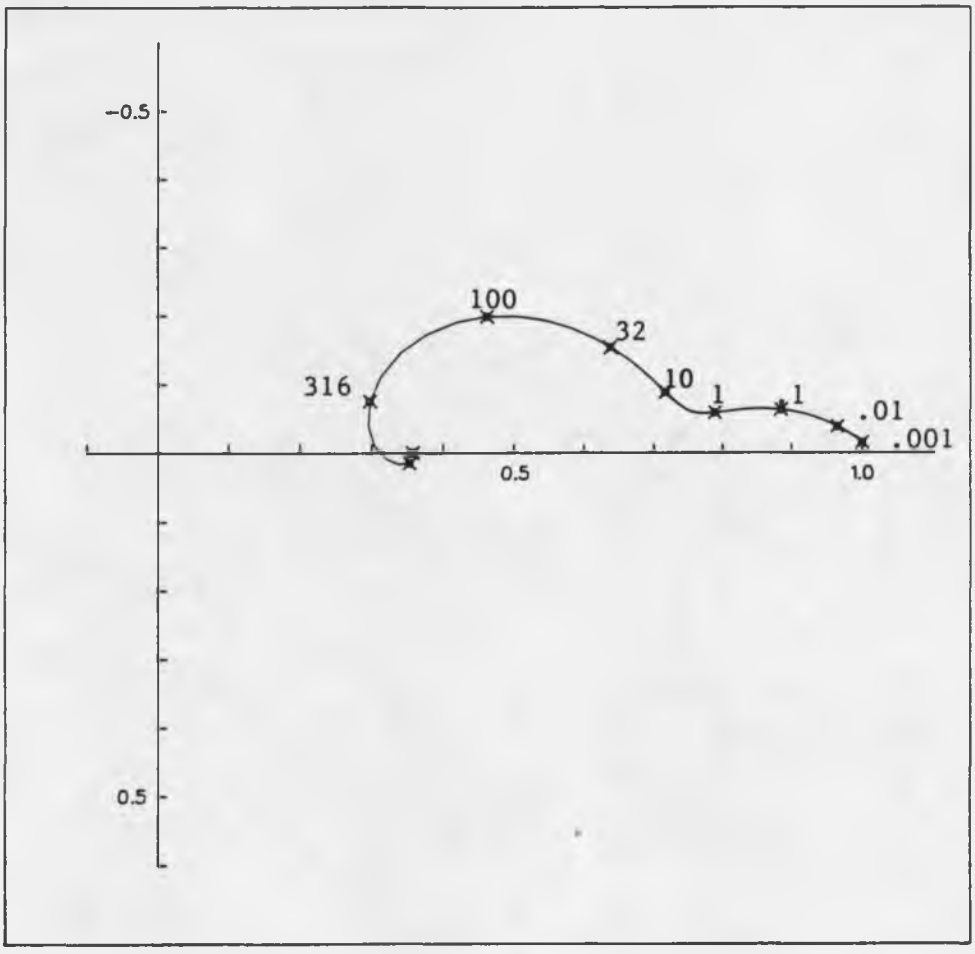

Figure 4.6a. Mutual impedance on a homogeneous, anisotropic half-space with Cole-Cole resistivities and a ratio of vertical to horizontal R of 1.-- Computed for a 100 meter dipole-dipole array at an N of 6 for frequencies between .001 and 10,000 Hertz. The mean dc conductivity is .01 mhos/m. For horizontal and vertical resistivities, m = .30, t_o = 1.0, c = .5. Normalization factor is 931.5 x 10^{-6}.

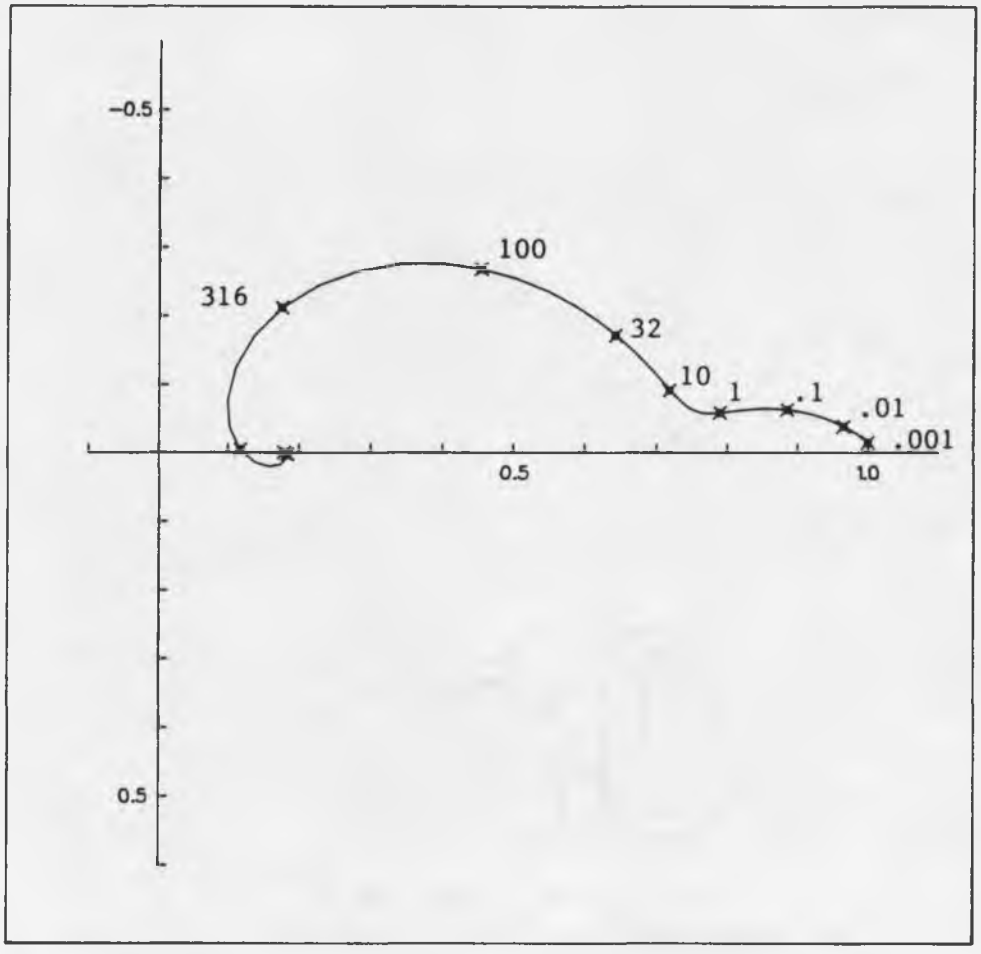

Figure 4.6b. Mutual impedance on a homogeneous, anisotropic half-space with Cole-Cole resistivities and a ratio of vertical to horizontal R of 4.-- Computed for a 100 meter dipole-dipole array at an N of 6 for frequencies between .001 and 10,000 Hertz. The mean dc conductivity is .01 mhos/m. For horizontal and vertical resistivities, m = .30, t_o = 1.0, c = .5. Normalization factor is 931.5 x 10^{-6}.

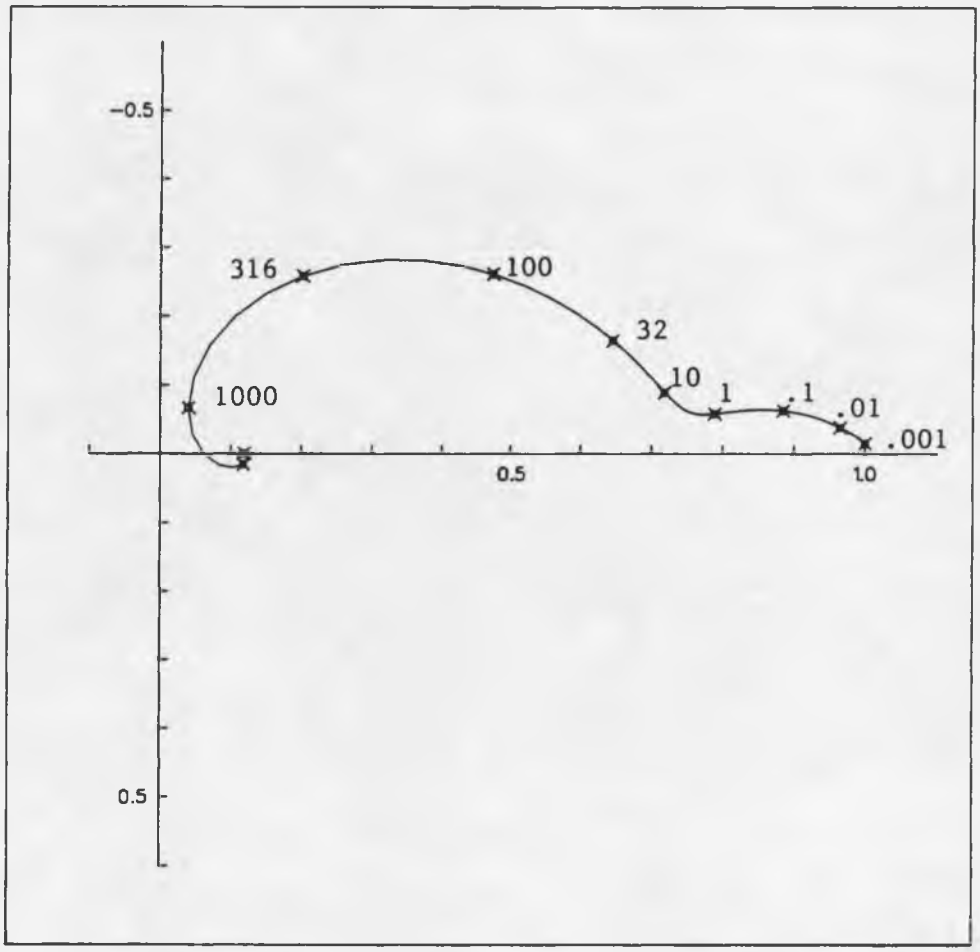

Figure 4.6c. Mutual impedance on a homogeneous, anisotropic half-space with Cole-Cole resistivities and a ratio of vertical to horizontal R of 9.--Computed for a 100 meter dipole-dipole array at an N of 6 for frequencies between .001 and 10,000 Hertz. The mean dc conductivity is .01 mhos/m. For horizontal and vertical resistivities, m = .30, t_o = 1.0, c = .5. Normalization factor is 931.5 x 10^{-6}.

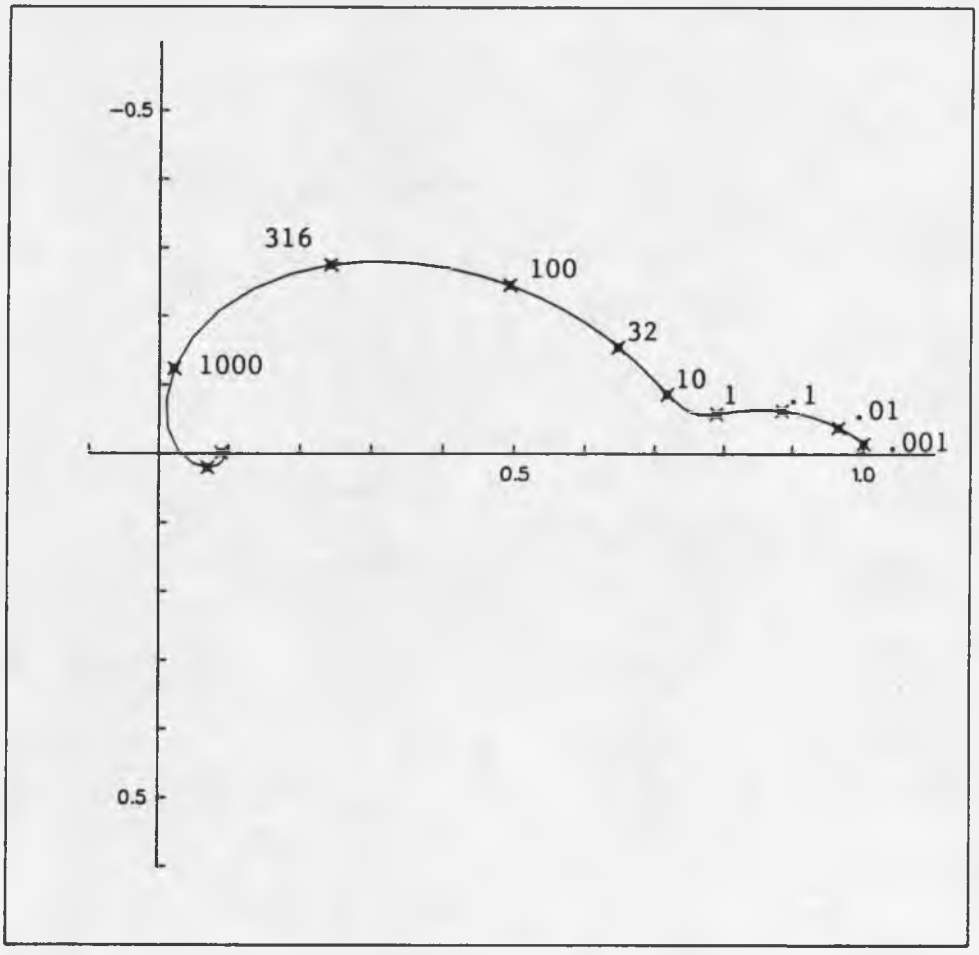

Figure 4.6d. Mutual impedance on a homogeneous, anisotropic half-space with Cole-Cole resistivities and a ratio of vertical to horizontal R of 16.--Computed for a 100 meter dipole-dipole array at an N of 6 for frequencies between .001 and 10,000 Hertz. The mean dc conductivity is .01 mhos/m. For horizontal and vertical resistivities, m = .30, t_o = 1.0, c = .5. Normalization factor is 931.6 x 10^{-6}.

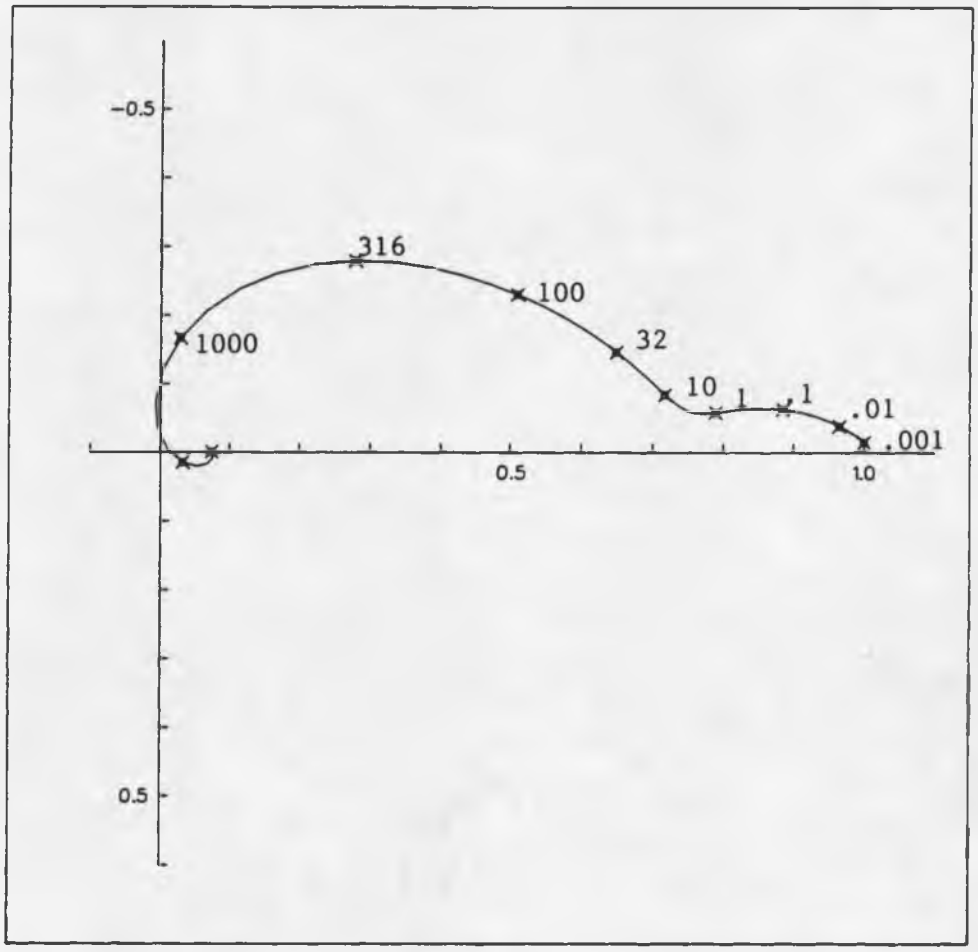

Figure 4.6e. Mutual impedance on a homogeneous, anisotropic half-space with Cole-Cole resistivities and a ratio of vertical to horizontal R of 25.--Computed for a 100 meter dipole-dipole array at an N of 6 for frequencies between .001 and 10,000 Hertz. The mean dc conductivity is .01 mhos/m. For horizontal and vertical resistivities, m = .30, t_o = 1.0, c = .5. Normalization factor is 931.5 x 10^{-6}.

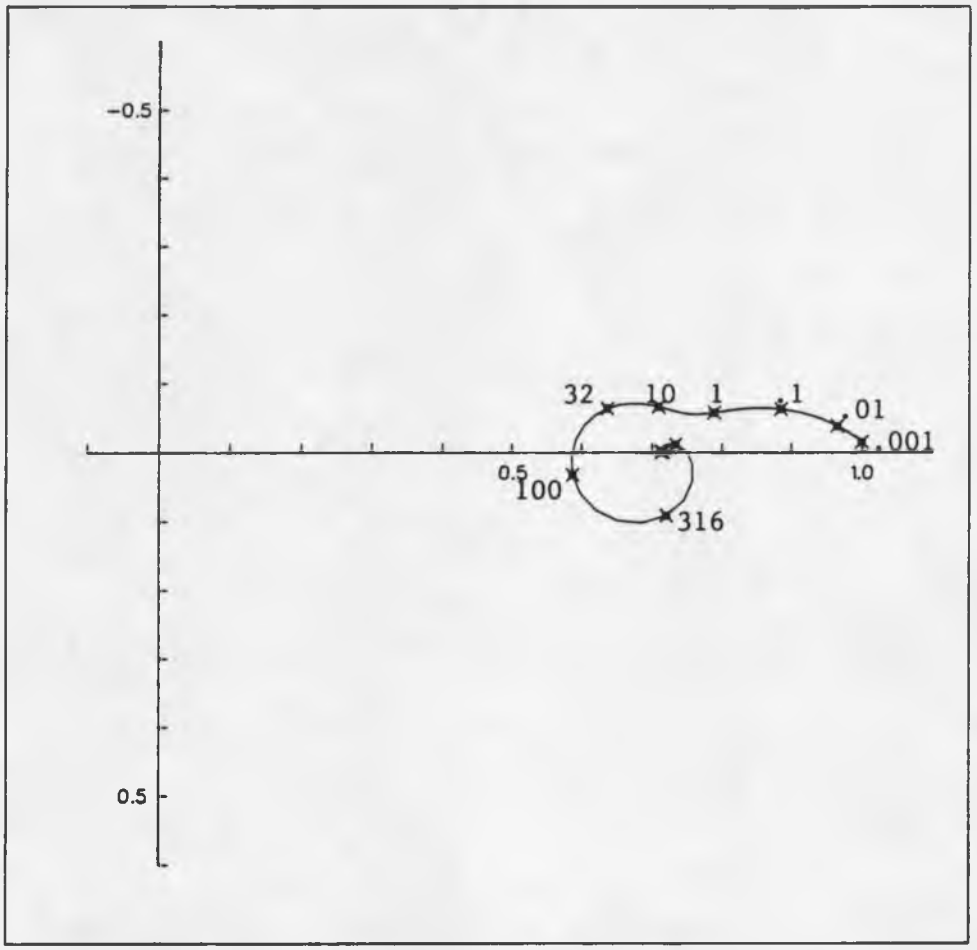

Figure 4.6f. Mutual impedance on a homogeneous, anisotropic half-space with Cole-Cole resistivities and a ratio of vertical to horizontal R of .25.--Computed for a 100 meter dipole-dipole array at an N of 6 for frequencies between .001 and 10,000 Hertz. The mean dc conductivity is .01 mhos/m. For horizontal and vertical resistivities, m = .30, t_o = 1.0, c = .5. Normalization factor is 931.5 x 10^{-6}.

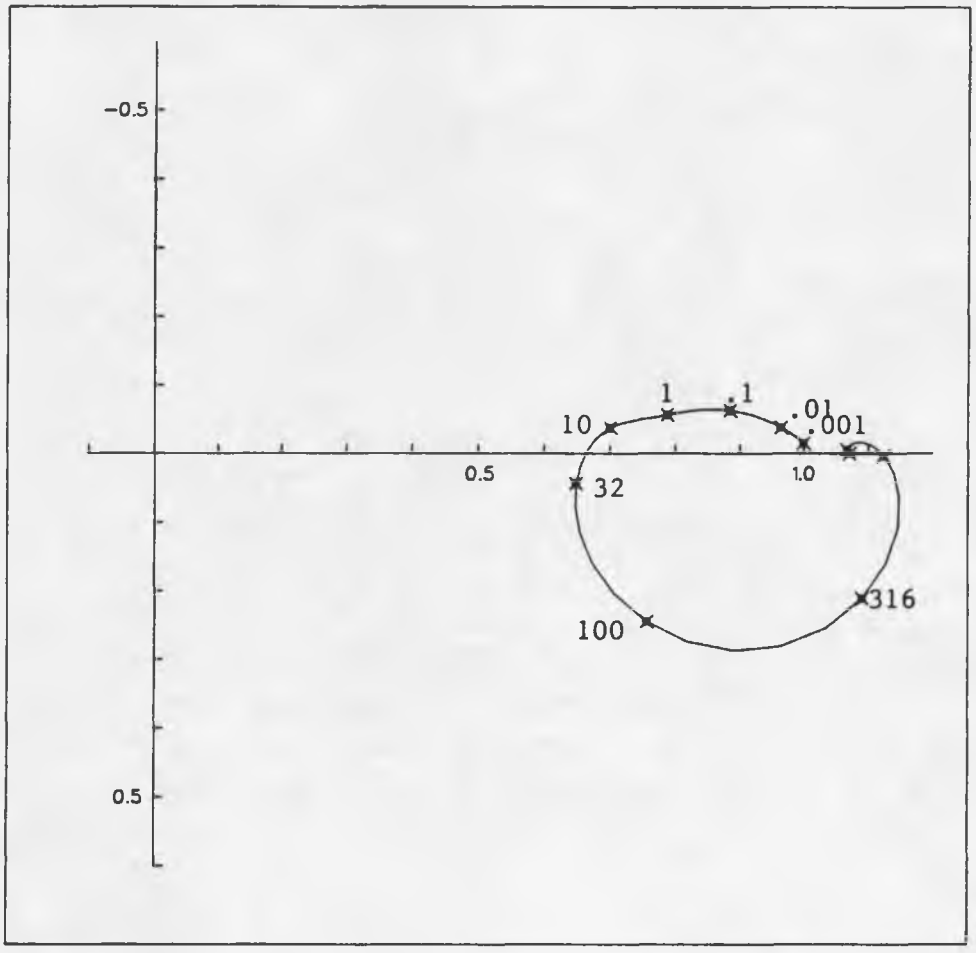

Figure 4.6g. Mutual impedance on a homogeneous, anisotropic half-space with Cole-Cole resistivities and a ratio of vertical to horizontal R of .1111.-- Computed for a 100 meter dipole-dipole array at an N of 6 for frequencies between .001 and 10,000 Hertz. The mean dc conductivity is .01 mhos/m. For horizontal and vertical resistivities, m = .30, t_o = 1.0, c = .5. Normalization factor is 931.5 x 10^{-6}.

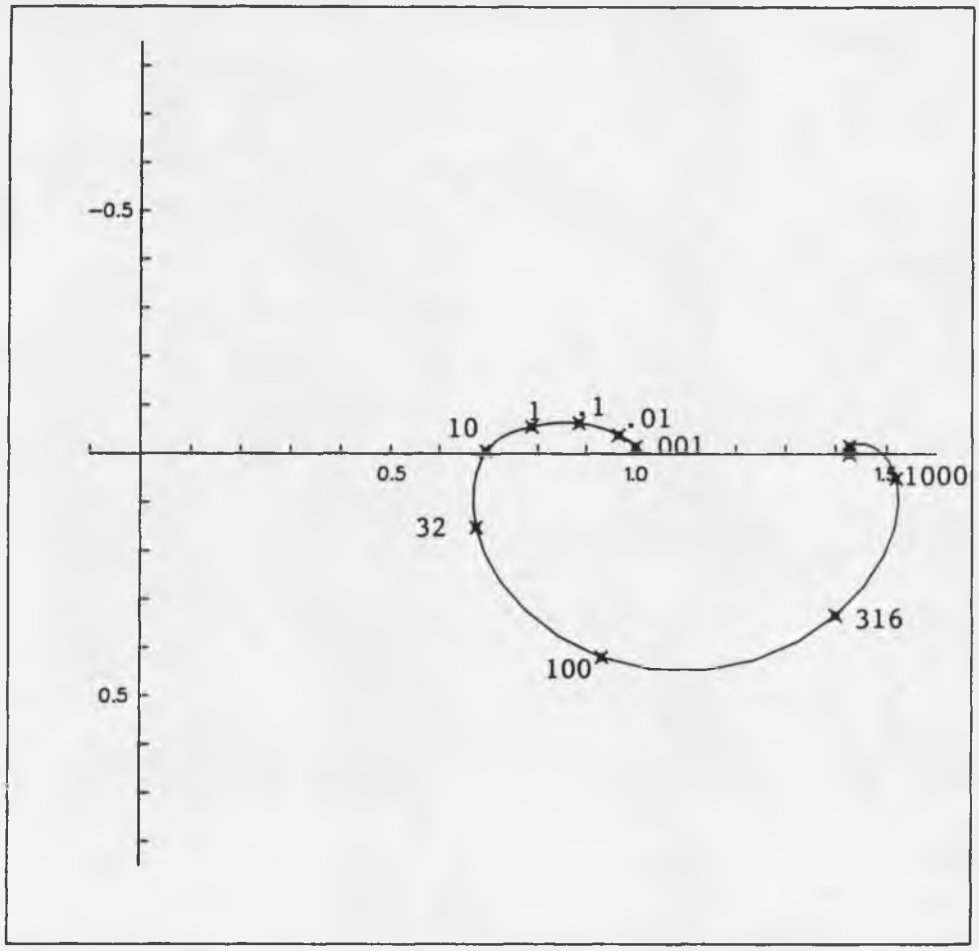

Figure 4.6h. Mutual impedance on a homogeneous, anisotropic half-space with Cole-Cole resistivities and a ratio of vertical to horizontal R of .0625.--Computed for a 100 meter dipole-dipole array at an N of 6 for frequencies between .001 and 10,000 Hertz. The mean dc conductivity is .01 mhos/m. For horizontal and vertical resistivities, m = .30, t_o = 1.0, c = .5. Normalization factor is 931.5 x 10^{-6}.

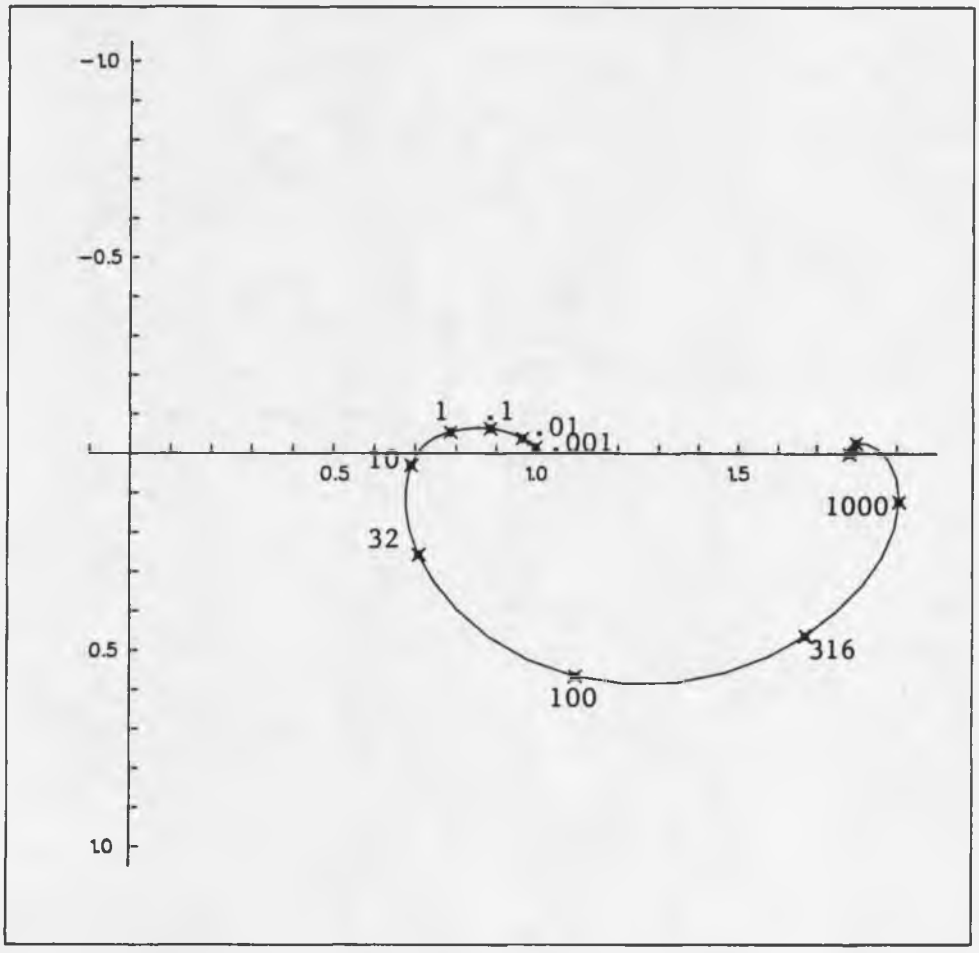

Figure 4.6i. Mutual impedance on a homogeneous, anisotropic half-space with Cole-Cole resistivities and a ratio of vertical to horizontal R of .04.--Computed for a 100 meter dipole-dipole array at an N of 6 for frequencies between .001 and 10,000 Hertz. The mean dc conductivity is .01 mhos/m. For horizontal and vertical resistivities, m = .30, t_o = 1.0, c = .5. Normalization factor is 931.5 x 10^{-6}.

half-space has independent horizontal and vertical complex resistivities, k^2 (the ratio of horizontal to vertical conductivities) is now complex.

Only horizontal and vertical values for the parameter R have been varied in Figures 4.6a-4.6i. The curves are quite similar to those calculated for real resistivities except that they have both a low frequency arc that corresponds to the IP effect and a high frequency response that is related to the EM coupling effect. The form and sign of the EM response is similar to the corresponding real case, but curves have been shifted towards the origin.

IP and EM effects are well separated, due largely to choice of the time constant, t_o. With t_o equal to 1.0 for horizontal and vertical Cole-Cole resistivities, the IP phase peak occurs at frequencies below 1 Hertz, where EM induction effects are negligible. If a smaller time constant had been chosen, the phase peak would be shifted to a higher frequency where separate IP- and EM-dominated responses would not be so readily visible.

EM effects start in the range of 3 to 10 Hertz and dominate the higher frequencies. One interesting effect is the second arc-like feature in Figure 4.6f between 10 and 100 Hertz. This feature is not related to the IP response but is only the effect of the interaction of the electromagnetic field with the anisotropy.

Other parameters in the Cole-Cole resistivity model can be varied instead of the dc resistivity term. Figures 4.7a and 4.7b show the effect of varying the horizontal and vertical m while holding other parameters constant. Figure 4.7a shows the effect of increasing the m in the horizontal resistivity function by a factor of two and decreasing m in the vertical resistivity function by a factor of two. Figure 4.7b shows the opposite situation, with the vertical m increased with respect to the horizontal m.

At frequencies up to about 10 Hertz, mutual impedance is dominated by the Q(r) function, which is responding to the geometric mean of the horizontal and vertical resistivities. Whether horizontal or vertical m is increased makes no difference, and the response is identical for both cases. When compared to the isotropic case in Figure 4.6a, the arc representing the IP response has flattened and the quadrature component has increased. The gentler slope for the low-frequency arc shows that the effective frequency dependence, c, is decreased by the anisotropy.

At higher frequencies where EM effects dominate, varying m has a similar influence as varying the resistivity. This should not be surprising since R and m occur as a product in the Cole-Cole function. Increasing the horizontal m value and decreasing the vertical m value causes a rising curve on Figure 4.7a between 10 and 100

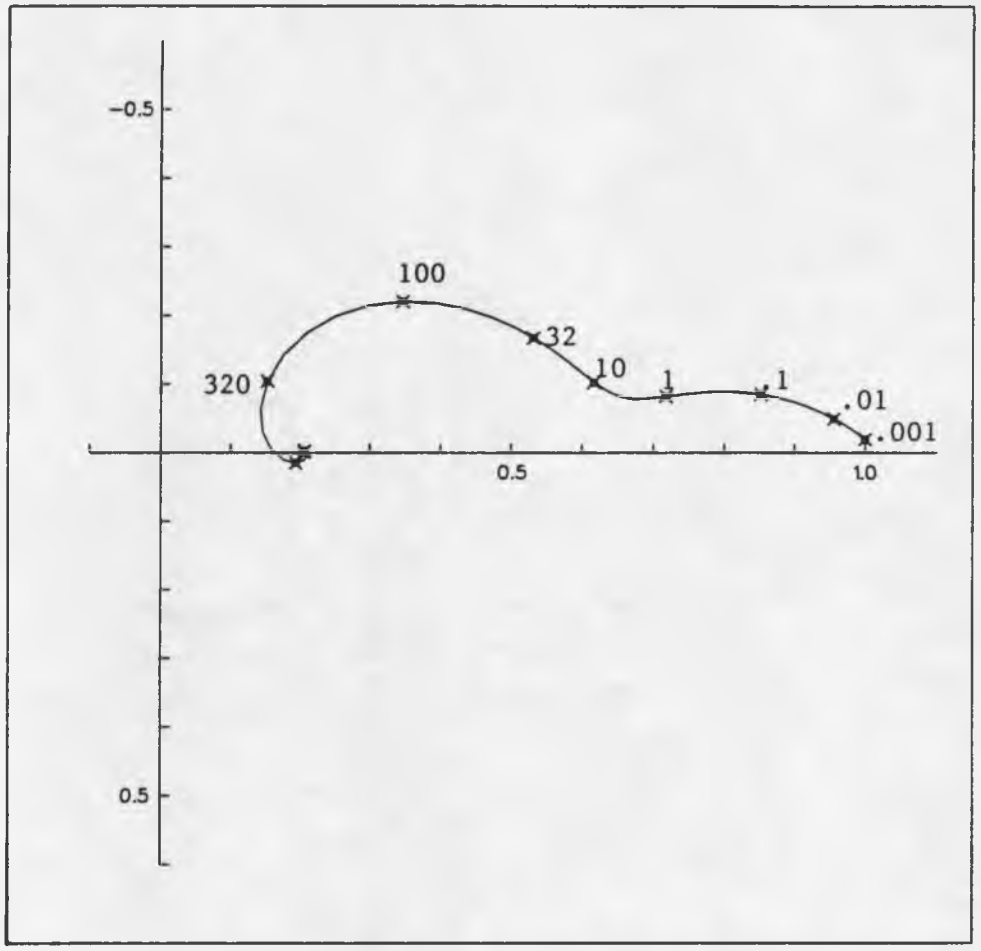

Figure 4.7a. Mutual impedance on a homogeneous, anisotropic half-space with Cole-Cole resistivities. Horizontal m = .60 and vertical m = .15.--Computed for a 100 meter dipole-dipole array at an N of 6 for frequencies between .001 and 10,000 Hertz. The horizontal and vertical resistivities have R = 100 ohm-m; t_o = 1.0, and c = .5. Normalization factor is 927.5 x 10^{-6}.

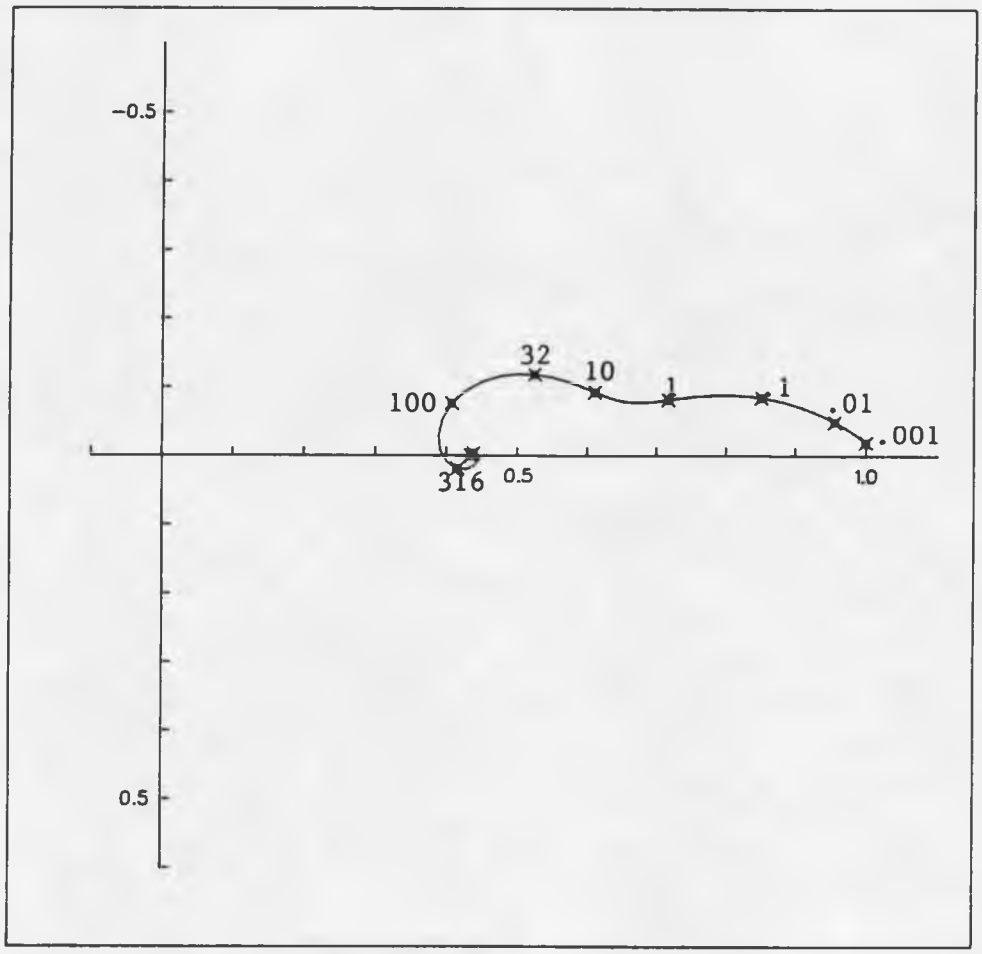

Figure 4.7b. Mutual impedance on a homogeneous, anisotropic half-space with Cole-Cole resistivities. Horizontal m = .15 and vertical m = .60.-- Computed for a 100 meter dipole-dipole array at an N of 6 for frequencies between .001 and 10,000 Hertz. The horizontal and vertical resistivities have R = 100 ohm-m; t_o = 1.0, and c = .5. Normalization factor is 927.5 x 10^{-6}.

Hertz. The curve in Figure 4.7b between 10 and 100 Hertz looks like the curve in Figure 4.6f where the ratio of the vertical to horizontal resistivity is 4. Two phase peaks occur between dc and 100 Hertz, but the IP response is not significant above 3 Hertz. The phase peak at about 32 Hertz is from EM coupling.

Increasing the horizontal t_o and decreasing the vertical by factors of 2, the same as was done for m, and had no noticeable effect on the normalized curve in the complex plane at either the high or low frequency. Coupling curves behaved the same as the complex, isotropic case. No figures were made to illustrate this since all curves appear the same as in Figure 4.6a. The mutual impedance is relatively insensitive to anisotropy related to the time constant. Much larger variations in the horizontal and vertical t are required to make a noticeable difference.

Figures 4.8a-4.8e, 4.9a- 4.9e and 4.10a-4.10e illustrate the increasing complexity that can be introduced by placing a layer over the half-space. In this study, I have chosen the first layer to have a thickness equal to the dipole length. It is isotropic and weakly polarizable, with Cole-Cole parameters of m = .1, t_o = .1, and c = .5. According to Figure 6 of Pelton et al. (1978), this can be empirically related to about 2 percent by volume sulphides with a grain size of 3 to 5 mm. The second layer always has

an isotropic m = .3, t_o = 1 and c = .5. The ratio of horizontal to vertical R is varied in the second layer.

Figures 4.8a-4.8e are for the case of a 100-meter-thick, 500 ohm-meter overburden over an anisotropic half-space. The calculations have been made with a 100 meter dipole-dipole array at an N spacing of 6. As a general rule, it is assumed that at an N of 6, the depth of investigation is approximately one and a half to two dipole lengths.

The coupling curves have characteristics of both the high over low resistivity layering and the anisotropy of the second layer. At low frequency, the IP response is quite similar to that calculated for a half-space with the properties of the second layer. The coupling curves are largely responding to the anisotropy of the second layer between 10 and 1000 Hertz. With a resistive overburden at low frequency, enough current flows in the second layer to influence the field measured on the surface. However, as the frequency is increased, the current flows closer to the surface and the electromagnetic fields respond more to the resistive surface layer. For curves associated with increased horizontal conductivity (Figures 4.8b and 4.8c), the imaginary part reaches a relative maximum between 100 and 1000 Hertz, then decreases steadily, changing sign at about 1000 Hertz

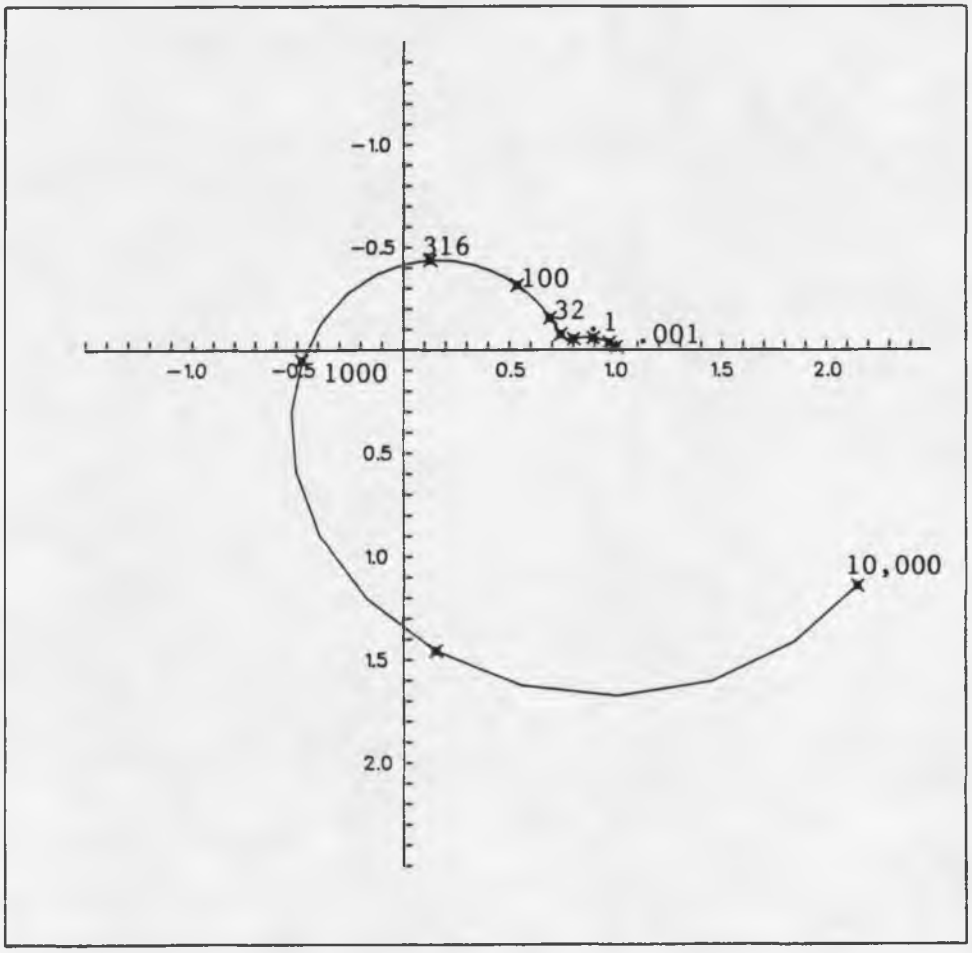

Figure 4.8a. Mutual impedance on a two-layer earth with Cole-Cole resistivities. First layer dc resistivity is 500 ohm-m. Second layer has a ratio of vertical to horizontal resistivity of 1. -- Computed for a 100 meter dipole-dipole array at an N of 6 for frequencies between .001 and 10,000 Hertz. The first layer is isotropic, with m = .10, t_o = .1, and c = .5. The second layer has a mean dc resistivity of 100 ohm-m and horizontal and vertical m = .3, t_o = 1.0, and c = .5. Normalization factor is 1116 x 10^{-6}.

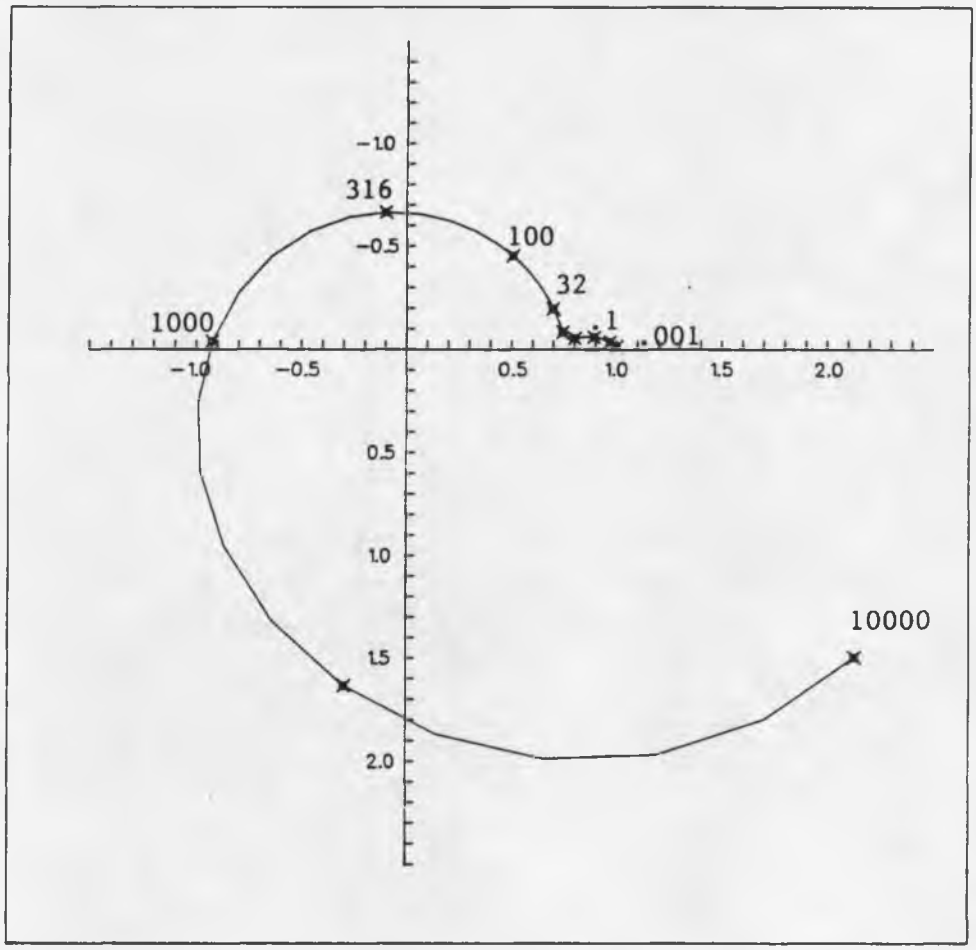

Figure 4.8b. Mutual impedance on a two-layer earth with Cole-Cole resistivities. First layer dc resistivity is 500 ohm-m. Second layer has a ratio of vertical to horizontal resistivity of 4. -- Computed for a 100 meter dipole-dipole array at an N of 6 for frequencies between .001 and 10,000 Hertz. The first layer is isotropic, with m = .10, t_o = .1, and c = .5. The second layer has a mean dc resistivity of 100 ohm-m and horizontal and vertical m = .3, t_o = 1.0, and c = .5. Normalization factor is 1116 x 10^{-6}.

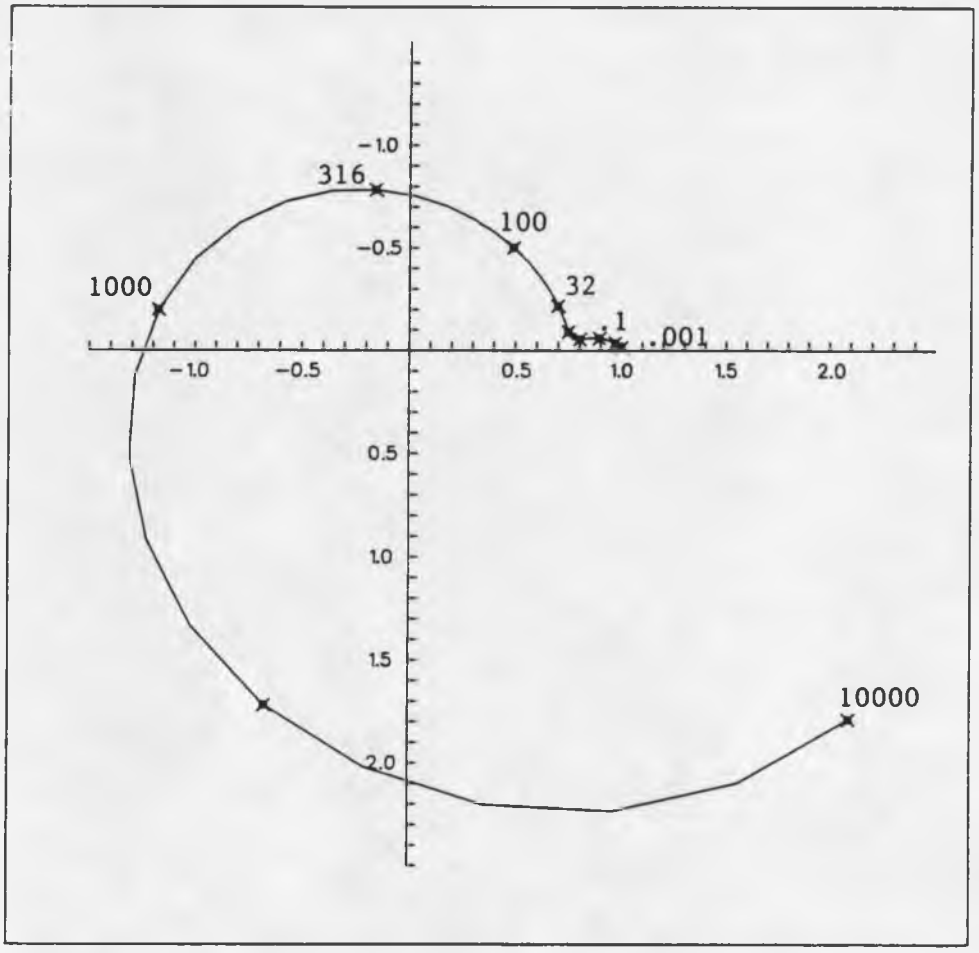

Figure 4.8c. Mutual impedance on a two-layer earth with Cole-Cole resistivities. First layer dc resistivity is 500 ohm-m. Second layer has a ratio of vertical to horizontal resistivity of 16. -- Computed for a 100 meter dipole-dipole array at an N of 6 for frequencies between .001 and 10,000 Hertz. The first layer is isotropic, with m = .10, t_o = .1, and c = .5. The second layer has a mean dc resistivity of 100 ohm-m and horizontal and vertical m = .3, t_o = 1.0, and c = .5. Normalization factor is 1116 x 10^{-6}.

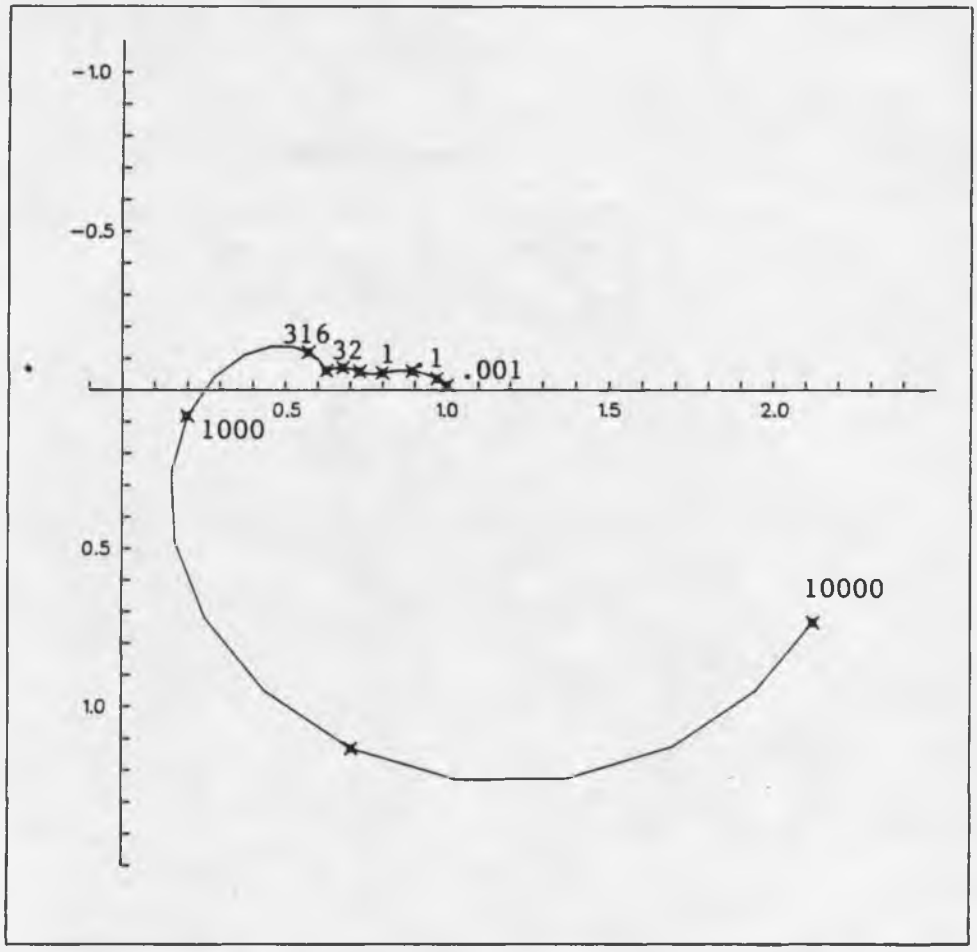

Figure 4.8d. Mutual impedance on a two-layer earth with Cole-Cole resistivities. First layer dc resistivity is 500 ohm-m. Second layer has a ratio of vertical to horizontal resistivity of .25. -- Computed for a 100 meter dipole-dipole array at an N of 6 for frequencies between .001 and 10,000 Hertz. The first layer is isotropic, with m = .10, t_o = .1, and c = .5. The second layer has a mean dc resistivity of 100 ohm-m and horizontal and vertical m = .3, t_o = 1.0, and c = .5. Normalization factor is 1116 x 10^{-6}.

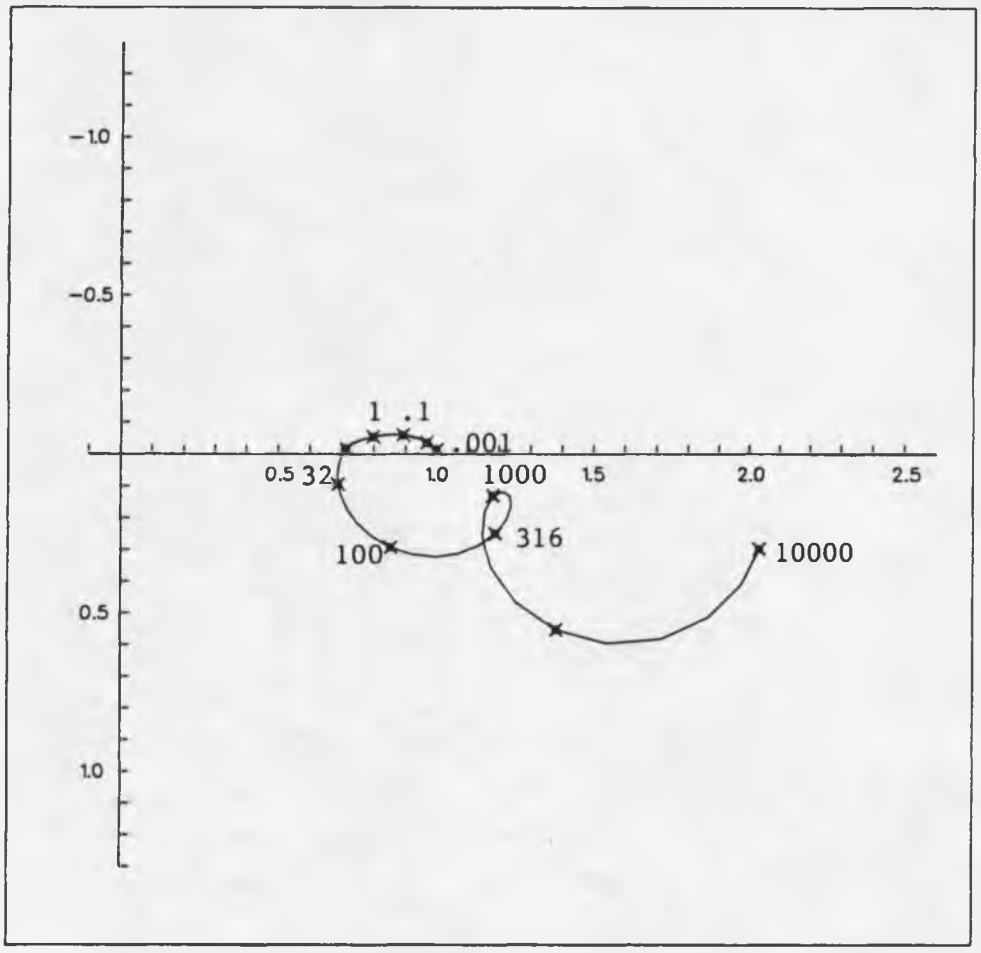

Figure 4.8e. Mutual impedance on a two-layer earth with Cole-Cole resistivities. First layer dc resistivity is 500 ohm-m. Second layer has a ratio of vertical to horizontal resistivity of .0625. -- Computed for a 100 meter dipole-dipole array at an N of 6 for frequencies between .001 and 10,000 Hertz. The first layer is isotropic, with m = .10, t_o = .1, and c = .5. The second layer has a mean dc resistivity of 100 ohm-m and horizontal and vertical m = .3, t_o = 1.0, and c = .5. Normalization factor is 1116 x 10^{-6}.

and tracking through the third and fourth quadrant of the complex plane.

For the models with increased vertical conductivity in Figures 4.8d and 4.8e, both the anisotropy of the second layer and the layering contribute to the negative coupling effects in the curves. An interesting feature is the closed loop in the frequency range of 100 to 3200 Hertz on Figure 4.8e. This is apparently the result of the contrast between the first and second layer. This feature would most likely show up as a notch in a field survey where sampling may not be sufficiently dense to fully detail the curve. Notching was also noted by Wynn (1979) in his models.

In Figures 4.9a-4.9e I have changed the first layer dc resistivity term to 50 ohm-meters. This represents a case where the overburden is slightly more conductive than the bedrock. The curves are as expected for the cases of an isotropic second layer and second layers with increased horizontal conductivity. The major changes occur in Figures 4.9d and 4.9e. Figure 4.9d develops a second arc-like feature between 1 and 100 Hertz, with a peak at about 32 Hertz. A notch develops at 100 Hertz, then a positive coupling curve follows.

On Figure 4.9e, results are even more spectacular. A closed loop develops between about 1 and 200 Hertz. A

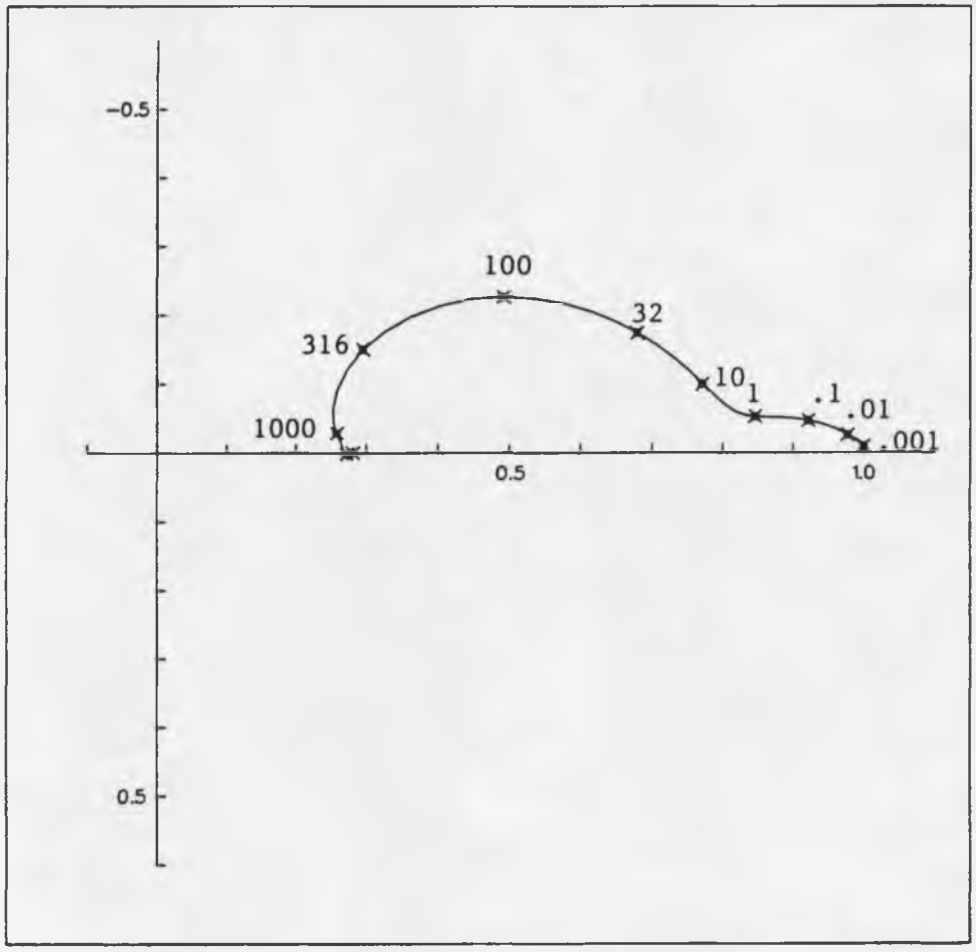

Figure 4.9a. Mutual impedance on a two-layer earth with Cole-Cole resistivities. First layer dc resistivity is 50 ohm-m. Second layer has a ratio of vertical to horizontal resistivity of 1. -- Computed for a 100 meter dipole-dipole array at an N of 6 for frequencies between .001 and 10,000 Hertz. The first layer is isotropic, with m = .10, t_o = .1, and c = .5. The second layer has a mean dc resistivity of 100 ohm-m and horizontal and vertical m = .3, t_o = 1.0, and c = .5. Normalization factor is 761 x 10^{-6}.

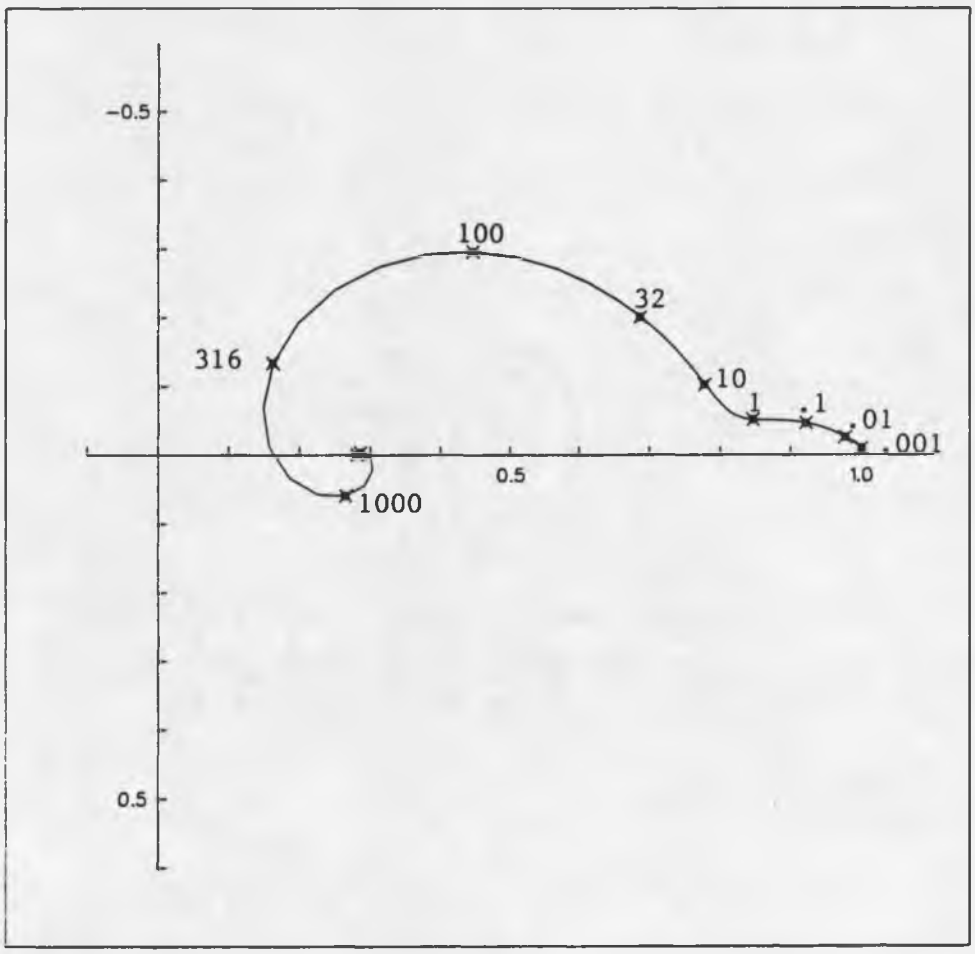

Figure 4.9b. Mutual impedance on a two-layer earth with Cole-Cole resistivities. First layer dc resistivity is 50 ohm-m. Second layer has a ratio of vertical to horizontal resistivity of 4. -- Computed for a 100 meter dipole-dipole array at an N of 6 for frequencies between .001 and 10,000 Hertz. The first layer is isotropic, with m = .10, t_o = .1, and c = .5. The second layer has a mean dc resistivity of 100 ohm-m and horizontal and vertical m = .3, t_o = 1.0, and c = .5. Normalization factor is 761 x 10^{-6}.

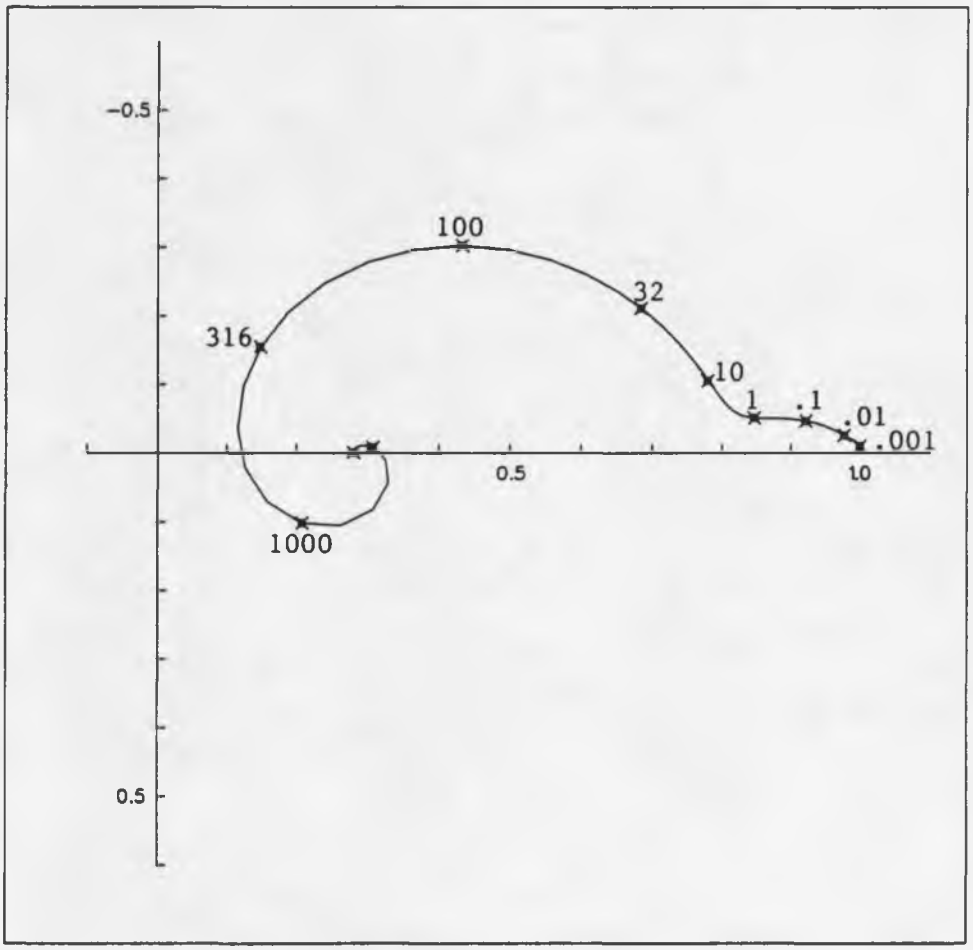

Figure 4.9c. Mutual impedance on a two-layer earth with Cole-Cole resistivities. First layer dc resistivity is 50 ohm-m. Second layer has a ratio of vertical to horizontal resistivity of 16. -- Computed for a 100 meter dipole-dipole array at an N of 6 for frequencies between .001 and 10,000 Hertz. The first layer is isotropic, with m = .10, t_o = .1, and c = .5. The second layer has a mean dc resistivity of 100 ohm-m and horizontal and vertical m = .3, t_o = 1.0, and c = .5. Normalization factor is 761 x 10^{-6}.

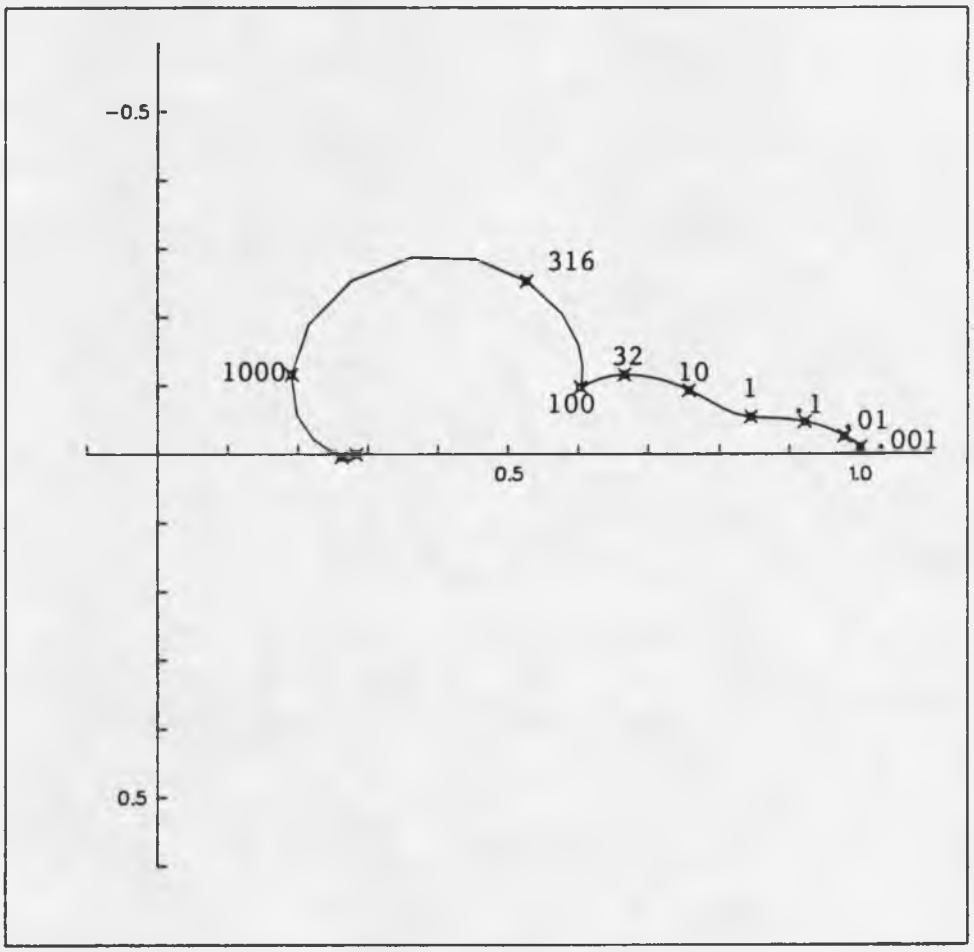

Figure 4.9d. Mutual impedance on a two-layer earth with Cole-Cole resistivities. First layer dc resistivity is 50 ohm-m. Second layer has a ratio of vertical to horizontal resistivity of .25. -- Computed for a 100 meter dipole-dipole array at an N of 6 for frequencies between .001 and 10,000 Hertz. The first layer is isotropic, with m = .10, t_o = .1, and c = .5. The second layer has a mean dc resistivity of 100 ohm-m and horizontal and vertical m = .3, t_o = 1.0, and c = .5. Normalization factor is 761 x 10^{-6}.

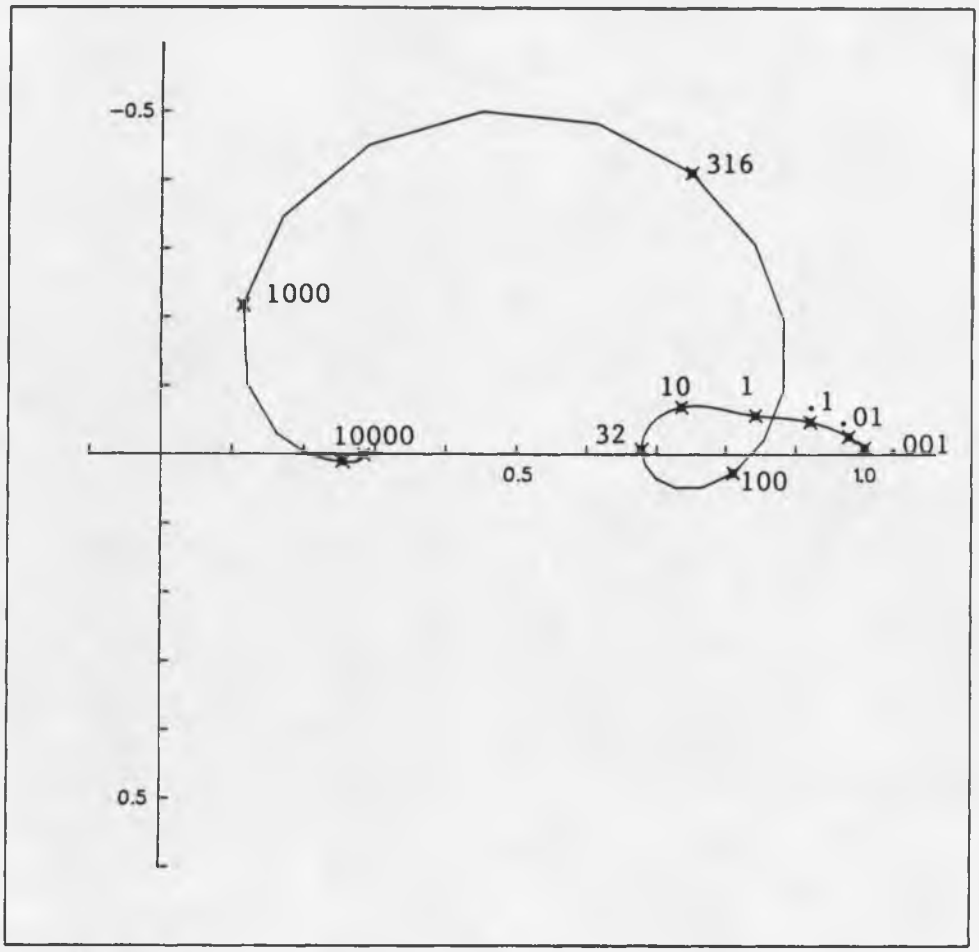

Figure 4.9e. Mutual impedance on a two-layer earth with Cole-Cole resistivities. First layer dc resistivity is 50 ohm-m. Second layer has a ratio of vertical to horizontal resistivity of .0625. -- Computed for a 100 meter dipole-dipole array at an N of 6 for frequencies between .001 and 10,000 Hertz. The first layer is isotropic, with m = .10, t_o = .1, and c = .5. The second layer has a mean dc resistivity of 100 ohm-m and horizontal and vertical m = .3, t_o = 1.0, and c = .5. Normalization factor is 761 x 10^{-6}.

double-bumped spectra is apparent at low frequencies up to 32 Hertz, with peaks occurring at about .1 and 10.

Figures 4.10a-4.10e represent the case of a first layer that has a dc resistivity five times as conductive as the second layer. The first layer is 100 meters thick and has a resistivity of 20 ohm-meters. Its Cole-Cole parameters m, t_o, and c are unchanged from the previous models. The second layer is the same as in the previous models. Again, the calculation is for an N of 6 with a 100 meter dipole-dipole array. At low frequencies the shape of the curve is changed significantly, even though the IP properties are identical and conventional wisdom would indicate that the second layer should be detected at this N spacing.

I interpret the results in the following way. The conductive overburden is concentrating current near the surface. In the IP frequency range, the received voltage appears to be affected by the shorter time constant of the surface layer. For Figures 4.10a-4.10c, the low-frequency arc appears to peak at 1 Hertz, then go through an inflection point between 1 and 10 Hertz before continuing with the expected positive EM coupling curve.

At higher frequencies, the properties of the first layer and the low to high resistivity contrast between layers still appears to control the shape of coupling curves. For models with increased horizontal conductivity, the

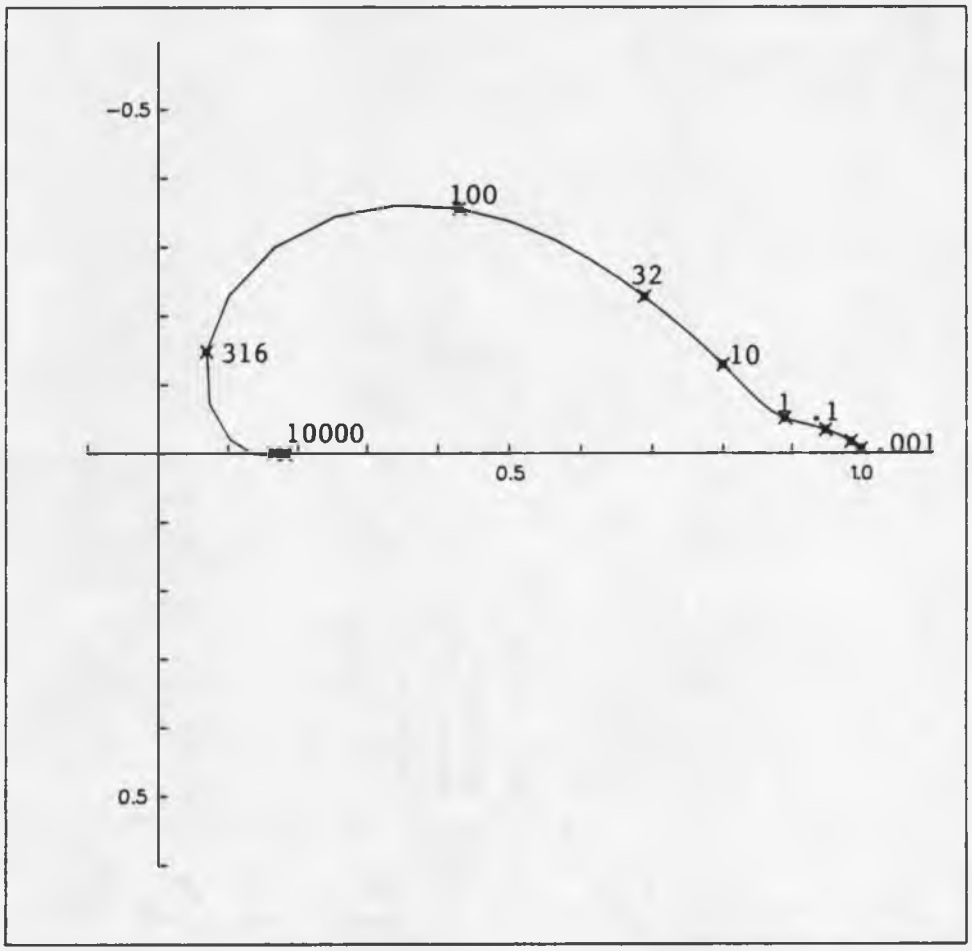

Figure 4.10a. Mutual impedance on a two-layer earth with Cole-Cole resistivities. First layer dc resistivity is 20 ohm-m. Second layer has a ratio of vertical to horizontal resistivity of 1. -- Computed for a 100 meter dipole-dipole array at an N of 6 for frequencies between .001 and 10,000 Hertz. The first layer is isotropic, with m = .10, t_o = .1, and c = .5. The second layer has a mean dc resistivity of 100 ohm-m and horizontal and vertical m = .3, t_o = 1.0, and c = .5. Normalization factor is 471.1 x 10^{-6}.

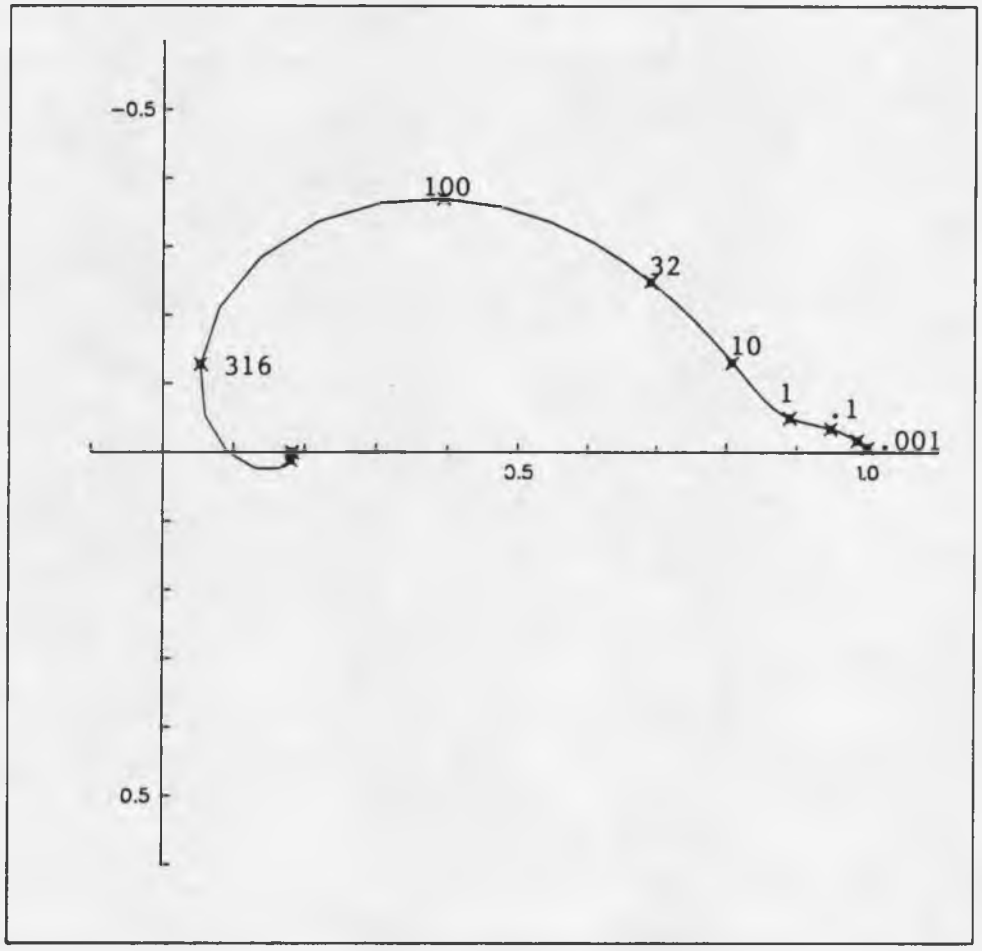

Figure 4.10b. Mutual impedance on a two-layer earth with Cole-Cole resistivities. First layer dc resistivity is 20 ohm-m. Second layer has a ratio of vertical to horizontal resistivity of 4. -- Computed for a 100 meter dipole-dipole array at an N of 6 for frequencies between .001 and 10,000 Hertz. The first layer is isotropic, with m = .10, t_o = .1, and c = .5. The second layer has a mean dc resistivity of 100 ohm-m and horizontal and vertical m = .3, t_o = 1.0, and c = .5. Normalization factor is 471.1 x 10^{-6}.

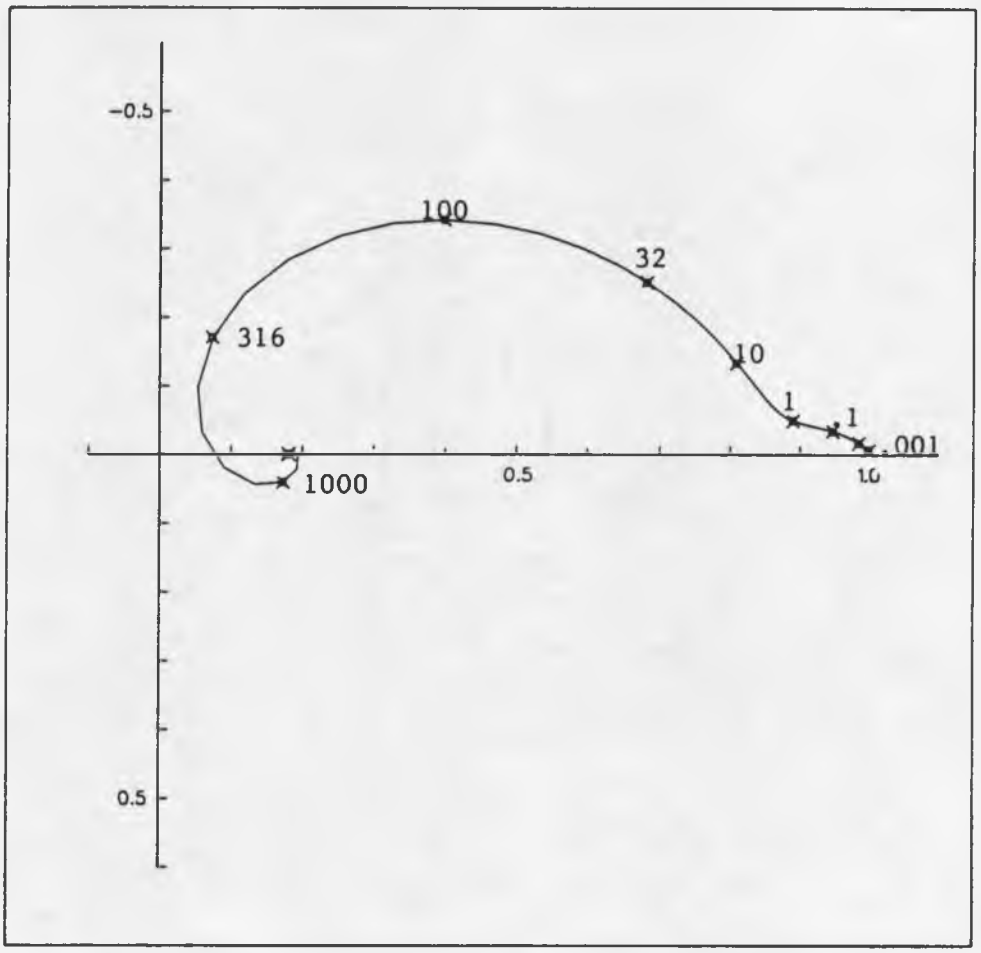

Figure 4.10c. Mutual impedance on a two-layer earth with Cole-Cole resistivities. First layer dc resistivity is 20 ohm-m. Second layer has a ratio of vertical to horizontal resistivity of 16. -- Computed for a 100 meter dipole-dipole array at an N of 6 for frequencies between .001 and 10,000 Hertz. The first layer is isotropic, with m = .10, t_o = .1, and c = .5. The second layer has a mean dc resistivity of 100 ohm-m and horizontal and vertical m = .3, t_o = 1.0, and c = .5. Normalization factor is 471.1 x 10^{-6}.

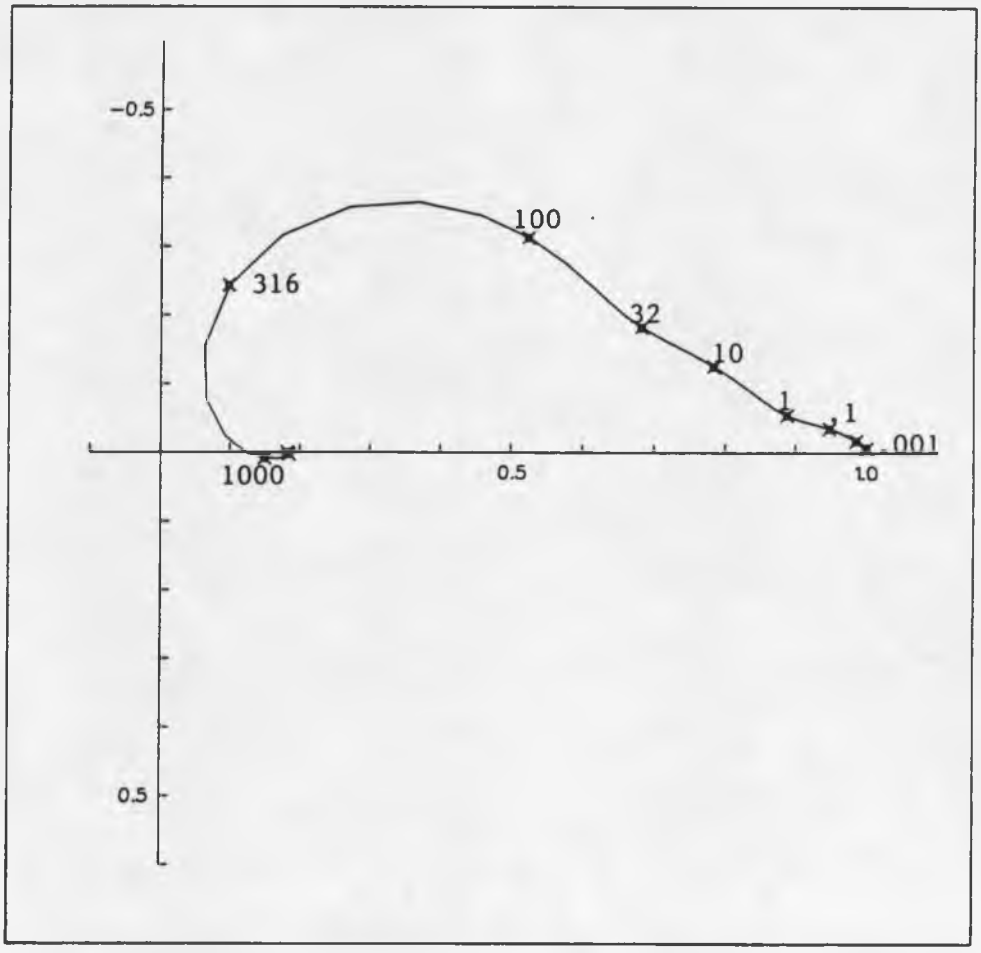

Figure 4.10d. Mutual impedance on a two-layer earth with Cole-Cole resistivities. First layer dc resistivity is 20 ohm-m. Second layer has a ratio of vertical to horizontal resistivity of .25. -- Computed for a 100 meter dipole-dipole array at an N of 6 for frequencies between .001 and 10,000 Hertz. The first layer is isotropic, with m = .10, t_o = .1, and c = .5. The second layer has a mean dc resistivity of 100 ohm-m and horizontal and vertical m = .3, t_o = 1.0, and c = .5. Normalization factor is 471.1 x 10^{-6}.

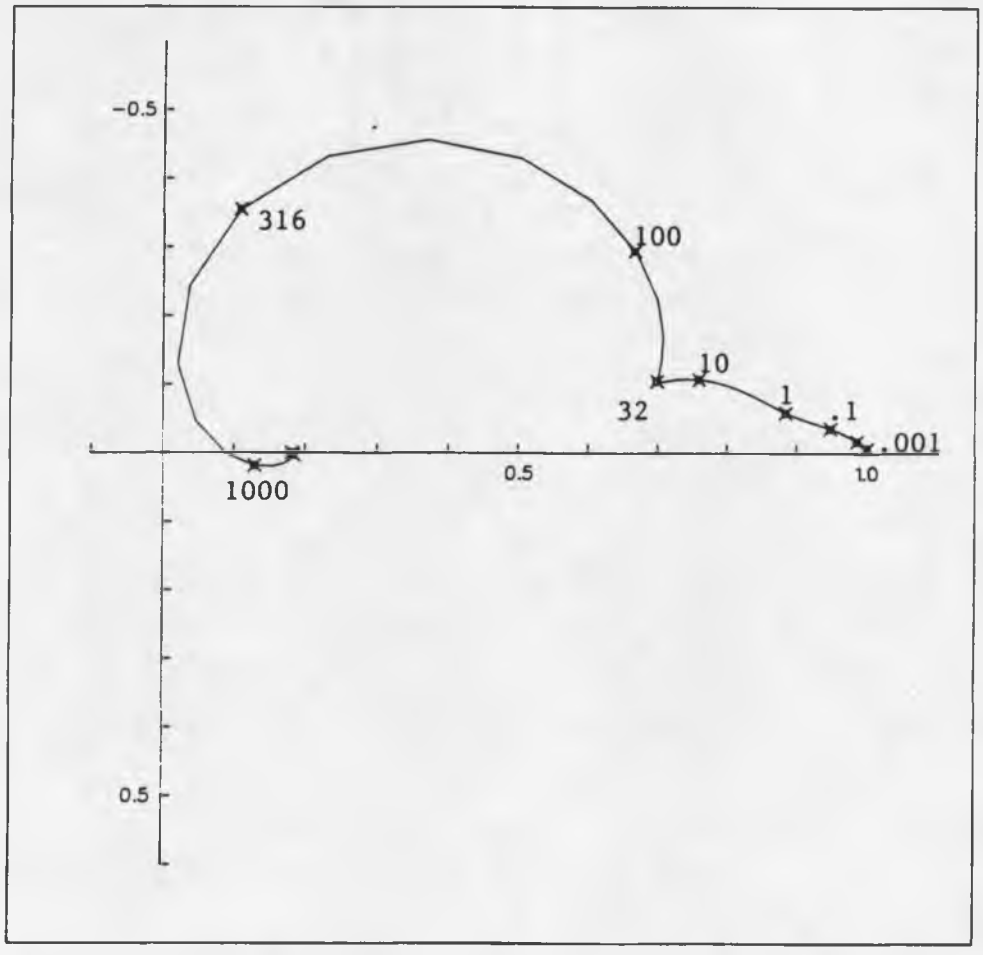

Figure 4.10e. Mutual impedance on a two-layer earth with Cole-Cole resistivities. First layer dc resistivity is 20 ohm-m. Second layer has a ratio of vertical to horizontal resistivity of .0625. -- Computed for a 100 meter dipole-dipole array at an N of 6 for frequencies between .001 and 10,000 Hertz. The first layer is isotropic, with m = .10, t_o = .1, and c = .5. The second layer has a mean dc resistivity of 100 ohm-m and horizontal and vertical m = .3, t_o = 1.0, and c = .5. Normalization factor is 471.1 x 10^{-6}.

curves all have a very similar shape, indicating a small influence of the second layer anisotropy. Curves diverge only slightly between 50 and 500 Hertz.

For the models with increased vertical conductivity (Figures 4.10d and 4.10e), the situation is complicated. On Figure 4.10d, inflection points develop on the curve at about 1 and 32 Hertz. Again, the slight peak at 10 Hertz and the low at 32 Hertz are EM effects and do not reflect the IP response of either layer. This is seen in 4.10e, where a sharp notch has developed at 32 Hertz. The inflection seems to mark the transition from: (1) the low-frequency behavior that is responding to a weighted average of the first and second layers, to (2) a positive coupling response that reflects layering.

CHAPTER 5

CONCLUSIONS

The analytical solution for a two-layer anisotropic earth with complex resistivity has been presented. My results are compatible with Wait's solution (1982) for a multi-layer earth and contrast with Wynn's results (1979). The solution has been written in a form which takes advantage of existing software for the computation of electric fields on a multi-layer earth with complex, isotropic resistivities. While modifying that software, an error that influences results for multi-layered models with complex resistivities was identified and corrected.

Computations have been made for both half-space and two-layer models, with resistivities ranging from real and isotropic to complex and anisotropic. Results are different from those previously published and appear to fit a simple physical explanation that correlates the coupling response on a two-layer earth to that occurring on a half-space under conditions of increased horizontal or vertical conductivity. Both increased horizontal conductivity for a half-space and a conductive first layer in a two-layer model cause an increase in lateral current flow and both produce positive coupling curves. Increased vertical conductivity or a

second layer that is more conductive than the first layer causes a relative increase in vertical current flow and can produce negative coupling curves. As predicted by Wait (1966a), the mutual impedance of grounded wires on an anisotropic half-space provides diagnostic information about the anisotropy, that is not available in either DC resistivity measurements or inductive EM soundings.

Two-layer models with real anisotropic resistivities have been computed for two of the models of Wynn (1979) and have produced quite different results. His assertion that anisotropy can cause the normalized amplitude between dc and .1 Hertz to exceed 1 could not be verified. Notching and even closed loops were observed in some layered models, but it was not clear whether this result was caused by the anisotropy of a layer or simply reflected a strong contrast in the layer properties.

To model polarizable, anisotropic layers, horizontal and vertical conductivities can be represented by independent Cole-Cole models. For the few models computed here, Cole-Cole parameters were selected to represent intermediate properties of porphyry-copper mineralization. For large time constants, the complex resistivity causes a low frequency arc and a left lateral shifting of the mutual impedance curve when data are plotted in the complex plane. At higher frequencies, curves have the same form and plot in

the same quadrant as in the real case. Varying parameters other than resistivity in the Cole-Cole model produces results consistent with physical reasoning. Variations in m (chargeability) can cause similar results as variations in R (dc resistivity term).

Two-layer cases have been computed to show the influence of overburden on response of a target at depth. Conductive overburden can obscure the response of the second layer. Not enough transmitted current flows in the second layer to influence the field measured at the surface. The high-frequency EM effects that are indicative of the anisotropic behavior of the second layer are subdued. When conductive overburden is present, simple rules for the depth of penetration of a dipole-dipole array do not hold.

When the first layer is more resistive, currents penetrate deeper and second layer properties can be more easily detected. Anisotropic behavior can be recognized over a wider frequency range. Layering appears to affect the high frequencies and, at least for increased vertical conductivities, can produce local closed loops on mutual impedance curves, when plotted in the complex plane.

Results of this study suggest that measurements of the mutual impedances of grounded wires are useful in the interpretation of the subsurface electrical properties. In particular, information is available in the EM coupling

component of multi-frequency IP measurements that is not readily available in conventional EM, IP or DC resistivity measurements. Many mineralized environments, targets for subsurface water, and even oil environments appear to be associated with vertically oriented fractures, veins or boundaries. Locally these environments might be approximated by the microanisotropic resistivity model studied here. Negative coupling curves might be indicators of such environments. High resistivity surface layers are not required to produce negative coupling effects.

This study also has relevance to problems in the recognition and separation of IP and electromagnetic effects in geophysical exploration systems. The goal in making multifrequency IP measurements is often to derive a description of IP properties of the ground over a wide frequency range. The detailed IP response allows prediction of the size and volume percent of mineralization and, potentially, discrimination between economic and uneconomic targets.

To separate the IP response from mutual impedance, the usual approach is to fit an empirical model that supposedly represents separately the responses of low frequency IP effects and higher frequency EM effects. Methods have concentrated on empirical techniques because of problems computing responses of physical models that represent all the complexities of the mutual impedance curve.

Because the goal of these decoupling schemes is to derive the complex apparent resistivity of the equivalent half-space, a direct approach to this problem would be to invert the data to an anisotropic half space. When the IP response can be represented by a single Cole-Cole model, a simple, 5 parameter model, involving horizontal and vertical resistivity and a single m, t_o, and c could be used. This physical model could match both positive and negative coupling curves over the frequency for which measurements are not complicated by the effects of layering. Complex resistivity and electromagnetic effects would be treated in a more realistic fashion, and better resolution of the IP response at high frequency should be possible.

An area of active research is measurement of the IP effect using ungrounded sources and/or receivers. The anisotropic model suggests that this type of measurement could produce results different from those measured with the grounded receiver and transmitter combination. If the transmitter or receiver (or both) are ungrounded loops, the Q(r) function is zero. For the uniform-layered, microanisotropic model, mutual impedance is only a function of P(r), which depends only on the horizontal conductivity function.

Currently, little is known about the anisotropy of resistivity in typical exploration environments. Thus it is impossible to judge its influence on inductive IP measure-

ments. Certainly it can be expected to be significant in deposits such as porphyry-copper and disseminated gold deposits where vertically oriented structures, veins and stockworks are common. More case histories and more three-dimensional measurements of the electrical properties of rocks are required to properly assess the advantages and disadvantages of grounded versus inductive methods.

SELECTED BIBLIOGRAPHY

Anderson, W. L., 1974, Electromagnetic fields about a finite electric wire source, U.S. Geological Survey Report USGS-GD-74-041, 209 p.

Anderson, W. L., 1979, Computer program: Numerical integration of related Hankel transforms of orders 0 and 1 by adaptive digital filtering, Geophysics, v. 44, 1287-1305.

Anderson, W. L. and Smith, B. D., 1984, Nonlinear least-squares inversion of transient induced polarization data (Program NLSTIP), U.S. Geological Survey Open-File Report 84-514, 63 p.

Anderson, W. L. and Smith, B. D., 1986, Nonlinear least-squares inversion of frequency-domain induced polarization data (program NLSIP), U.S. Geological Survey Open-File Report 86-280, 33 p.

Bertin J. and Loeb, J., 1976, Experimental and theoretical aspects of induced polarization, 2 vols.; Berlin, Gebruder Borntrager.

Brown, R. J., 1985, EM coupling in multifrequency IP and a generalization of the Cole-Cole impedance model, Geophysical Prospecting, v. 33, 282-302.

Chlamtac, M. and Abramovici, F., 1981, The electromagnetic fields of a horizontal dipole over a vertically inhomogeneous and anisotropic earth, Geophysics, v. 46, 904-915.

Coggon, J. H., 1984, New three-point formulas for inductive coupling removal in induced polarization, Geophysics, v. 49, 307-309.

Cole, K. S. and Cole, R. H., 1941, Dispersion and absorption in dielectrics, I. Alternating current characteristics, Journal of Chemical Physics, v. 9, 341- 351.

Dey, A. and Morrison, H. F., 1973, Electromagnetic coupling in frequency and time-domain induced-polarization surveys over a multilayered earth, Geophysics, v. 38, 380-405.

Fraser, D. C., Keevil, N. B., Jr., and Ward, S. H., 1964, Conductivity spectra of rocks from the Craigmont ore environment, Geophysics, v. 29, 832-847.

Fuller, B. D. and Ward, S. H., 1970, Linear system description of the electrical parameters of rocks, IEEE Transactions on Geoscience, v. GE-8, 7-18.

Grant, F. S. and West, G. F., 1965, Interpretation theory in applied geophysics, New York, McGraw-Hill.

Hallof, P. G, 1974, The IP phase measurement and inductive coupling, Geophysics, v. 39, 650-665.

Hallof, P. and Pelton, W. H., 1980, The removal of inductive coupling effects from spectral I. P. data, presented at the 50th Annual SEG meeting.

Halverson, M. D., Zinn, W. G., McAlister, E. O. Ellis, R. B. and Yates, W. C., 1981, Assessment of results of broad band spectral IP field tests, in Sumner, J. S. (ed.), Advances in Induced Polarization and Resistivity, Tucson, University of Arizona, 255-294.

Hill, D. G., 1972, A laboratory investigation of electrical anisotropy in precambrian rocks, Geophysics, v. 37, 1022-1038.

Hohmann, G. W., 1973, Electromagnetic coupling between grounded wires on the surface of a two layer earth, Geophysics, v. 38, 854-863.

Hohmann, G. W., 1975, Three-dimensional induced polarization and electromagnetic modeling, Geophysics, v. 40, 309-324.

Hohmann, G. W. and Ward, S. H., 1981, Electrical methods in mining geophysics, in Skinner, B. J. (ed.), Economic Geology Seventy-Fifth Anniversary Volume, 1905-1980. El Paso, Economic Geology Publishing Co., 806-828.

Kauahikaua, J., 1989, Personal communication. Geophysicist, U.S. Geological Survey, Hawaiian Volcano Observatory, Hawaii National Park, Hawaii, 96718.

Kauahikaua, J. and Anderson, W. L., 1979, Programs EMCUPL and SCHCPL, Computation of electromagnetic coupling on a layered half-space with complex conductivities: U.S. Geological Survey Open-File Report 79-1430, 91 p.

Keller, G. V. and Frischknecht, F. C., 1966, Electrical methods in geophysical prospecting: New York, Pergamon Press.

Kinghorn, G. F., 1967, Electrical methods for deep subsurface exploration, IEEE Trans. on Geoscience Electronics, v. GE-5, 51-62.

Le Manse, D. and Vasseur, G., 1981, Electromagnetic field of sources at the surface of a homogeneous conducting half-space with horizontal anisotropy: Application to fissured media, Geophysical Prospecting, v. 29, 803-821.

Madden T. R. and Cantwell, T., 1967, Induced polarization, a review, in Mining Geophysics, v. II, Tulsa, Society of Exploration Geophysicists, 373-400.

Major, J. and Silic, J., 1981, Restrictions on the use of Cole-Cole dispersion models in complex resistivity interpretation, Geophysics, v. 46, 916-931.

Millet, F. B., 1967, Electromagnetic coupling of collinear dipoles on a uniform half-space, in Mining Geophysics, v. II, Theory, Tulsa, Society of Exploration Geophysicists, 401-419.

Nablusi, K. A. and Wait, J. R., 1982, Transient coupling between finite circuits on an anisotropic conducting half-space, Geophysical Prospecting, v. 30, 470-485.

Pelton, W. H., Ward, S. H., Hallof, W. R., Sill, W. R., and Nelson, P. H., 1978, Mineral discrimination and removal of inductive coupling with multi-frequency IP, Geophysics, v. 43, 588-603.

Ramachandran Nair, M. and Sanyal, N., 1980, Electromagnetic coupling in IP measurements using some common electrode arrays over a uniform half-space, Geoexploration, v. 18, 97-109.

Sinha, A. K., 1968, Electromagnetic fields of an oscillating dipole over an anisotropic earth, Geophysics, v. 33, 346-353.

Sinha, A. K. and Bhattacharya, P. K., 1967, Electric dipole over an anisotropic and inhomogeneous earth, Geophysics, v. 32, 652-667.

Sommerfeld, A. N., 1964, Partial differential equations in physics, New York, Academic Press

Song, L., 1984, A new decoupling scheme, Exploration Geophysics, v. 15, 99-112.

Stratton, J. A., 1941, Electromagnetic Theory, New York, McGraw-Hill, 615 p.

Sumner, J. S., 1976, Principles of induced polarization for geophysical exploration: Amsterdam, Elsevier.

Sunde, E., D., 1949, Earth conduction effects in transmission systems: New York, D. Van Nostrand Co., Inc.

Trofimenkoff, F. N., Johnston, R. H., and Haslett, J. W., 1982, Electromagnetic coupling between parallel lines on a uniform earth, IEEE Trans. Geoscience Electronics, v. GE-20, 197-200.

Tyne, E. D., 1981, Field study of first and second-order transient induced polarization and electromagnetic coupling at Woodlawn, in Whitely, R. J. (ed.), Geophysical case study of the Woodlawn ore body, New South Wales, Australia, New York, Pergamon, 375-422.

Van Voorhis, G. D., Nelson, P. H., and Drake, T. L., 1973, Complex resistivity spectra of porphyry copper mineralization, Geophysics, v. 38, 49-60.

Wait, J. R. (ed.), 1959a, Overvoltage research and geophysical applications: New York, Pergamon Press Inc.

Wait, J. R., A phenomenological theory of overvoltage for metallic particles, in Wait, J. R. (ed.), 1959b, Overvoltage research and geophysical applications: New York, Pergamon Press Inc., 22-28.

Wait, J. R., The variable frequency method, in Wait, J. R. (ed.), 1959c, Overvoltage research and geophysical applications: New York, Pergamon Press Inc., 29-49.

Wait, J. R., 1966a, Electromagnetic fields of a dipole over an anisotropic half space, Canadian J. Phys., v. 44, 2387-2401.

Wait , J. R., 1966b, Fields of a horizontal dipole over a stratified anisotropic half-space, IEEE Trans. on Antennas and Propagation, v. AP-14, 790-792.

Wait, J. R., 1981, written communication. [A letter from J. R. Wait to J. Wynn detailing the inconsistencies in Wynn's derivations.] Regent's Professor Emeritus, University of Arizona, Tucson, Az.

Wait, J. R., 1982, GeoElectromagnetism, New York, Academic Press, 268 p.

Wait, J. R., 1989, Complex resistivity of the earth, in Kong, J. A. (ed.), Progress in Electromagnetics Research, Amsterdam, Elsevier, v. 1, 1-175.

Wang, J., Zhan, K., Shien, L., and Yan, L., 1985, Fundamental characteristics of an approximate correction method for electromagnetic coupling in frequency-domain induced polarization, Geophysics, v. 44, 1245-1265.

Ward, S. H., 1967, Electromagnetic Theory for Geophysical Applications, in Mining Geophysics, v. II, Theory, Tulsa, Society of Exploration Geophysicists, 10-198.

Washburne, J., 1982, Parameterization of spectral induced polarization data and in situ and laboratory spectral induced polarization measurements: West Shasta copper zinc district, Shasta, Ca., M.S. Thesis, Colo. Sch. of Mines, 228 p.

Wong, J., 1979, An electrochemical model of the induced polarization phenomenon in disseminated sulphide ores, Geophysics, v. 44, 1245-1265.

Wong, J. and Strangway, D. W., 1981, Induced polarization in disseminated sulphide ores containing elongated mineralization, Geophysics, v. 46, 1258-1268.

Wynn, J. C., 1974, Electromagnetic coupling in induced polarization, University of Arizona Ph.D. thesis, 137 p.

Wynn, J. C., 1979, Electromagnetic coupling with a collinear array on a two layer anisotropic earth, U. S. Geologic Survey Professional Paper 1077. Washington D. C., U. S. Government Printing Office.

Wynn, J. C. and Zonge, K. L., 1975, EM coupling, its intrinsic value, its removal and the cultural coupling problem, Geophysics, v. 40, 831-850.

Wynn, J. C. and Zonge, K. L., 1977, Electromagnetic coupling, Geophysical Prospecting, v. 25, 29-51.

Xiong, Z., Luo, Y., Wang, S., and Wu, G., 1986, I.P. and EM modeling of a 3-D body buried in a 2-layered anisotropic earth, Geophysics, v. 51, 2235-2246.

Zonge, K. L., 1972, Electrical properties of rocks as applied to geophysical prospecting, Ph.D. thesis, University of Arizona, 153 p.

Zonge K. L. and Wynn J. C., 1975, Recent advances and applications in complex resistivity measurements, Geophysics, v. 40, 851-864.